

Functional Analysis of Arabidopsis SPA Proteins in Plant Growth Control

Inaugural-Dissertation

zur

Erlangung des Doktorgrades
der Mathematisch-Naturwissenschaftlichen Fakultät
der Universität zu Köln

vorgelegt von

Petra Christina Fackendahl

aus Nettetal

2012

Berichterstatter: Prof. Dr. Ute Hoecker
Prof. Dr. Martin Hülskamp

Prüfungsvorsitzender: Prof. Dr. Wolfgang Werr

Tag der mündlichen Prüfung: 25.05.2011

Contents

Contents	I
Abbreviations	III
Abstract	V
Zusammenfassung	VI
I. Introduction	1
I.1. Photoreceptors and light signal transduction in <i>Arabidopsis thaliana</i>	1
I.2. Repressors of photomorphogenesis: the COP1/SPA complex	7
I.3. The SPA proteins and their function in light-regulated plant development	10
I.4. Arabidopsis leaf growth and development	13
I.5. Aims of this thesis	17
II. Results	18
II.1. Role of SPA proteins in Arabidopsis leaf size control	18
II.1.1. Detailed phenotypic characterization of <i>spa</i> mutants	18
II.1.2. Involvement of transcription factors in SPA/COP1-regulated leaf growth	25
II.2. Characterization of <i>spa</i> null mutants	27
II.2.1. Identification of <i>spa2</i> and <i>spa4</i> mutant null alleles	27
II.2.2. Generation of a <i>spa</i> quadruple null mutant	30
II.3. SPA4 structure function analysis	33
II.3.1. Role of the SPA4-N-terminus in light-grown seedlings	33
II.3.2. Role of the SPA4 N-terminus in adult plant development	43
II.4. SPA1 structure function analysis	45
II.4.1. Light-induced de-stabilization of SPA1 is dependent on the N-terminus and the coiled-coil domain	46
II.4.2. The SPA1 N-terminus partially contributes to seedling photomorphogenesis in a <i>spa</i> triple mutant background	48
II.4.3. Complementation of ΔNT -SPA1 constructs in adult <i>spa</i> triple mutants	52
II.5. Mapping of an <i>spa1</i> enhancer mutant	53
II.5.1. The <i>28g</i> locus shows an enhanced <i>spa1</i> mutant phenotype in light-grown seedlings but not in flowering time	54
II.5.2. Mapping of the <i>28g</i> locus	56
III. Discussion	59
III.1. Role of COP1/SPA in Arabidopsis leaf size regulation	59
III.2. SPA proteins are important but not essential for Arabidopsis development	64
III.3. Role of the SPA4 N-terminus in light-dependent seedling morphogenesis and plant size control	67
III.4. The SPA1-N terminus and coiled-coil domain are involved in light-dependent SPA1 protein de-stabilization	72
III.5. The SPA1 N-terminus is of different importance in seedling photomorphogenesis and leaf size regulation in a <i>spa</i> triple mutant background	74
III.6. The <i>28g</i> locus specifically enhances the <i>spa1</i> mutant phenotype in seedling development	78
IV. Materials and Methods	81
IV.1. Materials	81

IV.1.1. Chemicals and antibiotics	81
IV.1.2. Enzymes, kits, antibodies and radioactivity	81
IV.1.3. Oligonucleotides	81
IV.1.4. Bacterial strains	83
IV.1.5. Cloning vectors	83
IV.1.6. Plant lines	84
IV.2. Work with <i>Arabidopsis thaliana</i>	86
IV.2.1. Seed sterilization	86
IV.2.2. Plant growth	87
IV.2.3. Measurement of hypocotyl length	87
IV.2.4. Quantification of leaf size	88
IV.2.5. Determination of flowering time	88
IV.2.6. Microscopy of <i>Arabidopsis</i> leaves	88
IV.2.7. Screening of transgenic plants	89
IV.2.8. Screening of an <i>Arabidopsis</i> T-DNA insertion mutant collection	89
IV.2.9. Molecular mapping	89
IV.3. Molecular biology methods	90
IV.3.1. Standard molecular biology methods	90
IV.3.2. Cloning	90
IV.3.3. Bacterial transformation and plasmid isolation	90
IV.3.4. Sequence Analyses	91
IV.3.5. Transient transformation	91
IV.3.6. Fluorescence microscopy	92
IV.3.7. Plant transformation	92
IV.3.8. Genomic DNA preparation	92
IV.3.9. RNA isolation	92
IV.3.10. Transcript analysis by RT-PCR	92
IV.3.11. Transcript analysis by REALTIME-PCR	92
IV.3.12. RNA blot analysis	93
IV.3.13. Preparation of DNA Probes for RNA blot analysis	93
IV.4. Biochemical methods	94
IV.4.1. Total protein isolation from <i>Arabidopsis</i>	94
IV.4.2. SDS-polyacrylamidgelelectrophoresis (SDS-PAGE)	94
IV.4.3. Immunoblot analysis	94
IV.5. Cloning strategies	95
IV.5.1. Construction of 35S: <i>GFP-SPA4</i> full-length and deletion constructs	95
IV.5.2. Constructs for SPA1 structure-function analysis	97
V. Supplement	99
VI. References	105
Danksagung	118
Erklärung	119

Abbreviations

α - ³² P-dATP	2'-desoxyadenosin-5'triphosphate, radioactive labelled at α -P-atom
aa	amino acid
35S	35S promoter from Cauliflower Mosaic Virus
°C	degree Celsius
μ g	microgram
μ l	microlitre
μ m	micrometre
B, Bc	blue light, continuous B
bHLH	basic helix-loop-helix
bp	base pair
BR	Brassinosteroids
CaMV	Cauliflower Mosaic Virus
cDNA	complementary DNA
cc	coiled-coil structure
cm	centimetre
Col-0	Columbia; ecotype of <i>Arabidopsis thaliana</i>
D	darkness
DNA	deoxyribonucleic acid
et al.	et alerni (Lat.) and others
FL	full-length
FR, FRc	far-red light, continuous FR
GA	gibberelic acid
GFP	green fluorescent protein
h	hour
HA	Influenza hemagglutinin
kb	kilo bp
kDa	kilo Dalton
l	litre
LB	T-DNA left border
LD	long day
Ler	Landsberg <i>erecta</i> ; ecotype of <i>Arabidopsis thaliana</i>
M	molar; mol/l
mg	milligram
mM	millimolar
min	minute
mRNA	messenger RNA
MS	Murashige and Skoog medium
NLS	nuclear localization signal/sequence
nm	nanometre
ORF	open reading frame
p	promoter
PCR	polymerase chain reaction
Pfr	far red light absorbing phytochrome conformation
Phy	phytochrome
Pr	red light absorbing phytochrome conformation
R, Rc	red light, continuous R
RB	T-DNA right border
RLD	ecotype of <i>Arabidopsis thaliana</i>
RNA	ribonucleic acid

rpm	rounds per minute
RT-PCR	reverse transcription PCR
s	second
SD	short day
SEM	standard error of the mean
T-DNA	transferred DNA
UTR	untranslated region
UV	ultraviolet
WD	aspartic acid; tryptophan
WT	wild type
YFP	yellow fluorescent protein

Nomenclature:

<i>SPA1</i>	gene, locus, wild-type allele
<i>spa1</i>	mutant allele
SPA1	protein

Exception: Photoreceptors

<i>PHY</i>	gene, locus, wild-type allele
<i>phy</i>	mutant allele
PHY	apoprotein (without chromophor)
phy	holoprotein (with chromophor)

Abstract

For successful development, plants have to respond appropriately to environmental signals such as light quality and quantity. COP1/SPA complexes are important repressors of light signalling in darkness but also prevent overstimulation of the plant by light. In *Arabidopsis thaliana*, the four SPA proteins act in concert with COP1 as E3 ubiquitin ligase to regulate seedling development, photoperiodic flowering and leaf growth by promoting the degradation of transcription factors like HY5, HFR1 or CO via the 26S proteasome. SPA proteins share a typical domain structure including a C-terminal WD-repeat domain for substrate binding, a central coiled-coil domain, which is essential for SPA-SPA and SPA-COP1 interaction and an N-terminal part containing a kinase-like motif of unknown function.

In this study it was shown that the dwarfed phenotype of *spa* triple and weak *cop1* mutants is caused by a reduction in the number and the size of epidermal and mesophyll cells. Genetic interaction studies indicated that hyper-accumulation of COP1/SPA targets contributes to the reduced leaf size of *cop1* and *spa* mutants.

SPA4 was shown to be the key regulator of *COP1/SPA*-regulated plant growth. Here, a structure function analysis of *SPA4* revealed that the N-terminal part of the protein is dispensable for *SPA4* function in seedling de-etiolation and leaf size control, whereas its coiled-coil domain is essential. In contrast, the *SPA4* N-terminus is seemed to be involved in *SPA4* protein de-stabilization in adult plants.

It is known that the *SPA1* N-terminus is dispensable for seedling de-etiolation, but necessary for photoperiodic flowering control. In the present study, I could show that the *SPA1* N-terminus does not contribute to plant growth, but that it is involved in the light-induced de-stabilization of *SPA1*. Moreover, it was revealed that the coiled-coil domain is important for *SPA1* degradation, suggesting that *SPA* de-stabilization is dependent on *SPA-COP1* interaction.

cop1 null mutants are seedling lethal and therefore *Arabidopsis* development depends on *COP1* function. Here, the *SPA* proteins were shown to be important, but not essential for the survival of the plants as *spa* quadruple null mutants were tiny, but viable. This suggests that *COP1* is at least partially functional without the *SPA* proteins or acts in concert with other factors, but not vice versa.

Besides, a *spa1* enhancer mutant was mapped to a 46 kb region on chromosome 3. 16 gene loci are remaining as putative novel regulator of light signal transduction.

Zusammenfassung

Pflanzen müssen angemessen auf Umwelteinflüsse wie Lichtqualität und -quantität reagieren um sich erfolgreich zu entwickeln. COP1/SPA-Komplexe sind wichtige Repressoren der Lichtsignaltransduktion im Dunkeln aber verhindern auch eine Überstimulierung der Pflanze durch Licht. In *Arabidopsis thaliana* fungieren die vier SPA Proteine in Kooperation mit COP1 als E3 Ubiquitin Ligase, die die Keimlingsentwicklung, die Blühinduktion und das Blattwachstum steuert indem sie den Abbau von Transkriptionsfaktoren wie z.B. HY5, HFR1 oder CONSTANS durch das 26S Proteasom induzieren. Die SPA Proteine weisen eine typische Domänenstruktur auf, bestehend aus einer carboxy-terminalen WD-40 Repeat-Domäne, die Substratinteraktion vermittelt, einer zentralen Coiled-Coil Domäne, die für die Interaktion der SPAs miteinander und für die COP1-SPA Interaktion essentiell ist und einer amino-terminalen Region, die ein kinase-ähnliches Motiv aufweist, deren Funktion jedoch nicht bekannt ist.

In dieser Arbeit wurde gezeigt, dass der zwergwüchsige Phänotyp der *spa* Triplemutanten und der schwachen *cop1* Mutante sowohl durch eine Reduzierung der Zellzahl als auch durch eine verringerte Zellgröße von Epidermis- und Mesophyllzellen verursacht wird. Genetische Interaktionsstudien weisen darauf hin, dass erhöhte Akkumulation von COP1/SPA Substraten zu der verminderten Blattgröße von *cop1* und *spa* Mutanten beitragen.

SPA4 wurde als zentraler Regulator des *COP1/SPA*-gesteuerten Pflanzenwachstums identifiziert. Eine Struktur-Funktionsanalyse von *SPA4* offenbarte, dass der N-terminale Bereich des Proteins irrelevant für die *SPA4* Funktion bei der licht-induzierten Keimlingsentwicklung und dem Blattwachstum ist, während die Coiled-Coil Domäne essentiell für die Funktion von *SPA4* ist. Hingegen ist der *SPA4* N-Terminus mutmaßlich an der Destabilisierung des *SPA4* Proteins in adulten Pflanzen beteiligt.

Es ist bekannt, dass der N-Terminus von *SPA1* überflüssig für die Keimlingsentwicklung, jedoch essentiell für die Hemmung der Blühinduktion im Kurztag ist. In dieser Arbeit konnte gezeigt werden, dass der *SPA1* N-Terminus nicht zur Regulierung der Blattgröße beiträgt, aber in der lichtabhängigen Destabilisierung von *SPA1* involviert ist. Des Weiteren wurde nachgewiesen, dass auch die Coiled-Coil Domäne wichtig für den Abbau des *SPA1* Proteins im Licht ist. Dies deutet auf

eine Abhängigkeit der SPA1 Protein-Destabilisierung von der SPA-COP1 Interaktion hin.

cop1 Null Mutanten sind nicht in der Lage sich über das Keimlingsstadium hinaus zu entwickeln, daher ist die Entwicklung von Arabidopsispflanzen abhängig von der COP1 Funktion. Die Funktion der SPA Proteine ist zwar wichtig für die normale Entwicklung der Pflanzen, aber nicht essentiell, da gezeigt werden konnte, dass *spa* Quadruple Null Mutanten zwar extrem kleinwüchsig jedoch lebensfähig sind. Dies deutet darauf hin, dass in Abwesenheit der SPA Proteine, COP1 zumindest teilweise funktional ist oder aber gemeinsam mit anderen Proteinen fungiert, während im Gegensatz dazu die SPAs das Fehlen von COP1 nicht kompensieren können.

In einem weiteren Projekt wurde der Locus, der eine *spa1* enhancer Mutante kodiert bis auf einen 46 kb umfassenden Bereich auf Chromosom 3 kartiert. Noch 16 Gene kommen als Kandidat für einen potentiellen neuen Faktor in der Lichtsignaltransduktion in Frage.

I. Introduction

1.1. Photoreceptors and light signal transduction in *Arabidopsis thaliana*

Plants are sessile organisms; therefore, rapid and appropriate responses to environmental changes are essential for their successful growth and reproduction. Besides factors like temperature, nutrient and water availability, light plays an important role in plant development throughout the whole life cycle of a plant as it provides the primary source of energy and moreover, serves as an informational signal. Light regulates seed germination, seedling photomorphogenesis, phototropism, shade avoidance responses, induction of flowering and other developmental processes (Neff et al., 2000; Jiao et al., 2007). To mediate developmental changes in response to light, plants have evolved a highly complex regulatory network including various photoreceptors, transcription factors and components of the protein degradation machinery.

In plants, five distinct classes of photoreceptors, which can act redundantly, synergistically or antagonistically depending on the particular signalling pathway, perceive light signals (Chen et al., 2004; Franklin et al 2005). The three main families of photoreceptors are the red (R) and far-red (FR) light-absorbing phytochromes (phyA-phyE) (Sharrock and Quail, 1989; Clack et al., 1994) and the UV-A/blue light-absorbing cryptochromes (cry1-cry3) and phototropins (phot1 and phot2) (Lin, 2002; Chen et al., 2004). Additionally, zeitlupe (ztl)/ flavin-binding, kelch repeat, f-box1 (fkf1)/ lov-kelch protein2 (lkp2) perceive blue light and are involved in regulation of the circadian clock and flowering time control (Somers et al., 2004; Imaizumi et al., 2003; Schultz et al., 2001). Furthermore, UV-B light signals are mediated by the *UV RESISTANCE LOCUS 8 (UVR8)* pathway, in which the photoreceptor itself has not been identified yet (Favory et al., 2009) (Figure 1).

Phototropins contain a photosensory N-terminal part including two flavin mononucleotide (FMN) chromophore-binding LOV domains and a C-terminal serine/threonine kinase (Jiao et al., 2007) Phototropins are important for phototropism, chloroplast movement and stomatal opening (Briggs and Christie, 2002; Chen et al., 2004). In these processes phot1 is specialized for low blue light fluence rates, while phot2 is more important for high light responses (Liscum and Briggs, 1995; Sakai et al., 2000; 2001).

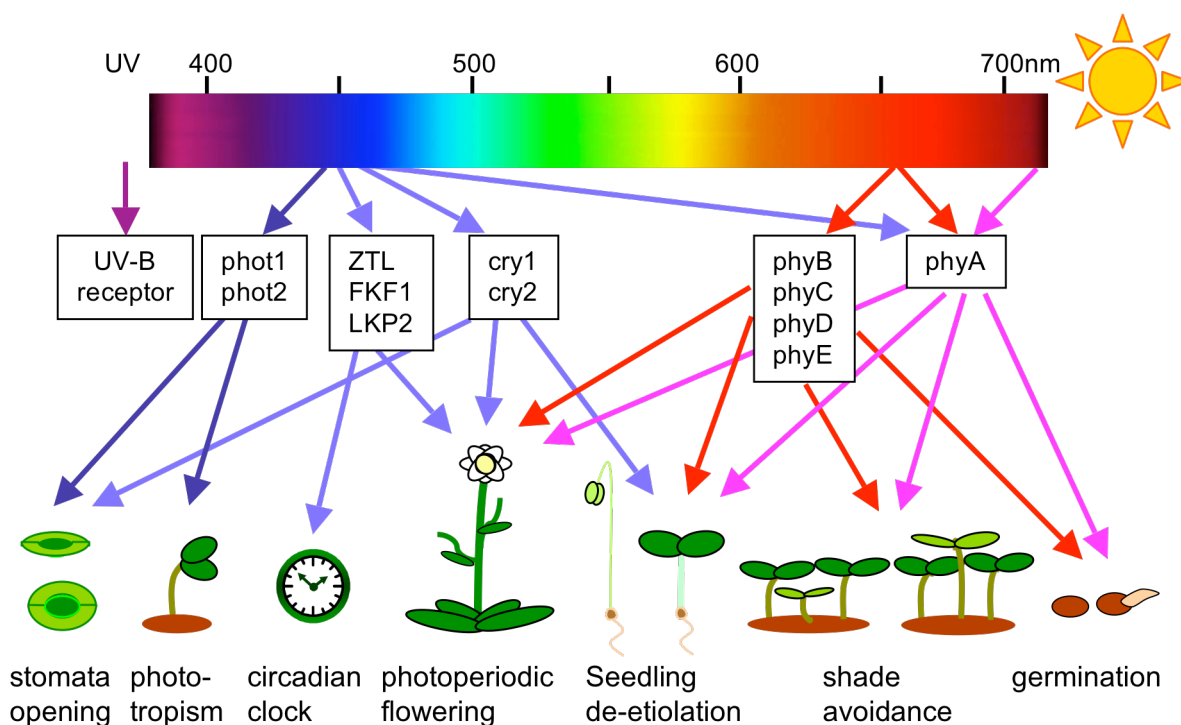


Figure 1. Light-dependent plant development is mediated by photoreceptors.

Distinct classes of photoreceptors perceive light signals of specific wave lengths, respectively and act synergistically or antagonistically to control various developmental processes. Phototropins, cryptochromes and the zeitlupe protein family mediate B and UV-A responses. Phytochromes B-E perceive R and phyA responds to B, FR and R. Phototropins regulate stomata opening and phototropism. The zeitlupe protein family is involved in circadian clock- and flowering time control. Cryptochromes control seedling de-etiolation, stomata opening and photoperiodic flowering. Phytochromes regulate germination, seedling de-etiolation, shade-avoidance responses and photoperiodic flowering.

Cryptochromes are photolyase-derived flavoproteins with an N-terminal PHR (photolyase-homology region) domain for chromophore (FAD and Pterin) binding and a C-terminal putative signalling DAS (CCT) domain, which is not yet fully characterized, but known to be important for blue light signalling in cry1 (Ahmad et al., 1995; Cashmore et al., 1999; Lin, 2002). cry1 is relatively light-stable and can be localized in the nucleus as well as in the cytoplasm, whereas cry2 is constitutively localized in the nucleus and is rapidly degraded in blue light (Guo et al., 1999; Yang et al., 2000; Lin et al., 1998; Wu and Spalding, 2007; Yu et al., 2007). cry1 is involved in seedling de-etiolation at higher fluence rates of blue light, while cry2 acts in response to low light intensities (Ahmad and Cashmore, 1993; Ahmad et al., 1998a; Lin et al., 1998). Furthermore, cry2 has a predominant role in the regulation of photoperiodic flowering time (Guo et al., 1998; Mockler et al., 2003; Liu et al., 2008).

In *Arabidopsis thaliana*, five genes (*PHYA-PHYE*) encoding phytochromes have been identified and characterized (Sharrock and Quail, 1989; Clack et al., 1994). Phytochromes are dimers with an N-terminal photosensory domain that covalently binds a single bilin chromophore and a C-terminal part containing several motifs for dimerization, protein-protein interaction, light-dependent nuclear localization and a histidin kinase-like domain (Neff et al., 2000; Jiao et al., 2007). Phytochromes are synthesized in the dark in a biologically inactive red light (R) absorbing Pr form and R perception leads to their activation via conversion to the biologically active far-red light (FR) absorbing Pfr form (Quail, 2002). Upon activation, the Pfr form translocates to the nucleus and phytochrome signalling is initiated (Sakamoto and Nagatani, 1996; Nagatani, 2004; Kircher et al., 1999; 2002). After absorption of FR, the Pfr form of phytochrome is converted back to the inactive Pr form (Rockwell et al., 2006). This reversible system of photoconversion leads to a dynamic photoequilibrium of Pr and Pfr in natural light conditions (Franklin and Quail, 2010). In contrast to the other phytochromes, the Pfr form of PhyA is rapidly degraded in response to light and controls the Very-Low-Fluence-Responses (VLFR) and far-red High-Irradiance-Responses (FR-HIR) (Neff et al., 2000; Kevei et al., 2007). The phytochromes PhyB-E are relatively light-stable in their Pfr form and mediate Low-Fluence-Responses (LFR) and red light High-Irradiance-Responses (R-HIR) (Neff et al., 2000; Kevei et al., 2007). However, recent studies revealed that also the relatively light-stable photoreceptor phyB is degraded in the nucleus, a process, which provides a mechanism for desensitization of the photoreceptor and for signal termination (Jang et al., 2010). All five phytochromes contribute to seed germination; seedling de-etiolation is regulated by phyA in FRc and B, whereas phyB plays a major role in R and W and cry1 and cry2 control seedling photomorphogenesis in B and UV-A (Jiao et al., 2007; Franklin and Quail, 2010). Photoreceptor action is also crucial for adult plant development. When growing in close proximity to other vegetation, plants perceive light with a reduced R:FR ratio which initiates a shade avoidance response. This process is characterized by enhanced elongation growth, reduced leaf growth, elongation of stems and petioles and increased apical dominance (Franklin and Quail, 2010). Shade avoidance is mediated mainly by phyB since *phyB* mutants exhibit an extreme constitutive shade avoidance phenotype (Somers et al., 1991). Also during transition from vegetative to reproductive development photoreceptors are important since plants need to monitor day length (photoperiod) to adjust their

development appropriately to seasonal changes (Jiao et al., 2007). *Arabidopsis thaliana* is a facultative long-day plant, which means that it flowers early in long days but also - yet much later - under short day conditions (Coupland et al., 1998). The transcription factor CONSTANS (CO) plays a central role in the photoperiodic induction of flowering in LD (Putterill et al., 1995). CO activates the transcription of the floral inducer *FLOWERING LOCUS T* (*FT*) in the leaf, subsequently the FT protein moves through the phloem to the shoot apical meristem (SAM) (An et al., 2004; Corbesier et al., 2007; Lin et al., 2007a; Mathieu et al., 2007; Turck et al., 2008). At the SAM FT interacts with the bZIP transcription factor *FLOWERING LOCUS D* (*FD*) and the FT/FD heterodimer induces flowering by activating floral meristem identity genes like *APETALA1* (*AP1*) and further floral promoters like *SUPPRESSOR OF OVEREXPRESSION OF CONSTANS 1* (*SOC1*) (Abe et al., 2005; Wigge et al., 2005; Yoo et al., 2005; Turck et al., 2008; Amasino, 2010). CO mRNA levels are controlled by the circadian clock and exhibit highest abundance in the afternoon, which coincides with light exposure under long-day conditions, therefore flowering can be induced (Suarez-Lopez et al., 2001; Yanovsky and Kay, 2002). CO protein levels are regulated on the post-transcriptional level in a light-dependent manner (Valverde et al., 2004; Turck et al., 2008). In short days CO is expressed in the dark, which leads to the poly-ubiquitination and subsequent degradation of the transcription factor via the 26S proteasome (Valverde et al., 2004; Laubinger et al., 2006, Jang et al., 2008). In this developmental switch phyA, cry2 and phyB possess antagonistic roles. phyA and cry2 stabilize the transcription factor CO in the light and thereby promote flowering in long days, while phyB promotes CO degradation and thus acts as a repressor of flowering (Guo et al., 1998; Mockler et al., 1999; 2003; Valverde et al., 2004).

Downstream of the photoreceptors, light signal transduction is mediated via highly complex transcriptional regulatory networks, which coordinate activation and repression of specific downstream genes (Jiao et al., 2007). In *Arabidopsis*, more than 20% of the genes are light-regulated e.g. by various transcription factors that bind to their cis-regulatory elements (LIGHT RESPONSIVE ELEMENTS, LREs) (Ma et al., 2001; Tepperman et al., 2001). Some of these transcription factors are specific for distinct light qualities, while others have a more general role as they respond to various light conditions (Jiao et al., 2007). Many components involved in light signal

transduction were identified by classical genetic approaches using phenotypic screens for mutants, which are defective in skoto- or photomorphogenesis. Dark-grown wild-type seedlings exhibit a long hypocotyl, closed cotyledons and a closed apical hook. Light exposure induces the inhibition of hypocotyl elongation, opening of the apical hook, expansion of cotyledons and synthesis of chlorophyll (Figure 2). Mutants of factors that act positively on light signal transduction show a reduced light response, whereas mutants of light-signalling repressors display an enhanced light response or constitutive photomorphogenesis even in darkness.

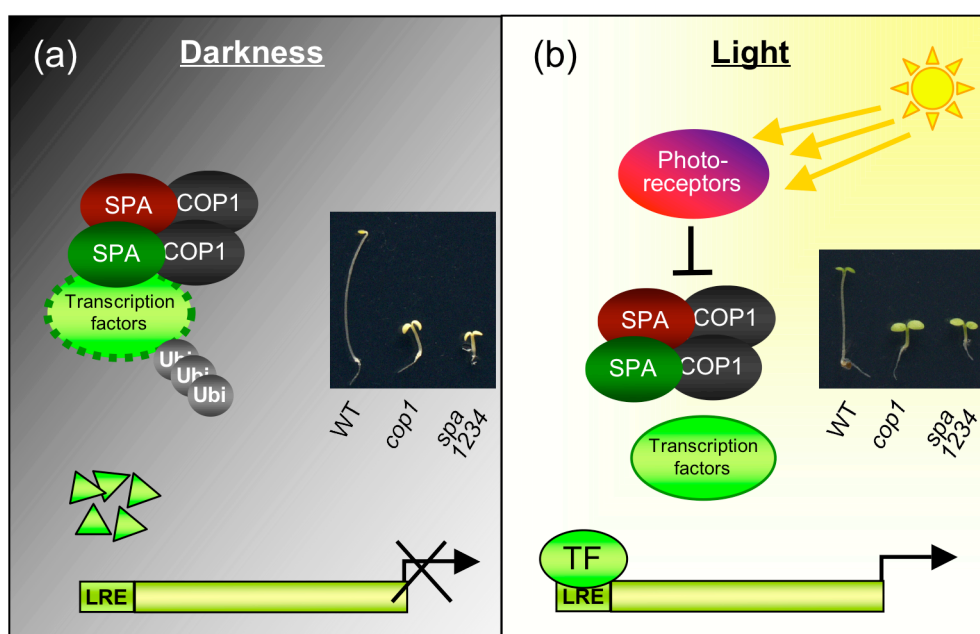


Figure 2. The COP1/SPA complex acts as a repressor of photomorphogenesis.

(a) In darkness, the COP1/SPA complex targets photomorphogenesis promoting transcription factors for degradation by ubiquitination. Therefore wild-type seedlings exhibit a long hypocotyl and closed cotyledons, whereas *cop1* and *spa* quadruple mutants exhibit a constitutive photomorphogenesis phenotype.

(b) Upon light perception by photoreceptors most of COP1/SPA activity is inhibited. Therefore transcriptional activators are active and by binding to Light Responsive Elements of light-induced genes gene expression is induced and thereby photomorphogenesis is promoted. In wild-type seedlings hypocotyl elongation is inhibited, cotyledons expand and chlorophyll is produced. Light-grown *cop1* and *spa* quadruple mutants show an enhanced photomorphogenic phenotype. (Photographs taken from Hoecker, 2005)

The MYB transcription factor LONG AFTER FAR-RED (LAF1) is a positive regulator of gene expression downstream of FR (Ballestros et al., 2001). *LONG HYPOCOTYL IN FAR-RED (HFR1)* encodes a bHLH transcription factor and is involved in positive regulation of FR and B responses like seedling development and shade avoidance responses (Fairchild et al., 2000; Duek and Fankhauser, 2003; Sessa et al., 2005).

Mutant analyses showed that the bZIP transcription factor LONG HYPOCOTYL 5 (HY5) acts in all light conditions to promote various aspects of light-induced seedling development, like the inhibition of hypocotyl elongation or accumulation of anthocyanins (Oyama et al., 1997; Chattopadhyay et al., 1998; Ulm et al., 2004). HY5 binds directly to G-box DNA sequences of LREs of its target genes and analysis of HY5 genomic binding sites identified >3000 in vivo targets in the *A. thaliana* genome, most of them light-responsive genes and transcription factor genes; suggesting HY5 to be a high hierarchical regulator of the transcription cascades that promote photomorphogenesis (Chattopadhyay et al., 1998; Lee et al., 2007). HY5 furthermore integrates light- and phytohormone signalling, including GA, auxin, cytokinin and ABA (Lau and Deng, 2010; Cluis et al., 2004; Sibout et al., 2006; Vandenbussche et al., 2007; Alabadi et al., 2008; Chen et al., 2008). *HY5 HOMOLOG (HYH)* is mainly required in B-dependent seedling development (Holm et al., 2002). The B-box containing proteins SALT TOLERANCE HOMOLOG 2 (STH2/BBX21) and STH3/LZF1/BBX22 have been shown to act as positive regulators of seedling de-etiolation (Datta et al., 2007; 2008). Moreover, recent studies revealed that both proteins are involved in the regulation of shade avoidance (Crocco et al., 2010). Important negative regulators of light signal transduction are the bHLH transcription factors PHYTOCHROME-INTERACTING FACTORS (PIFs), which act to repress seed germination in darkness and promote seedling skotomorphogenesis as well as shade-avoidance (Leivar and Quail, 2011).

One mechanism of photoreceptor-mediated light signal transduction is direct binding of the photoreceptors to transcription factors to activate or repress gene expression. *cry2* was shown to interact with the bHLH transcription factor CIB1 (CRYPTOCHROME-INTERACTING-BASIC-HELIX-LOOP-HELIX 1) in a blue-light dependent manner to promote *cry2*-dependent floral transition (Liu et al., 2008). Also phytochromes were shown to regulate transcription factors directly. Upon R perception and nuclear import of the active Pfr form of the photoreceptor, phytochromes physically interact with the PIF proteins (Duek and Fankhauser, 2005; Monte et al., 2007). The phy-PIF interaction leads to phosphorylation, ubiquitination and degradation of the transcription factors via the 26S proteasome (Bauer et al., 2004; Shen et al., 2005; 2007; Al-Sady et al., 2006). Light-induced degradation of the PIF proteins is necessary for light responses and enables plants to alter gene

expression rapidly in response to light (Franklin and Quail, 2010). In contrast, under long-term R exposure the interaction between phytochromes and PIF proteins leads to the degradation of phyB, providing a negative feedback loop to modulate light signal transduction (Al-Sady et al., 2008; Jang et al., 2010).

However, most transcription factors such as LAF1, HFR1 or HY5 do not directly interact with photoreceptors. The regulation of light signal transduction mediated by these transcriptional activators involves light-dependent post-translational modifications and subsequent degradation or stabilization of the transcription factors (Figure 2). It is known that LAF1, HFR1 and HY5 are targets of the E3 ubiquitin ligase CONSTITUTIVELY PHOTOMORPHOGENIC 1 (COP1), which acts in concert with other proteins, like the SUPPRESSOR OF PHYTOCHROME A-105 (SPA) proteins to target the positively acting transcription factors for degradation via the 26S proteasome in darkness (Seo et al., 2003; Duek et al., 2004; Jang et al., 2005; Yang et al., 2005b; Osterlund et al., 2000b). Also the light-labile photoreceptors phyA and cry2 have been shown to be targets of COP1 (Seo et al., 2004; Wang et al., 2001; Shalitin et al., 2002).

1.2. Repressors of photomorphogenesis: the COP1/SPA complex

COP1 belongs to a group of 11 *COP/DE-ETIOLATED/FUSCA* (*COP/DET/FUS*) genes that were identified in phenotypic screens for mutants displaying a constitutive photomorphogenic phenotype in darkness (Chory et al., 1989b; 1991; Deng et al., 1991). Furthermore, *cop/det/fus* mutants display elevated protein levels of transcription factors like HY5 and HFR1, which positively regulate light signal transduction (Osterlund et al., 2000a; 2000b; Sajio et al., 2003; Duek et al., 2004; Jang et al., 2005; Yang et al., 2005b). Thereby *COP/DET/FUS* proteins were identified as negative regulators of photomorphogenesis (Hoecker, 2005).

COP/DET/FUS members as well as CULLIN 4 (CUL4) and DAMAGED DNA-BINDING PROTEIN 1 (DDB1) are highly conserved also in animals. In humans for example, hCOP1 act together with hDDB1 and hDET1 in a CUL4-based E3 ligase to mediate the ubiquitination and subsequent degradation of the transcription factor c-Jun (Wertz et al., 2004). In this type of E3 ubiquitin ligase CULLIN4 is the scaffold protein and DDB1 serves as linker to multiple WD40 proteins, which act as substrate

receptors and are referred to as DDB1-CUL4-associated factors (DCAFs) (Jackson and Xiong, 2009).

To date there are three different complex formations known in Arabidopsis, which include members of the COP/DET/FUS protein family. These complexes are involved in the negative regulation of various light signalling responses but also contribute to DNA damage repair, cell cycle control and other developmental processes (Zhu et al., 2008; Chen et al., 2006; 2010; Schwechheimer and Isono, 2010; Biedermann and Hellmann, 2011). The COP9 signalosome (CSN) is an eight-subunit protein complex in Arabidopsis (Wei et al., 1994) and regulates the activity of CULLIN-based E3 ubiquitin ligase complexes by de-neddylation of the CULLIN subunit (Lyapina et al., 2001; Schwechheimer et al., 2001; Wei et al., 2008; Schwechheimer and Isono, 2010). The CDD complex, consisting of COP10, DDB1a and DET1 (Yanagawa et al., 2004), was found to associate with CUL4 and RING-BOX 1 (RBX1) in a high molecular complex to repress photomorphogenesis and flowering, but also other developmental processes in Arabidopsis (Bernhardt et al., 2006; Chen et al., 2006; 2010). The third group are the tetrameric COP1/SPA complexes, likely consisting of a COP1 homo-dimer and a variable combination of two SPA molecules, which are thought to act in a CUL4 complex as well (Zhu et al., 2008; Chen et al., 2010). All three complexes are thought to function in concert in the ubiquitination and subsequent degradation of photomorphogenesis-promoting transcription factors via the 26S proteasome (Yanagawa et al., 2004; Chen et al., 2006; 2010). However, the exact coordination between these complexes is not known.

The E3 ubiquitin ligase COP1 was shown to be a key regulator of photomorphogenesis, which is predominantly active in darkness (Osterlund et al., 1999; Ma et al., 2002). The COP1 protein contains a C-terminal WD-repeat domain, a coiled-coil motif and an N-terminal RING domain (Deng et al., 1992, Yi and Deng, 2005) (Figure 3). How COP1 activity is regulated by light is mainly unknown. COP1 has been shown to be nuclear-localized in darkness and thereby can act as repressor of light signal transduction, whereas in the light COP1 is predominantly localized in the cytoplasm (von Arnim and Deng, 1994; von Arnim et al., 1997; Subramanian et al., 2004). Since this mechanism is very slow (von Arnim et al., 1997) it cannot explain the rapid accumulation of certain COP1-targeted transcription factors like HFR1 or LAF1 after two hours of light treatment (Duek et al., 2004; Jang

et al., 2007) as well as the massive change in gene expression, which occurs quickly upon light perception (Tepperman et al., 2001; Ma et al., 2001). The direct interaction of COP1 with the photoreceptors cry1, cry2, phyA and phyB might suppress COP1 activity in the light (Yang et al., 2001; Wang et al., 2001; Seo et al., 2004). Nevertheless, also in light, residual nuclear COP1 is active to prevent an over-stimulation of the plant by light, since light-grown *cop1* mutant seedlings exhibit an increased response to light (McNellis et al., 1994a; von Arnim and Deng, 1994). On the other hand, COP1 is involved in the light-induced degradation of the light-labile photoreceptors phyA and cry2 as well as phyB, suggesting a negative feedback regulation (Seo et al., 2004; Shalitin et al., 2002; Jang et al., 2010). An alternative mechanism to regulate COP1 activity could be a light-induced conformational change or re-arrangement of the different COP complexes upon post-translational modifications of various compounds of these complexes.

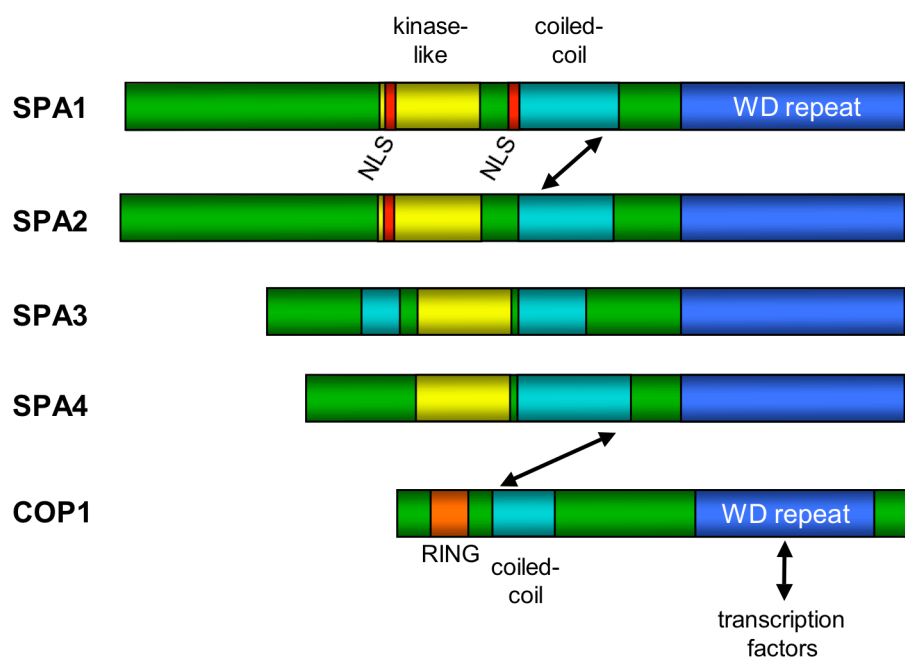


Figure 3. Domain structure of the SPA proteins and COP1.

All SPA proteins and COP1 contain a C-terminal WD-repeat domain that provides interaction with their substrates and at least one coiled-coil domain that allows SPA-SPA homo- or hetero-dimerization and COP1-COP1 dimerization as well as COP1-SPA interaction. SPA proteins exhibit an N-terminal kinase-like domain of unknown function and SPA1 and SPA2 contain nuclear localization sequences (NLS). COP1 contains an N-terminal RING-finger motive typical for a subclass of E3 ubiquitin ligases. Arrows indicate protein-protein interaction.

1.3. The SPA proteins and their function in light-regulated plant development

In Arabidopsis, there are four SPA proteins present (SPA1-SPA4) of which SPA1 was first identified as a suppressor of a weak *phyA* mutation (Hoecker et al., 1998). All members of the SPA protein family share a similar domain structure, consisting of a C-terminal WD repeat domain, a coiled-coil motif, and an N-terminal kinase-like domain (Hoecker et al., 1999; Laubinger and Hoecker, 2003; Laubinger et al., 2004; Zhu et al., 2008) (Figure 3). The SPA proteins exhibit highest sequence similarity to COP1 within the WD-repeat domain, which is essential for protein-protein interaction with transcription factors like HY5 or HFR1 (Hoecker et al., 1999; Saijo et al., 2003; Yang et al., 2005a). Furthermore, all SPAs have been shown to physically interact with each other and COP1 via their respective coiled-coil domains (Hoecker and Quail, 2001; Laubinger and Hoecker 2003; Saijo et al., 2003; Laubinger et al., 2004). The function of the SPA N-terminus and its kinase-like domain has not been identified yet. Based on their sequence similarity, the SPA proteins can be divided into two sub-groups. SPA1 and SPA2, in contrast to SPA3 and SPA4, contain a longer N-terminal extension and nuclear localization sequences (NLS) (Hoecker et al., 1999; Laubinger and Hoecker, 2003; Laubinger et al., 2004) (Figure 3). SPA1 and SPA2 are constitutively localized in the nucleus and produce nuclear speckles (Hoecker et al., 1999; Laubinger et al., 2004; Zhu et al., 2008). In comparison, SPA4 is cytoplasmic- as well as nuclear-localized but only forms nuclear speckles when it is coexpressed with SPA1, indicating that SPA1 can recruit SPA4 into nuclear speckles (Hoecker et al., 1999; Laubinger et al., 2004; Zhu et al., 2008).

A *spa* quadruple mutant exhibits a similar constitutive photomorphogenic seedling phenotype like a weak *cop1* mutant allele (Deng et al., 1991; Laubinger et al., 2004). Analyses of several *spa* double and triple mutant combinations revealed that the SPA proteins have partially redundant as well as distinct functions in various stages of plant development (Laubinger and Hoecker, 2003; Laubinger et al., 2004; Laubinger et al., 2006; Fittinghoff et al., 2006; Balcerowicz et al., 2010) (Figure 4). *SPA1* and *SPA2* are both sufficient to suppress seedling photomorphogenesis in darkness, whereas in light-grown seedlings *SPA1* is the most important regulator and acts in concert with *SPA3* and *SPA4* to repress hypocotyl elongation (Laubinger et al., 2004; Fittinghoff et al., 2006). Recent studies showed that the COP1/SPA complex acts as a repressor of stomata development and epidermal cell differentiation in darkness,

since in contrast to wild-type seedlings, *cop1* as well as *spa* multiple mutants constitutively produced stomata and fully differentiated epidermal pavement cells in dark-grown seedlings (Kang et al., 2009; Ranjan et al., 2011).

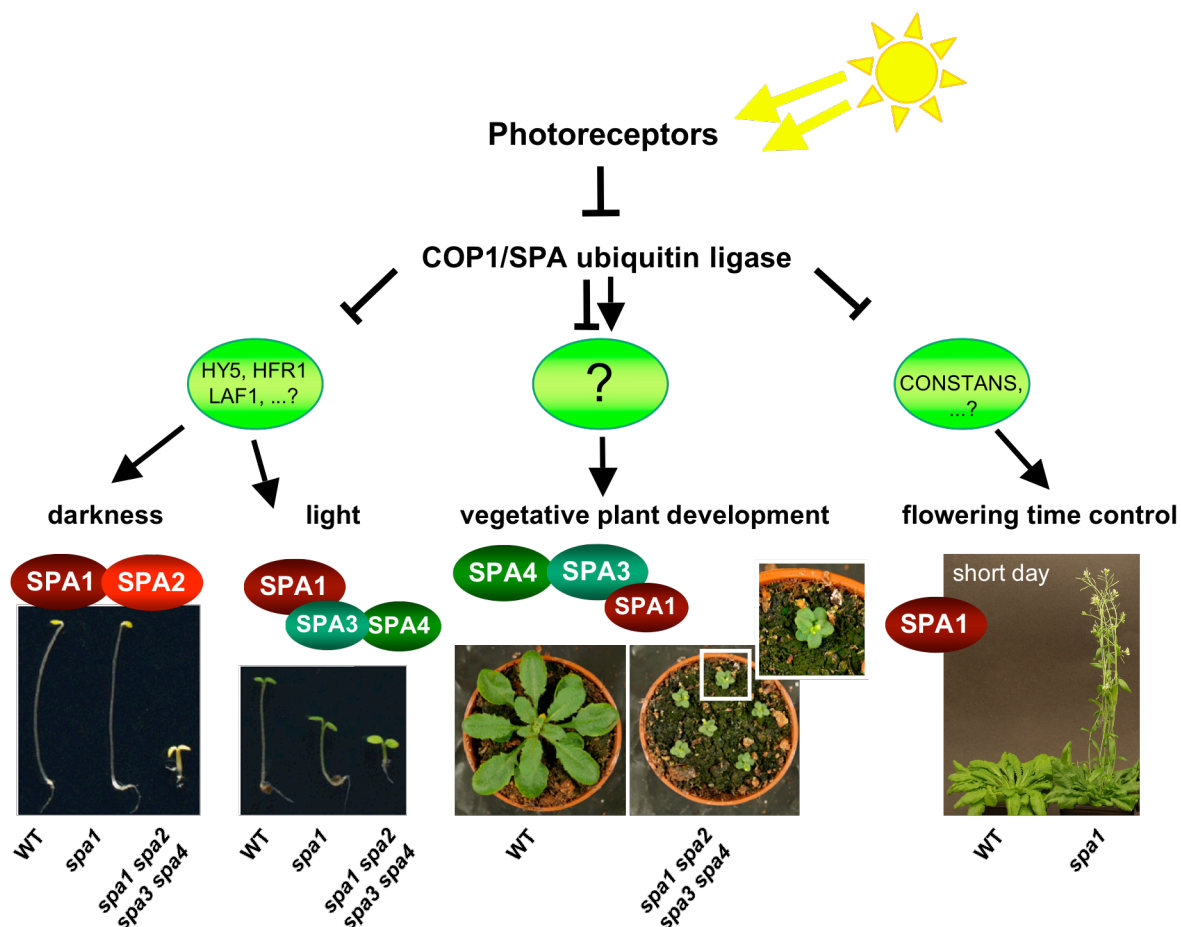


Figure 4. SPA proteins have overlapping but also distinct functions in Arabidopsis development.

The COP1/SPA complex represses light signal transduction by targeting positively acting transcription factors for degradation.

SPA1 and SPA2 are sufficient for seedling development in darkness, whereas SPA1 acts in concert with SPA3 and SPA4 to regulate seedling development in response to light. The transcription factors HFR1, LAF1 and HY5 are COP1/SPA targets in seedling stage.

SPA3 and SPA4 are the predominant regulators of vegetative plant growth. In this developmental stage the target transcription factors are not known yet.

SPA1 is necessary and sufficient to suppress early flowering in non-inductive SD by promoting the degradation of the floral inducer CO. (Photographs taken from Hoecker, 2005; Laubinger et al., 2006)

Additionally, SPA proteins and COP1 control the photoperiodic induction of flowering in Arabidopsis, since *cop1* as well as *spa* mutants display an early-flowering phenotype under non-inductive short-day conditions and COP1 as well as SPA1 are known to target the transcriptional activator CO for degradation in darkness (Laubinger et al., 2006; Jang et al., 2008; Liu et al., 2008). Furthermore, the SPA

proteins and COP1 are also involved in vegetative plant development. A *spa* quadruple mutant plant exhibits an extremely dwarfed phenotype, similar to a strong *cop* mutant (McNellis et al., 1994a; Laubinger et al., 2004). Analyses of various *spa* triple mutants revealed that in the regulation of leaf size *SPA2* has nearly no function, whereas *SPA3* and *SPA4* play a major role and also *SPA1* contributes to leaf growth (Laubinger et al., 2004; Fittinghoff et al., 2006). For *SPA1* it was shown that it regulates leaf-growth control non-cell-autonomously in the phloem as well as in mesophyll cells (Ranjan et al., 2011). However, the targets of the COP1/*SPA* complex in *SPA*-regulated leaf growth control have not been identified yet (Figure 4).

Analyses of transgenic *spa1* mutants expressing various deletion derivatives of *SPA1* showed that the deletion of either its coiled-coil domain or its WD-repeat domain failed to rescue the *spa1* mutant phenotype of FRc grown seedlings, suggesting that both domains are essential for *SPA1* function (Fittinghoff et al., 2006; Yang and Wang, 2006). In contrast, *SPA1* function in seedling de-etiolation was not impaired when the kinase-like domain or the complete N-terminus of *SPA1* were deleted (Yang and Wang, 2006; Fittinghoff et al., 2006). In contrast, the *SPA1* N-terminus and the kinase-like domain are essential for *SPA1* function in photoperiodic flowering time control, as transgenic *spa1* mutants expressing *SPA1-ΔNT* or *SPA1-Δkin* deletion derivatives failed to rescue the early flowering phenotype of *spa1* mutants in short days (Fittinghoff, PhD thesis, 2008). In addition, the *SPA1* N-terminus seems to be involved in the regulation of *SPA1* stability and/or accumulation, since truncated *SPA1* protein accumulates to much higher levels than the full-length protein in FRc grown seedlings and adult plants (Yang and Wang, 2006; Fittinghoff et al., 2006; Fittinghoff, PhD thesis, 2008). Furthermore, it was shown that *SPA1* and *SPA2* protein levels are increased in a *cop1* mutant background, suggesting that *SPA* protein stability is at least in part dependent on COP1 (Yang and Wang, 2006; Zhu et al., 2008; Alexander Maier, unpublished).

Taken together, COP1/*SPA* complexes are important and possibly essential factors of light-regulated plant development even beyond seedling photomorphogenesis. However, the molecular basis of the distinct function of the *SPA* proteins, their individual function within the COP1/*SPA* complex as well as the regulation of the complex itself are unknown so far.

1.4. Arabidopsis leaf growth and development

In plants, new lateral organs like leaves develop from the shoot apical meristem (SAM) through a strictly coordinated combination of cell proliferation, cell differentiation and cell growth and expansion. As a result, final leaf size and shape within a particular plant species are quite uniform, when grown under comparable conditions (Krizek, 2009). In animals, total organ/body size is regulated mainly by intrinsic cues and “total mass control”, where altering the cell number and/or size usually does not affect the overall size or shape of organs (Potter and Xu, 2001). Furthermore, cell numbers in organs are additionally adjusted by apoptosis in animals, which does not occur in plant cell number control (Tsukaya, 2006; Conlon and Raff, 1999). In plants, organ morphogenesis and growth are in part controlled by genetic factors and phytohormones. But in contrast to animals, plant morphology is also highly dependent on environmental signals like nutrient and water availability, temperature as well as light quality and quantity (Bögre et al., 2008). The different endogenous and exogenous pathways build a complex signalling network to control final leaf size. Leaf growth is also regulated spatio-temporally. Cell proliferation is active throughout the developing leaf primordium, but decreases from the distal to the proximal region of the young leaf blade (Donnelly et al., 1999). Subsequent cell growth via increase in cytoplasmatic macromolecular mass and nuclear size as well as cell expansion by increasing cell volume through vacuolation, contribute to overall leaf size in plants (Sugimoto-Shirasu and Roberts, 2003; Fleming, 2006) (Figure 5). The period of cell proliferation has to be regulated to guarantee proper final leaf size. Mutations causing a premature arrest of cell proliferation result in decrease of organ size as seen in *klu* mutants. *KLUH* (*KLU*) encodes the cytochrome P450 monooxygenase CYP78A5, which promotes organ growth non-cell autonomously, since *KLU* expression is not strictly correlated with proliferating regions (Anastasiou et al., 2007). Organ size also involves protein degradation of growth promoting factors, as for instance the E3 ubiquitin ligase *BIG BROTHER* (*BB*) acts to restrict the period of cell proliferation within developing organs (Disch et al., 2006). The period of growth is also controlled by the growth restricting *DA1* and *DAR1*, which encode ubiquitin receptors (Li et al., 2008). Increase of organ size in *da1* mutants is due to an extended period of growth and not by alteration of cell size (Li et al., 2008). Various phenotypic screens in *Arabidopsis* for individuals exhibiting altered leaf size identified mutants, which can be classified in different groups according to their

changes (increase or decrease) in cell number and/or cell size (Berná et al., 1999; Pérez-Pérez et al., 2002; Horiguchi et al 2006a; 2006b). Most leaf size mutants have small leaves, due to decrease in both cell number and cell size (Horiguchi et al 2006a; 2006b). Some leaf size mutants are involved specifically in the directional control of cell growth or proliferation. *ANGUSTIFOLIA* is involved in polar cell elongation in leaf-width direction, whereas *ROTUNDIFOLIA 3* controls polarized cell growth along longitudinal direction (Tsuge et al., 1996). Cell proliferation along leaf-width axes is regulated by *AN3*, whereas *ROT4* controls cell number in leaf-length direction (Kim and Kende, 2004; Narita et al., 2004; Tsukaya, 2006).

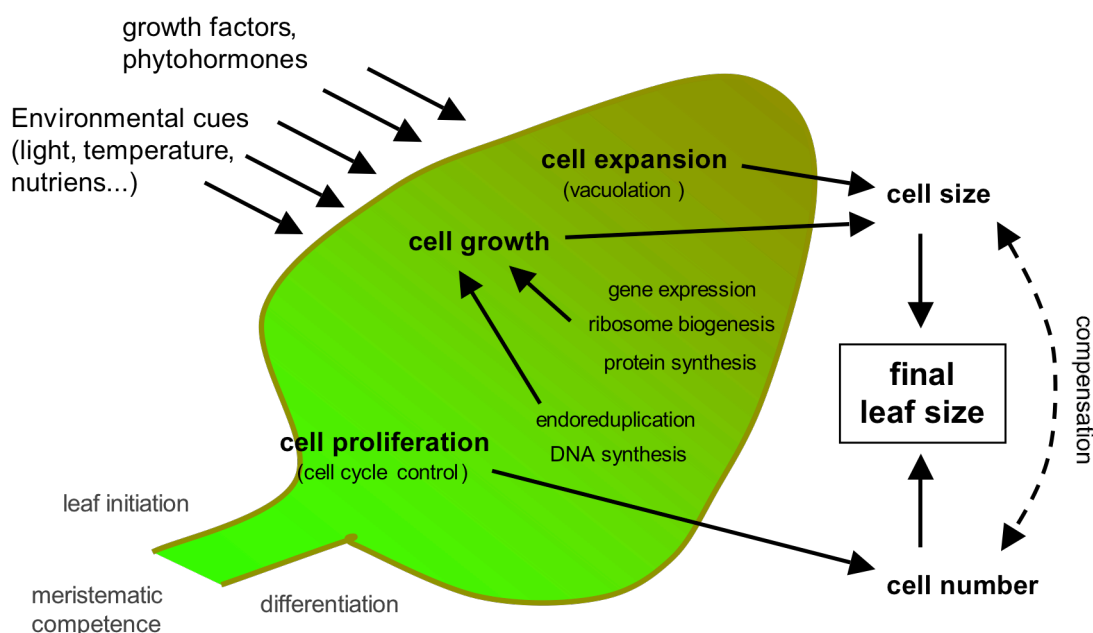


Figure 5. Pathways controlling final leaf size.

A simple schematic model for the regulation of leaf size. Intrinsic and environmental signals affect leaf size on the level of cell proliferation as well as cell growth (via increase in macromolecular mass) and cell expansion (via vacuolation-mediated increase of volume). Cell proliferation and cell expansion have suggested to be coordinated organ-wide as e.g. decrease in cell number can lead to increased cell size (compensation).

Defects in phytohormone perception or signalling often cause dwarfism, which can be related to cell proliferation and/or cell growth or cell differentiation control. Auxin promotes the extension period of cell proliferation via the transcription factor *AUXIN-RELATED GENE INVOLVED IN ORGAN SIZE (ARGOS)* which is an auxin-induced gene and acts upstream of *AINTEGUMENTA (ANT)*, a transcription factor that activates the cell-cycle driver *cyclin D3;1* (Krizek, 1999; Mizukami et al., 2000; Hu et al., 2003). But Auxin also contributes to cell elongation as *AUXIN BINDING*

PROTEIN 1 (ABP1) was shown to be important for coordination of cell division and cell expansion (Braun et al., 2008). Cytokinins (CKs) are important for cell division and stem cell maintenance (Werner and Schmülling, 2009). Moreover, CK signalling interconnects with light signalling, as the CK-induced ARABIDOPSIS RESPONSE REGULATOR 4 (ARR4) protein interacts with phyB and stabilizes the active Pfr form of the photoreceptor (Sweere et al., 2001). Moreover, *hy5* mutants show a reduced cytokinin response and cytokinin increases HY5 stability, suggesting HY5 to be a point of convergence between light signalling and cytokinin pathways (Vandenbussche et al., 2007). During shade avoidance, upregulation of the cytokinin-degradation gene CKX6 leads to a local decrease in CK and growth arrest of the leaf blade (Carabelli et al., 2007). Gibberellins (GAs) are mainly involved in leaf expansion (Fleet and Sun, 2005). GAs promote growth by initiating the proteolysis of the transcriptional repressing DELLA proteins. Upon perception of GA via the GID1 receptor and subsequent GID-DELLA interaction the latter are targeted for degradation by the E3 ubiquitin ligase SCF^{SLY1} (Schwechheimer and Willige, 2009). Recently, phenotypic analyses of *ga insensitive (gai) repressor of ga1 (rga) rga-like1 (rgl1) rgl2* della quadruple mutants and the F-box mutant *sleepy 1 (sly1)* in which DELLA degradation is inhibited showed that GA controls cell expansion as well as cell proliferation (Achard et al., 2009). DELLAs also have been shown to be involved in stress-induced growth modulation, involving abscisic acid (ABA) and ethylene-mediated reduction of GA levels (Achard et al., 2006). Mutants of brassinosteroid (BR) biosynthesis and signalling develop smaller organs mainly due to a defect in cell expansion (Clouse and Sasse, 1998; Szekeres et al., 1996; Bishop and Koncz, 2002). Although in the dwarfed mutant *det2*, which is defective in BR biosynthesis, fewer and smaller leaf cells compared to wild type have been observed (Nakaya et al., 2002).

GROWTH REGULATING FACTOR (GRF) genes encode transcription factors that interact with GRF INTERACTING FACTORS (GIFs) control leaf size by regulation of cell proliferation (Kim et al., 2003; Kim and Kende, 2004; Horiguchi et al., 2005; Lee et al., 2009). Some mutants, which are defective in cell proliferation, such as *gif1/angustifolia3 (an3)* are able to compensate this defect at least partially by so called “cell enlargement compensation” (Horiguchi et al., 2005). Conversely, in tobacco (*Nicotiana tabacum*) leaves overexpression of *ABP1* induces cell

enlargement with a compensating decrease in cell number (Jones et al., 1998). This suggests the existence of an organ-size checkpoint that controls cell size and cell number in developing organs. Plants can achieve immense cell enlargement by increasing their ploidy level through successive rounds of DNA replication (endoreduplication) and DNA content often correlates with cell size (Sugimoto-Shirasu and Roberts, 2003).

Light is an important environmental factor to affect plant morphology. As mentioned before, shade causes inhibition of leaf blade expansion and enhanced petiole elongation, which is mainly due to changes in cell expansion (Kozuka et al., 2005; Cookson and Granier, 2006). Daylength affects leaf expansion since leaf expansion is decreased by short days, whereas duration of leaf expansion is increased (Cookson et al., 2007). In addition, light has been shown to directly impact phytohormone levels in organs and thereby enables the plant to adjust growth to changing environments (Wolters and Jürgens, 2009).

Comparative analyses of genes that enhance leaf size revealed that multiple pathways control organ growth in a largely independent manner by affecting hormone, metabolite as well as transcript levels (Gonzalez et al., 2010). Additionally, final leaf size is organized from different tissue layers, such as epidermis, sub-epidermis, phloem and mesophyll cells (Savaldi-Goldstein et al., 2007; Bai et al., 2010; Ranjan et al., 2011). These findings suggest that leaf size (and shape) regulation is object of a highly complex molecular network.

Altogether, plant (organ) growth is based on spatially as well as temporally organized control of cell proliferation, differentiation and enlargement. Most pathways controlling organ size, whether based on intrinsic or external signals, are closely linked to each other and act in coordination to determine proper organ size. Nevertheless, there are still many open questions on how information from these different pathways are integrated in the genetic and molecular control of leaf size and shape.

Weak *cop1* mutants as well as *spa* quadruple mutants display an extremely dwarfed phenotype, indicating that the COP1/SPA complex is involved in the regulation of plant size in *Arabidopsis thaliana*. The cause for the reduced plant size of *cop1* and *spa* mutants as well as the mechanism how the COP1/SPA ubiquitin ligase contributes to plant size control remains to be determined.

1.5. Aims of this thesis

Besides their role in seedling photomorphogenesis and flowering time, the Arabidopsis COP1/SPA ubiquitin ligase complexes are involved in plant growth as *spa* and weak *cop1* mutants exhibit a dramatic reduction in leaf size. Therefore, one aim of my work was to investigate the role of COP1 and particularly the SPA proteins in plant growth. Detailed phenotypic analyses and genetic interaction studies should reveal the cause and possible targets of COP1/SPA in leaf size control. In addition, the importance of the SPAs was examined by generation and analysis of a *spa* quadruple null mutant, since it is known that *cop1* null mutants are seedling lethal and therefore *COP1* function is crucial for Arabidopsis development.

The SPA1 N-terminal domains are necessary for repression of flowering time in short days but dispensable for seedling development in *spa1* mutants and additionally they are thought to contribute to SPA1 de-stabilization. Structure function analyses of SPA1 as well as SPA4 were performed to test the functional requirement for the different SPA domains in the regulation of *COP1/SPA*-dependent leaf size and for SPA protein stability. To this end, various *SPA4* and *SPA1* deletion constructs were generated and examined in different *spa* mutant backgrounds for complementation of the mutant phenotypes and for their impact on SPA4 or SPA1 protein stability, respectively.

In an additional project I aimed to identify a *spa1* enhancer mutant, which was generated by EMS mutagenesis of *spa1* mutant seeds via positional cloning.

II. Results

II.1. Role of SPA proteins in Arabidopsis leaf size control

Cell number is a primary determinant of organ size, although parallel and/or subsequent cell expansion amplifies and modifies its effect, thereby contributing to the final size and shape of lateral organs (Tsukaya, 2005). Analysis of the relationship between various growth variables in leaf development (e.g. cell size, cell number, expansion rates and duration of expansion) revealed that the final leaf area is determined early in development as it correlates with the maximal absolute leaf expansion rate and the cell number, but not with the duration of leaf expansion or the cell size (Cookson et al., 2005).

The COP1/SPA complex is involved in the regulation of plant size in Arabidopsis since weak *cop1* mutants as well as *spa* quadruple mutant plants exhibit an extremely dwarfed phenotype (McNellis et al., 1994a; Laubinger et al., 2004). Despite the fact that, among the SPA proteins, SPA3 and SPA4 are the main regulators of plant growth, also SPA1 contributes to plant size control, yet to a minor extent, whereas SPA2 has almost no function (Laubinger et al., 2004).

II.1.1. Detailed phenotypic characterization of *spa* mutants

The first step to determine the role of SPA function in leaf growth regulation was a detailed phenotypic characterization of various *spa* triple mutants. Typically, leaf area expansion forms a sigmoid-shaped curve when plotted on a linear scale (Cookson et al., 2005). To investigate leaf growth in *spa* mutants, the changes in leaf area over time were determined in the third leaf of wild-type and *spa* triple mutant plants. Under long-day conditions, wild-type Arabidopsis leaves expanded rapidly during the early stage of development, whereas *spa1 spa3 spa4* triple mutants showed a dramatically decreased growth rate as well as a reduction in final leaf size (Figure 6a, b). Comparing final leaf area of wild type and *spa* triple mutants at about 32 days after sowing showed that all *spa* triple mutants exhibited a significant reduction of total leaf size compared to wild type. *spa1 spa3 spa4* mutant leaves were 7 times smaller than wild-type leaves and therefore showed the strongest effect, but also in *spa2 spa3 spa4* mutants the final leaf area was reduced by around 60% (Figure 6B, left graph). *spa* triple mutants with a functional SPA4 exhibited a leaf area reduction of about one

third whereas *spa1 spa2 spa4* mutant leaves were about 50% smaller than wild-type leaves (Figure 6b, right graph). Also, the duration of leaf expansion was affected in *spa* triple mutants since *spa1 spa3 spa4* leaves stopped expanding after approximately 20 days while those of wild-type plants continued to expand even after 30 days (Figure 6b). Thus, the fact that the weakest effect on leaf size was observed in *spa* triple mutants retaining only functional *SPA4* suggest that *SPA4* is the main regulator of leaf growth.

Besides the regulation of leaf size, SPA proteins have been shown to be important for the regulation of photoperiodic flowering as they repress flowering under short-day conditions (Laubinger et al., 2006). While *spa1 spa3 spa4* triple mutants flowered extremely early in short days, flowering time in *spa2 spa3 spa4* mutants was not altered, indicating that *SPA1* is both necessary and sufficient to regulate photoperiodic flowering (Laubinger et al., 2006, Figure 6c). Comparing the flowering time of all *spa* triple mutants revealed that *SPA2* and also *SPA3* indeed have a negligible function in flowering time control, since *spa1 spa3 spa4* and *spa1 spa2 spa4* mutants flowered with less than 20 leaves in contrast to the wild type, which flowered with about 60 leaves (Figure 6c). In addition to *SPA1*, also *SPA4* appears to be involved in flowering time regulation to some degree since *spa* triple mutants containing only functional *SPA4* developed around 40 leaves until bolting and therefore flowered only slightly earlier than *spa1* single mutants, which flowered with around 45 leaves, but still significantly later than *spa1 spa3 spa4* and *spa1 spa2 spa4* mutants (Figure 6c). Thus, *spa* mutants exhibit the most severe early flowering phenotype when both *SPA1* and *SPA4* are absent. This indicates that both proteins are involved in photoperiodic flowering time control, but *SPA4* only contributes to a minor extent to this developmental switch, as *SPA4* alone, in contrast to *SPA1*, is not sufficient to fully suppress early flowering in short days.

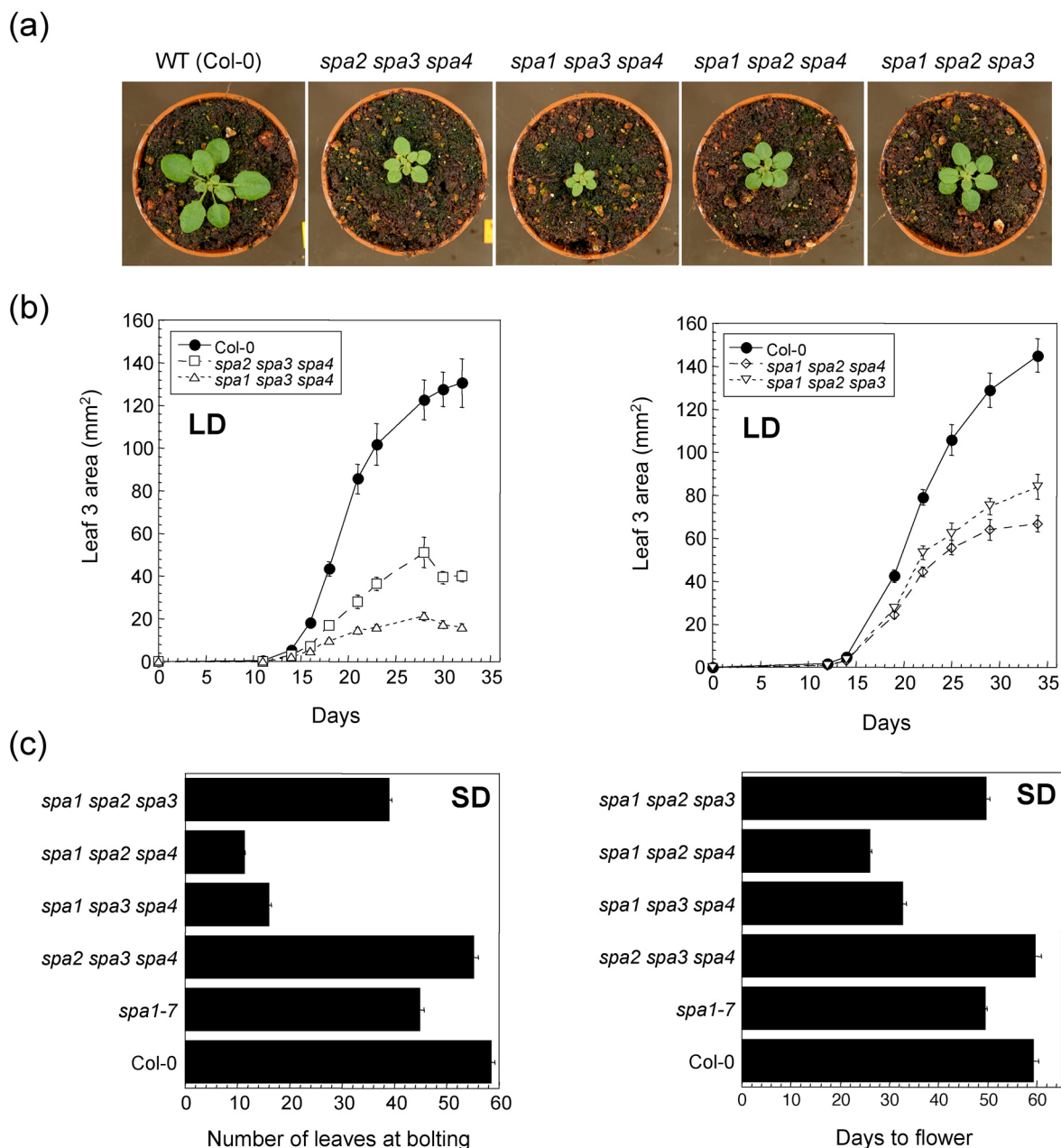


Figure 6. Plant size and flowering time of *spa* triple mutants.

(a) Visual phenotype of 3-week old wild-type (Col-0) and *spa* triple mutant plants grown under long-day (LD) conditions.

(b) Growth rates of the third rosette leaf of genotypes shown in (a). *spa2 spa3 spa4* and *spa1 spa3 spa4* (left panel) and *spa1 spa2 spa4* and *spa1 spa2 spa3* mutants (right panel) were grown in LD (16 hrs light/ 8 hrs darkness). Total leaf area was measured starting from the initiation of leaf 3 in a 2-5-day interval (n=10). Error bars indicate the standard error of the mean (SEM).

(c) Flowering time of wild-type (Col-0), *spa1* single and *spa* triple mutants grown under short-day (SD) conditions (8 hrs light/ 16 hrs darkness) Flowering time was determined by counting the number of rosette leaves at bolting (left panel) and the days to flower (right panel) (n=15). Error bars indicate the SEM.

To investigate whether the reduction in final leaf size in *cop1* and *spa* mutants is due to changes in cell expansion and/or cell proliferation, fully expanded leaves of 4-week-old LD-grown wild-type, *cop1-4* and *spa* triple mutant plants were analyzed microscopically. The average area of palisade cells of the third leaf was measured and total cell numbers per leaf were calculated from the final leaf area and the number of cells in a distinct leaf area. Figure 7c shows a microscopic observation of palisade cells in leaf tips from the genotypes shown in 7a. Compared to wild-type plants, *spa* mutants displayed a dramatic reduction in palisade cell size (Figure 7e) as well as in palisade cell number per leaf (Figure 7d). Palisade cell area in *spa1 spa3 spa4* mutants was reduced even more than in *spa2 spa3 spa4* mutants (Figure 7e). In addition, palisade cell number per leaf was decreased by approximately 60% in *spa1 spa3 spa4* mutants and approximately 40% in *spa2 spa3 spa4* mutant plants compared to wild type (Figure 7d). *cop1* mutants exhibited a similarly severe phenotype regarding both palisade cell number and size (Figure 7d,e). These data indicate that cell proliferation as well as cell expansion is affected in *cop1* and *spa* mutants.

Furthermore, epidermal cells of the third leaf of these genotypes were microscopically analyzed and both their epidermal cell number per leaf and their epidermal cell size were quantified. Figure 7f displays epidermal tissue observed using Collodium imprints of adaxial epidermal cells at the leaf tip. Similar to the data obtained by quantification of palisade cells, the total epidermal cell number and the average cell size in *cop1*, *spa1 spa3 spa4* as well as *spa2 spa3 spa4* mutant leaves were decreased (Figure 7g, h). Here, *spa2 spa3 spa4* mutants displayed only a 20% reduction in epidermal cell number (Figure 7g). However, an independent experiment showed a stronger reduction of cell number in *spa2 spa3 spa4* mutants compared to wild type (Supplemental Figure 1). Regarding epidermal cell size, all genotypes analyzed exhibited a reduction of at least 50% compared to wild type (Figure 7h). In summary, these results show that in *cop1* and in *spa* mutants cell proliferation as well as cell expansion are impaired, and both effects contribute to the dwarfed phenotype of *cop1* and *spa* mutant plants.

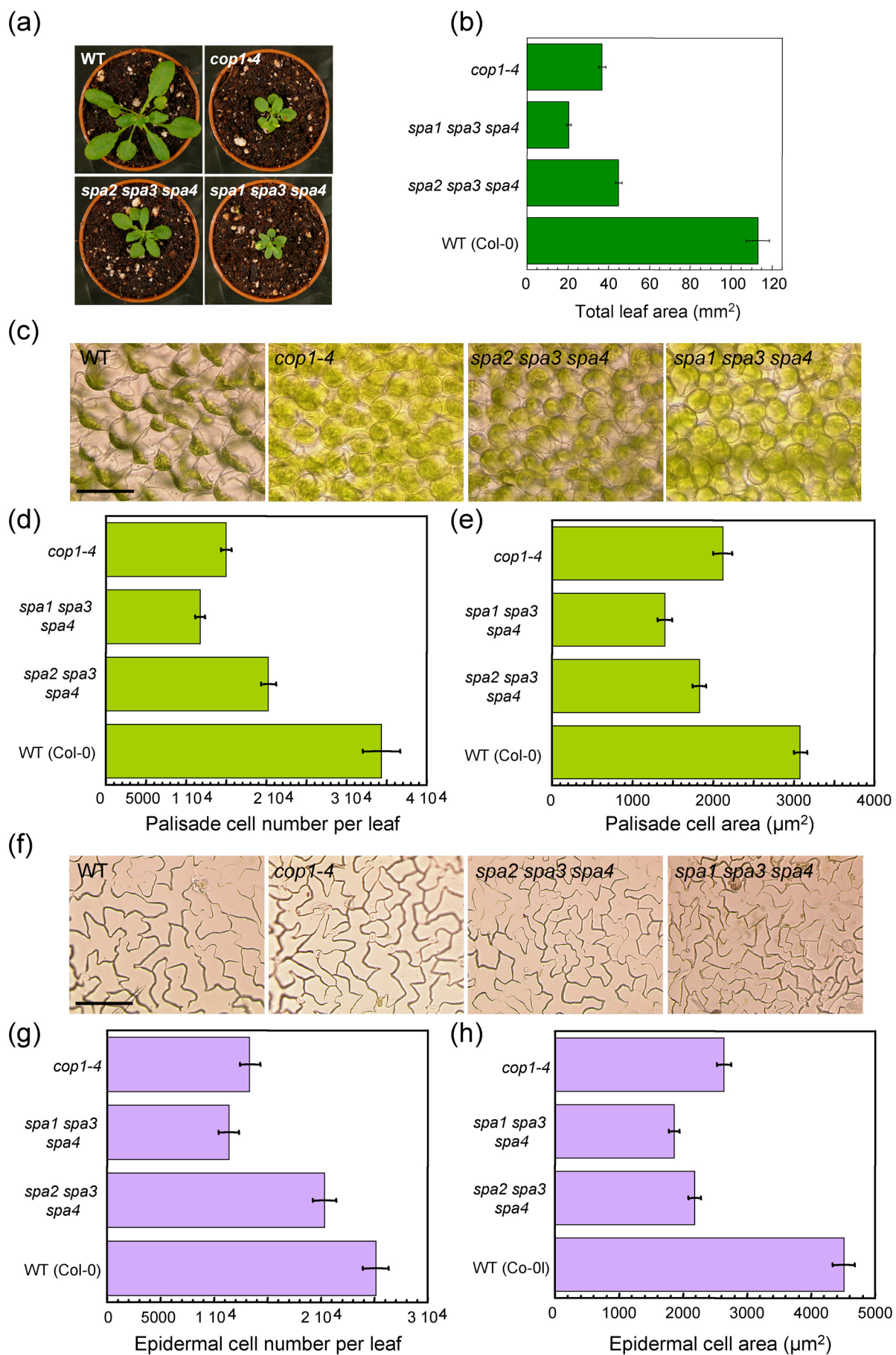


Figure 7. For description see next page.

← **Figure 7. The reduced plant size of *cop1* and *spa* mutants is due to a decrease in cell number and cell size.**

(a) Visual phenotype of 4-week old wild-type (Col-0), *cop1*, *spa2 spa3 spa4* and *spa1 spa3 spa4* mutant plants grown under long-day conditions.

(b) Quantification of total leaf area of the genotypes shown in (a). Error bars indicate the SEM.

(c) Visual phenotype of palisade cells of the genotypes shown in (a) (scale bar: 100 μ m).

(d) Quantification of average palisade cell number per leaf of the genotypes shown in (a). Error bars indicate the SEM.

(e) Quantification of average palisade cell size of the genotypes shown in (a). Error bars indicate the SEM.

(f) Visual phenotype of epidermal cells of the genotypes shown in (a) (scale bar: 100 μ m).

(g) Quantification of average epidermal cell number per leaf of the genotypes shown in (a). Error bars indicate the SEM.

(h) Quantification of average epidermal cell size of the genotypes shown in (a). Error bars indicate the SEM.

The same experimental procedure was performed on *spa1 spa2 spa4* and *spa1 spa2 spa3* triple mutants, which exhibited a less severe defect in leaf growth (Laubinger et al., 2004; Figure 6b, 8b). Also in these genotypes the total area of the third leaf (Figure 8b), the cell number per leaf as well as the average cell size of palisade (Figure 8c,d) and epidermal cells (Figure 8e,f) were reduced compared to the wild type, but the leaf phenotype, especially in the *spa1 spa2 spa3* mutant background, was less dramatic. *spa1 spa2 spa4* as well as *spa1 spa2 spa3* mutants displayed a significant reduction in total palisade cell number compared to wild type (Figure 8c). Also the area of palisade cells in *spa1 spa2 spa4* mutant plants was decreased noticeably, whereas *spa1 spa2 spa3* mutants exhibited only a minor reduction of average palisade cell area (Figure 8d). Total epidermal cell number of *spa1 spa2 spa4* mutants was decreased significantly, while *spa1 spa2 spa3* mutants showed only a slight reduction in cell number compared to wild type (Figure 8e). Furthermore, epidermal cells of *spa1 spa2 spa4* mutants were about 50% smaller than wild-type epidermal cells, whereas *spa1 spa2 spa3* mutants displayed a 20% reduction of average epidermal cell area compared to wild type (Figure 8f). These findings emphasize that SPA-regulated leaf growth is mediated via cell proliferation and cell growth. In addition, these results support the idea that the SPA proteins, and particularly SPA4, act as important factors in plant development by functioning in cell division as well as in cell growth control.

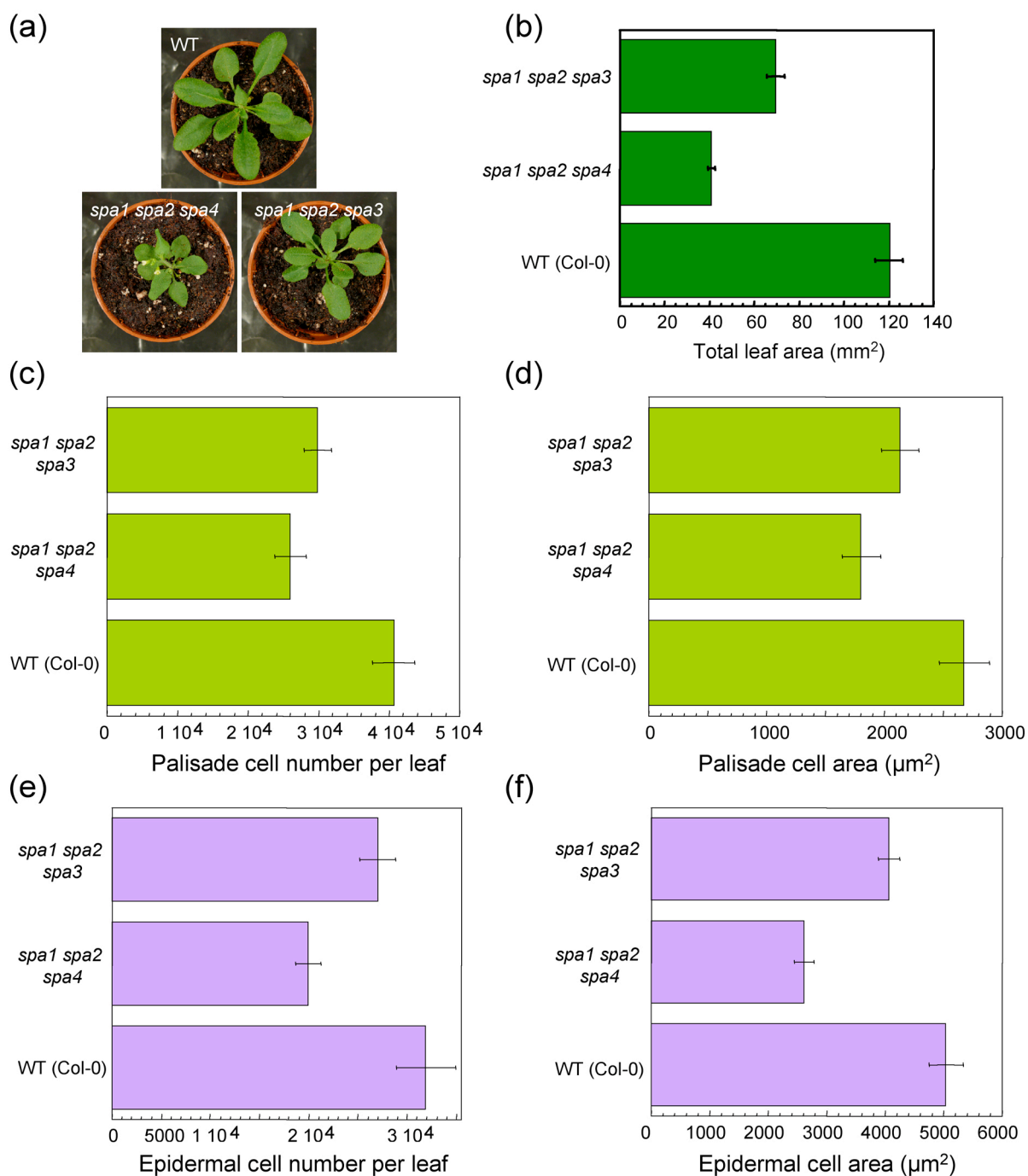


Figure 8. SPA4 is the main regulator of cell size and cell number control

(a) Visual phenotype of 4-week-old wild-type (Col-0), *spa1 spa2 spa4* and *spa1 spa2 spa3* mutant plants grown under long-day conditions.

(b) Quantification of total leaf area of the genotypes shown in (a). Error bars indicate the SEM.

(c, d) Quantification of average palisade cell number per leaf (c) and average palisade cell size (d) of the genotypes shown in (a). Error bars indicate the SEM.

(e, f) Quantification of average epidermal cell number per leaf (e) and average epidermal cell size (f) of the genotypes shown in (a). Error bars indicate the SEM.

II.1.2. Involvement of transcription factors in *SPA/COP1*-regulated leaf growth

An extremely dwarfed phenotype similar to that of weak *cop1* and *spa* multiple mutants was also described for overexpression lines of known COP1/SPA targets like CO, FT or HFR1 (Yoo et al., 2005; Onouchi et al., 2000; Yang et al., 2003). To investigate whether the dwarfed adult phenotype of *spa* and *cop1* mutants is caused by hyper-accumulation of these proteins, dwarfed *spa1 spa3 spa4* triple or quadruple mutants were crossed into mutant backgrounds of the known COP1/SPA targets CO, FT, HFR1 and HY5. In addition, various available *cop1* transcription factor double mutants were analyzed.

spa1 spa3 spa4 mutants with an additional mutation in CO resulted in late flowering dwarfed plants (Figure 9a, b, Supplemental Figure 2). Also, the additional mutation of the FT gene in the *spa* quadruple mutant background led to a late flowering and extremely dwarfed phenotype (Figure 9b, data not shown). The loss of HFR1 in a *spa1 spa3 spa4* mutant background was also not able to suppress the leaf size phenotype of the *spa* triple mutant (Figure 9b). On the contrary, *spa1 spa3 spa4 hy5* quadruple mutants, *cop1 hy5* as well as *cop1 sth2* double mutants showed a slightly increased plant size compared to the corresponding *spa* triple or *cop1* single mutants (Figure 9b). Nevertheless, none of the additional introduced mutations were able to fully restore the wild-type phenotype. Furthermore, *cop1-6 phyB* double mutants exhibited an increased leaf size compared to *cop1-6* single mutants, while on the other hand the constitutive shade avoidance phenotype of the *phyB* mutant was suppressed in the *cop1* mutant background (Figure 9b). These results, together with the fact that transcription factors like HY5 hyper-accumulate in *cop1* and *spa* mutants (Saijo et al., 2003; Zhu et al., 2008; Nixdorf and Hoecker, 2010), indicate that increased abundance of HY5 or STH2 at least in part contributes to the altered plant size phenotype of these mutants.

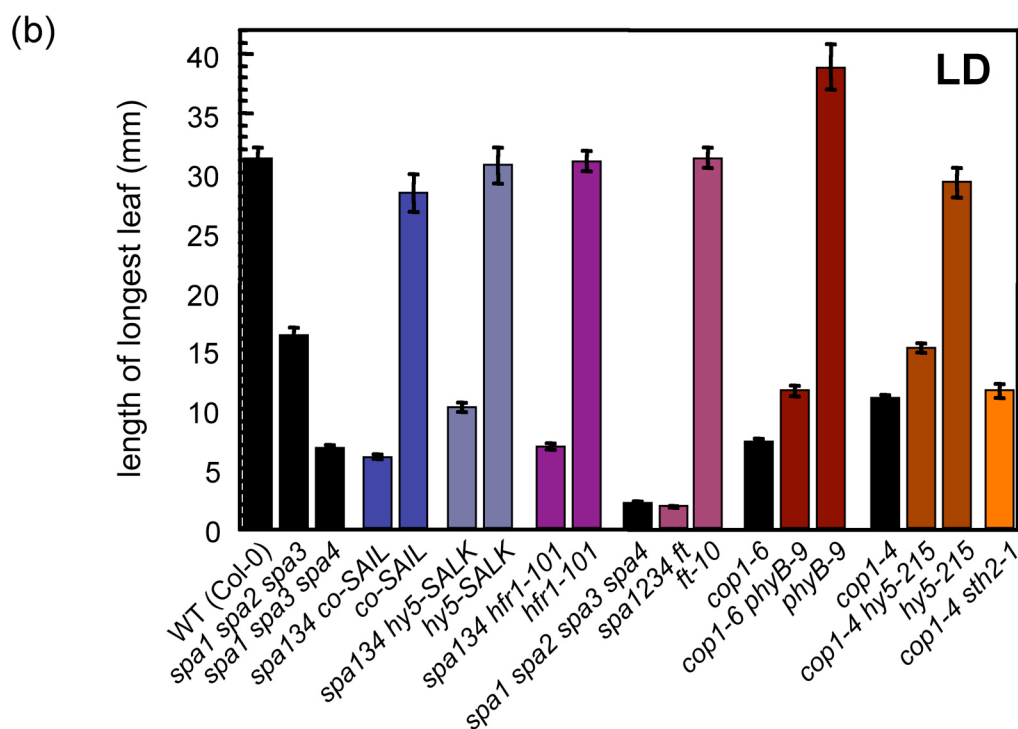
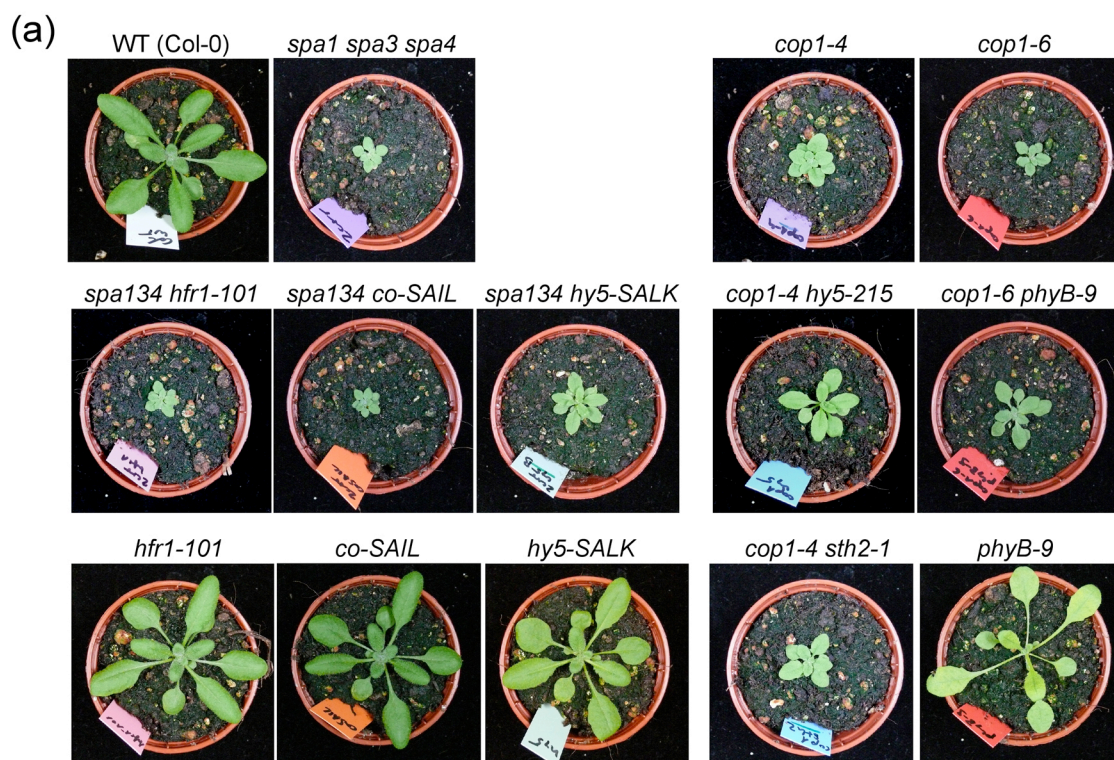


Figure 9. SPA/COP1-regulated leaf development is independent of CO and HFR1, but possibly involves other transcription factors like HY5 and STH2.

(a) Visual phenotypes of various *cop1* or *spa* transcription factor multiple mutant plants grown for 21 days in LD. Wild-type (Col-0), *spa1 spa3 spa4* and *cop1* mutant plants are shown as controls.

(b) Quantification of hypocotyl length of the genotypes shown in (a). Error bars indicate the SEM.

II.2. Characterization of *spa* null mutants

SPA proteins are thought to act together with the E3-ubiquitin ligase COP1 in a number of heterogeneous complexes, likely consisting of a COP1 homo-dimer and a SPA homo- or hetero-dimer (Zhu et al., 2008). The fact that SPA proteins have partially redundant functions makes it difficult to uncover the distinct functions of each single *SPA* gene. *spa* triple mutants, which contain only one functional *SPA* gene, were used to determine these functions. However, three of the four *spa* mutant alleles (*spa1-7*, *spa2-1*, *spa4-1*) used in triple mutant analyses so far still produce truncated mRNAs and thus do not represent true null alleles (Laubinger and Hoecker, 2003; Laubinger et al., 2004; Fittinghoff et al., 2006). Even in a *spa* quadruple mutant there might be some residual *SPA* function left. It is known also that *cop1* null mutants are lethal and therefore the SPA proteins cannot compensate for a loss of *COP1* function (McNellis et al., 1994a). But to answer the question whether COP1 has residual function in the absence of the SPA proteins, true null alleles for all *SPA* genes are needed. For this purpose a T-DNA library (C. Koncz, MPIZ, Cologne) was screened for *spa2* and *spa4* null mutant alleles and subsequently a *spa* quadruple mutant containing these alleles and the *spa3-1* and *spa1-100* null alleles was generated and characterized (Laubinger and Hoecker, 2003; Yang et al., 2005).

II.2.1. Identification of *spa2* and *spa4* mutant null alleles

In order to generate a *spa* quadruple null mutant, an Arabidopsis insertion mutant collection of 90000 lines, carrying the T-DNA of the *Agrobacterium* gene fusion vector pPCV6NFHy (Rios et al., 2002), was screened for mutations in the N-terminal part of *SPA2* and *SPA4*, respectively. For each locus one mutant allele was isolated. *spa2-2* carries a T-DNA insertion 1331 bp downstream of the ATG in the second exon (Figure 10a). The T-DNA insertion in *spa4-3* is located 150 bp upstream of the ATG in the first intron (Figure 10b). Populations segregating for the respective insertions in *SPA2* or *SPA4* were screened for homozygous *spa2-2* or *spa4-3* mutant plants using PCR-based markers flanking the respective insertion sites, thereby allowing to discriminate between wild-type (Col-0) and *spa2-2* or *spa4-3* mutant alleles, respectively. RT-PCR analysis using primers flanking the respective insertion site confirmed that neither *spa2-2* nor *spa4-3* mutant plants accumulated wild-type

SPA2 or *SPA4* transcripts (Figure 10c, e). Additionally, RNA blot analysis of RNA isolated from wild-type and *spa2* or *spa4* mutant seedlings using *SPA2*- or *SPA4*-specific probes revealed that, in contrast to the so far available *spa2-1* and *spa4-1* alleles, no truncated transcript was detectable in the newly isolated *spa2-2* and *spa4-3* alleles (Figure 10d, f). These results indicate that *spa2-2* as well as *spa4-3* mutant plants are disrupted in normal *SPA2* or *SPA4* function, respectively, and that the resulting alleles are indeed null mutations.

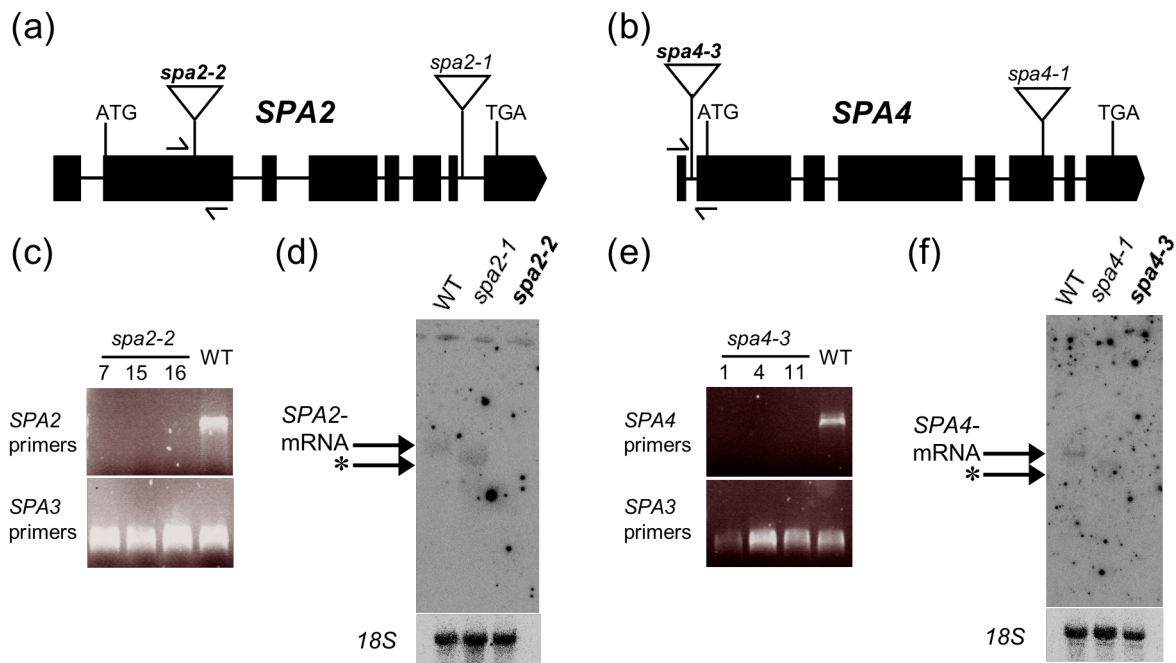


Figure 10. The T-DNA insertions in *spa2-2* and *spa4-3* cause null mutations.

(a, b) *SPA2* (a) and *SPA4* (b) genomic structure including schematic representation of T-DNA insertion sites (triangles) and position of gene-specific primers (arrows) used for RT-PCR presented in (c) and (e). Black rectangles represent the exons and lines denote the introns.

(c, e) RT-PCR analysis of wild-type (WT) and *spa2-2* (c) or *spa4-3* (e) mutant seedlings. Total RNA from three homozygous lines each was reverse-transcribed and subsequently amplified by PCR using primers flanking the respective T-DNA insertion site (*SPA2* primers, *SPA4* primers) and, as a control, *SPA3*-specific primers. Numbers indicate individual homozygous lines selected for analysis.

(d, f) RNA blot analysis of RNA isolated from dark-grown wild-type (WT) and *spa2* (d) or *spa4* (f) mutant seedlings which were transferred to Rc ($30 \mu\text{mol m}^{-2} \text{s}^{-1}$) for 4 hours. Blots were hybridized with a *SPA2*-specific probe (d) or a *SPA4*-specific probe (f). As a control for equal loading the blots were re-hybridized with an 18S-rRNA-specific probe. Asterisks mark truncated transcripts detected in the *spa2-1* and *spa4-1* alleles, respectively.

A fluence dose response curve in FRc showed that the *spa2-2* mutant did not show an altered responsiveness to light compared to the wild type (Figure 11a-c), as it was shown already for *spa2-1* (Laubinger et al., 2004). However, in contrast to previous results *spa2-1* as well as *spa2-2* mutants displayed a slightly shorter hypocotyl compared to wild type in Rc and Bc (Laubinger et al., 2004; Figure 11b, c). The *spa4-*

3 mutant allele exhibited a similarly increased responsiveness to light as the *spa4-1* mutant when compared to wild-type seedlings (Figure 11d-f). The *spa4-3* mutation suppressed hypocotyl growth most notably in Rc (Figure 11e) but also in FRc (Figure 11d) and Bc (Figure 11f) of lower fluence rates, as it was reported before for *spa4-1* (Laubinger and Hoecker, 2003). These results imply that, even though *spa2-1* and *spa4-3* mutants produced truncated transcripts, the function of the respective SPA gene is completely lost in these mutants.

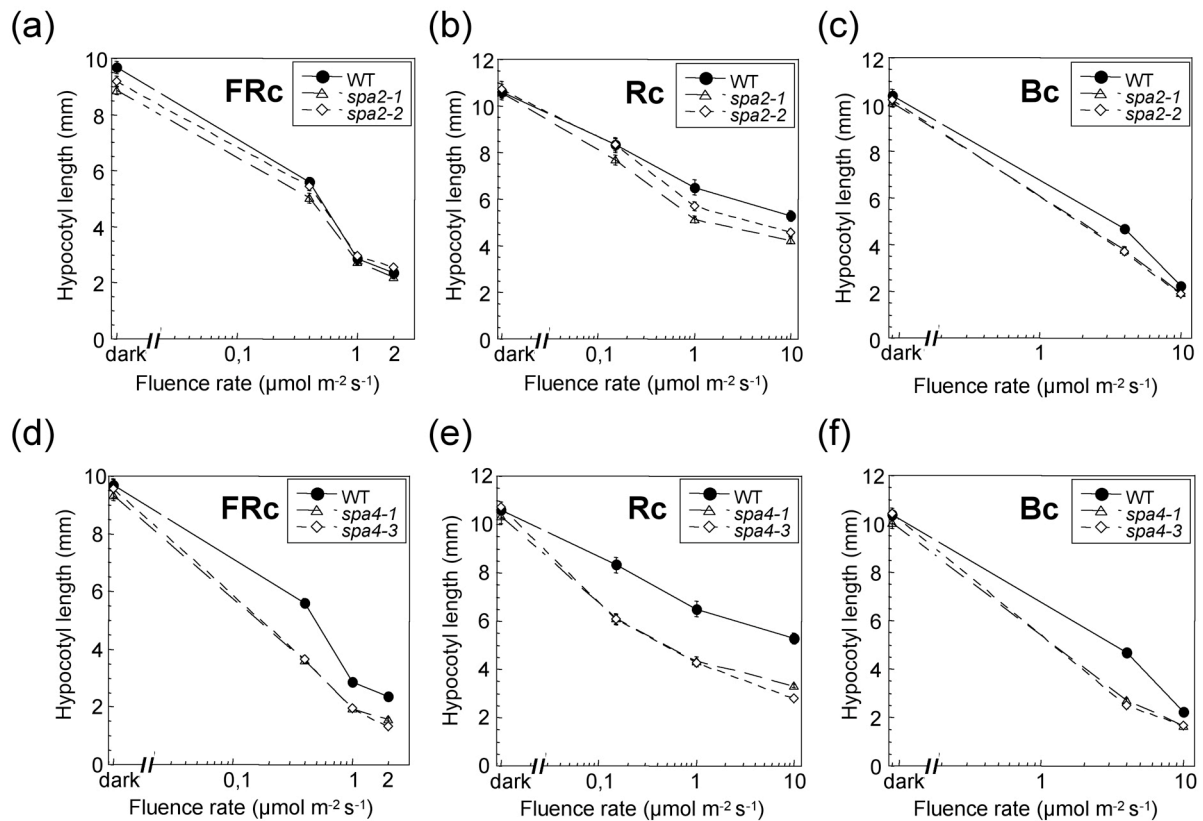


Figure 11. A *spa2* null mutation does not enhance the responsiveness of seedlings to light whereas the *spa4* null allele does.

(a, b, c) Hypocotyl length of wild-type (WT), *spa2-1* and *spa2-2* mutant seedlings grown in FRc (a), Rc (b), Bc (c) of various fluence rates. Error bars indicate the SEM.
 (d, e, f) Hypocotyl length of wild-type (WT), *spa4-1* and *spa4-3* mutant seedlings grown in FRc (d), Rc (e), Bc (f) of various fluence rates. Error bars indicate the SEM.

II.2.2. Generation of a *spa* quadruple null mutant

Now having null mutant alleles for all four *SPA* genes, the aim was to generate a *spa* quadruple null mutant to answer the question whether the *SPA* proteins are essential for *Arabidopsis* development similarly to *COP1* as *cop1* null mutant alleles are seedling lethal (McNellis et al., 1994a). For this reason the already available *spa1-100* and *spa3-1* null alleles as well as the newly identified *spa2-2* and *spa4-3* mutant alleles were crossed to obtain double mutants for further crossings. Homozygous F2 progenies of these crosses were verified using PCR-based markers, which discriminate the wild-type and the respective *spa* mutant allele. To obtain *spa* quadruple null mutant plants the *spa1 spa3* and *spa2 spa4* double mutants were crossed. The F2 was screened via seedling phenotype in light and darkness, as a previously generated *spa* quadruple mutant shows an extreme constitutively photomorphogenic phenotype (Laubinger et al, 2004). To facilitate screening and subsequent propagation of *spa* quadruple null mutant seeds, it was additionally screened for segregating *spa1 spa2 spa3 SPA4+/-* mutants, which are much bigger plants and exhibit an enhanced responsiveness to light compared to the wild type. Moreover, the null allele containing *spa1 spa2* and *spa3 spa4* double mutants as well as all four *spa* triple mutant combinations were generated by crossing the *spa1 spa3* double mutant with a *spa2* or *spa4* single mutant as well as by crossing the *spa2 spa4* double mutant with a *spa1* or *spa3* single mutant, respectively. To work in a *spa* triple null background will help to distinguish the functions of the individual *SPA* genes more precisely.

The hypocotyl phenotype of the newly generated *spa* mutants in dark- and light-grown seedlings were compared to wild type and the respective previously used *spa* mutants (Figure 12). Figure 12a displays a representation of dark-grown wild-type, *spa* double, triple and quadruple mutant seedlings. The respective newly generated *spa* mutant seedlings are shown on the right side. Figure 12b shows the same genotypes as in (a) grown in FRc ($0.4 \mu\text{mol m}^{-2} \text{s}^{-1}$) but without the *spa1 spa2* double mutant, which is indistinguishable from a *spa1* single mutant under these conditions (Laubinger et al., 2004). Quantification of hypocotyl length of dark- (Figure 12c) and FRc-grown (Figure 12d) wild-type and *spa* mutant seedlings revealed that the *spa* null mutants were indistinguishable from the previously used *spa* mutants. Furthermore, *spa* quadruple null mutants exhibited a phenotype quite similar to the

previously used *spa* quadruple mutant (Figure 12a, b). Hence, *spa* quadruple null mutants are, in contrast to *cop1* null mutants, viable.

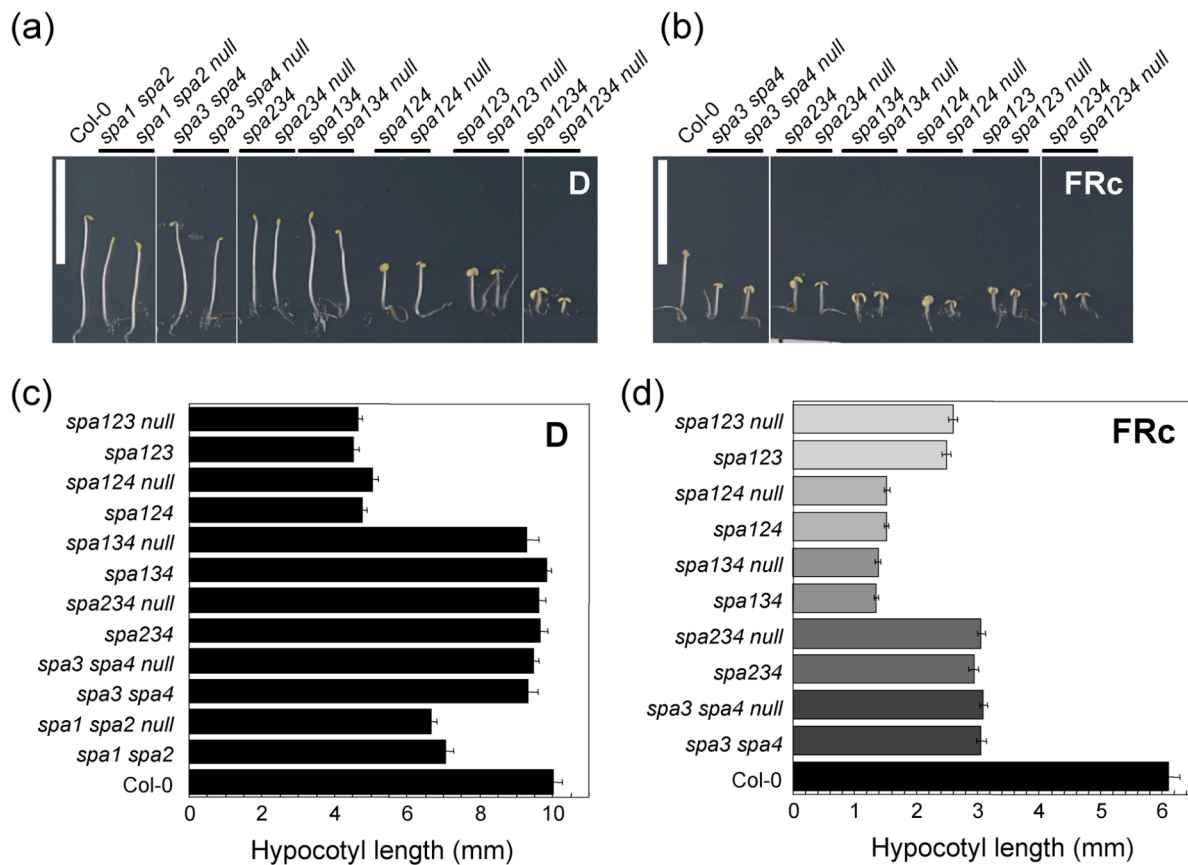


Figure 12. Seedling phenotype of *spa* double and *spa* triple null mutants.

(a, b) Visual phenotypes of wild-type (Col-0) and various *spa* double and *spa* triple mutant seedlings grown in darkness (a) or FRc ($0.4 \mu\text{mol m}^{-2} \text{s}^{-1}$) (b) for 4 days. For each genotype 2 different alleles are shown. Mutants containing previous available alleles (left): *spa1-7*, *spa2-1*, *spa3-1*, *spa4-1*. *spa*-null multiple mutants containing the null alleles *spa1-100*, *spa2-2*, *spa3-1*, *spa4-3* are always shown on the right. Scale bar: 10 mm.

(c, d) Quantification of hypocotyl length of seedlings shown in (a) and (b). *spa*-null multiple mutants are always shown on top. Error bars indicate the SEM.

Also in the adult plant stage *spa* null mutants demonstrate the same phenotype as the previously characterized *spa* mutants (Figure 13a). The *spa* quadruple null mutant is, despite its tiny size, able to reach adult stage, to flower (Figure 13b) and to produce seeds (data not shown). These findings show that the SPA proteins - in contrast to COP1 - are important, but not essential, for Arabidopsis development and that COP1 may have residual functions without the SPA proteins or that there might be additional factors involved in COP1-dependent signalling pathways.

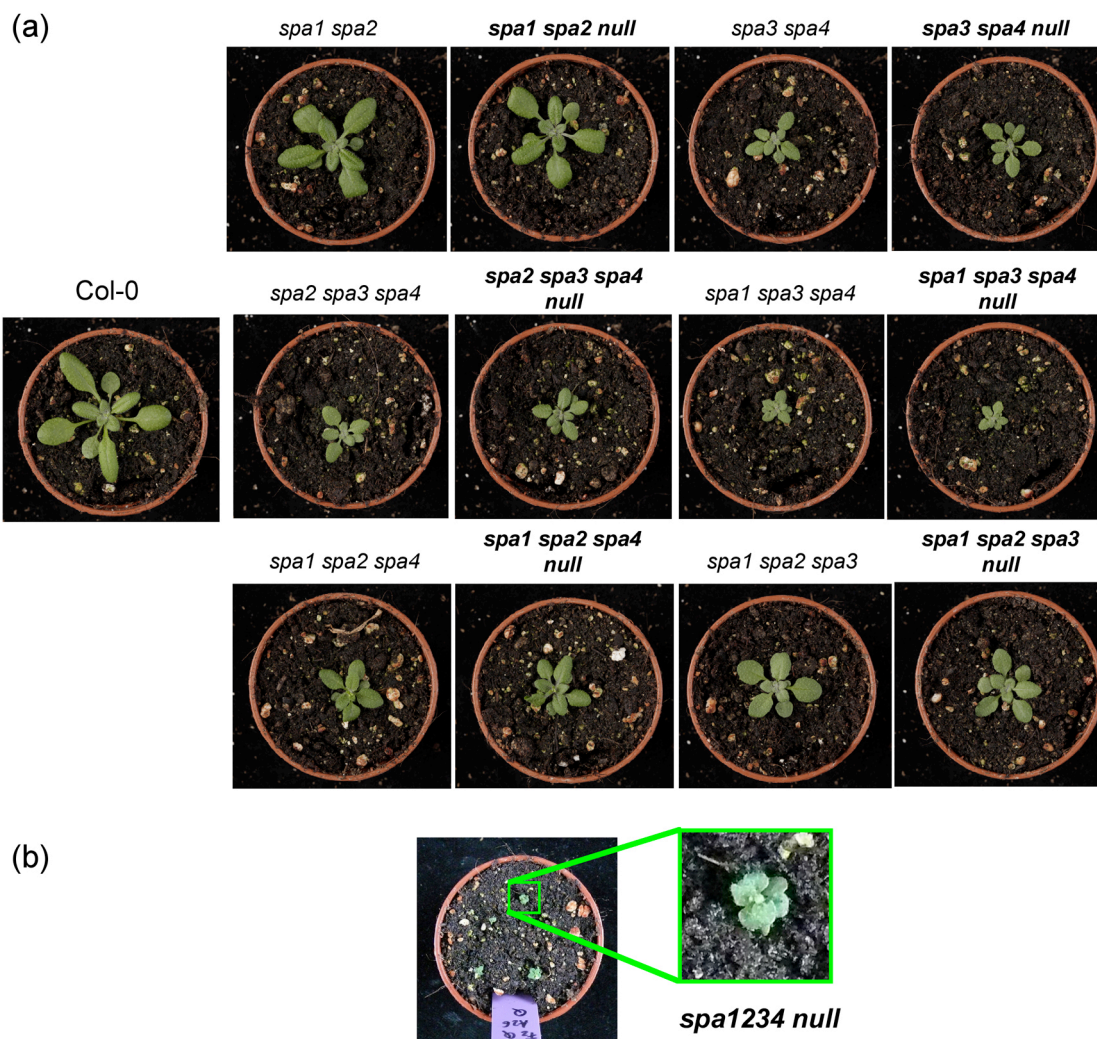


Figure 13. Plant size of *spa* mutant plants containing null alleles.

(a) Visual phenotypes of wild-type (Col-0), *spa* double and *spa* triple mutant plants grown in LD for 21 days. *spa* mutants containing the null alleles were compared with previously available mutants. Previous available alleles are *spa1-7*, *spa2-1*, *spa3-1* and *spa4-1*. *spa*-null multiple mutants carry the null alleles *spa1-100*, *spa2-2*, *spa3-1* and *spa4-3*.

(b) Phenotype of a *spa* quadruple null mutant, grown in LD for 23 days.

II.3. SPA4 structure function analysis

The four *SPA* loci encode WD-repeat proteins, which in addition contain coiled-coil domains and an N-terminal kinase-like domain (Figure 3). In case of *SPA1* it was shown that the WD-repeat domain is essential for *SPA1* function since it is involved in binding of DDB1 and the transcription factors HY5 and HFR1 (Chen et al., 2010; Saijo et al., 2003; Yang et al., 2005a). The coiled-coil domains of the *SPA* proteins are essential for *SPA* function as they mediate binding to COP1 and other SPAs (Hoecker and Quail, 2001; Laubinger and Hoecker, 2003; Saijo et al., 2003). Previous analyses showed that the N-terminus is not required for normal *SPA1* function in seedling photomorphogenesis, whereas it is essential to suppress early flowering in short days (Fittinghoff et al., 2006; Kirsten Fittinghoff, PhD thesis, 2008). Analysis of various *spa* triple mutants revealed redundant as well as distinct functions of the individual *SPA* genes in different light conditions and developmental stages. *SPA1* regulates seedling photomorphogenesis, photoperiodic flowering and also contributes to leaf size control, whereas *SPA4* is involved mainly in leaf growth regulation and light-regulated seedling development but also contributes to suppression of flowering in SD in Arabidopsis (Laubinger et al., 2004, Fittinghoff et al., 2006, Laubinger et al., 2006; this study).

II.3.1. Role of the SPA4-N-terminus in light-grown seedlings

To test whether the coiled-coil domain, the kinase-like domain or the whole N-terminus is essential for *SPA4* function, *SPA4* deletion constructs were generated and transformed into a *spa3 spa4* mutant background. As a positive control the *SPA4* full-length cDNA was used. The *SPA4* full-length and deletion derivatives were fused to an N-terminal GFP epitope and expressed under the control of a dual 35S CaMV promoter (Curtis and Grossniklaus, 2003). Because *SPA4*, in contrast to *SPA1*, has no known NLS sequence and to ensure that the truncated versions of the *SPA4* protein are transported to the nucleus, additional constructs were generated in which an artificial *SV40 NLS* (modified after Matsushita et al., 2003) was fused to the respective *SPA4* cDNAs (Figure 14a).

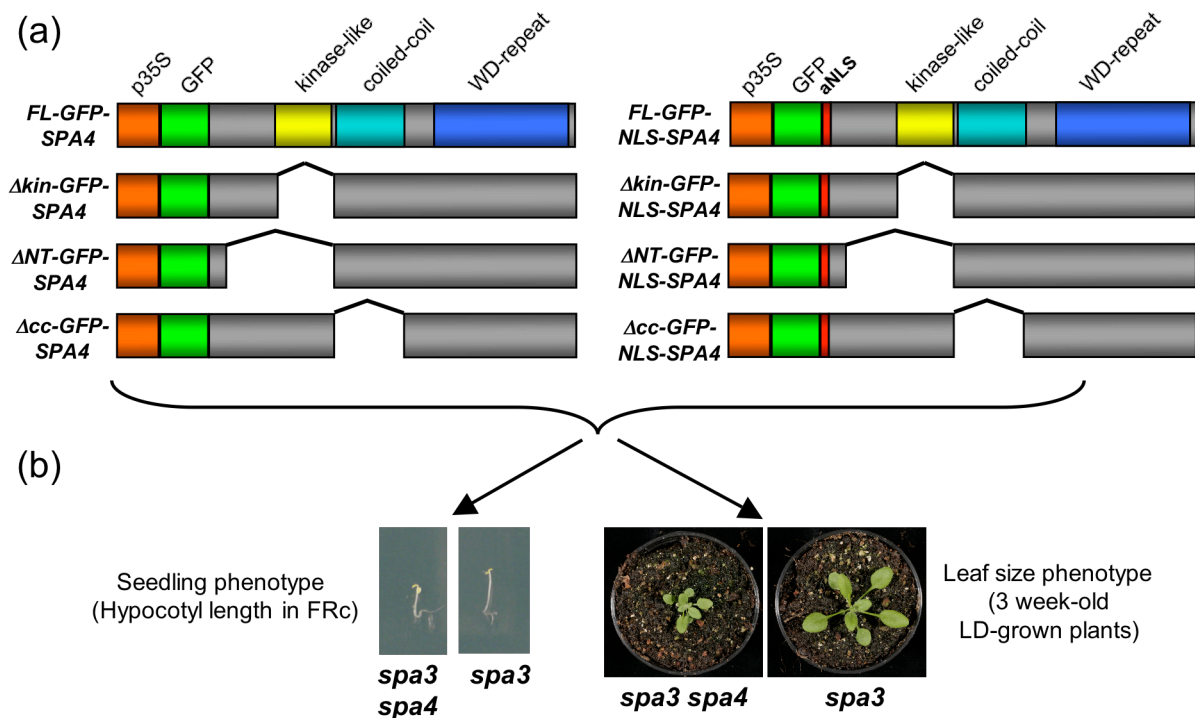


Figure 14. GFP-SPA4 full-length and deletion constructs and strategy of the SPA4 structure-function analysis.

(a) Schematic representation of full-length *SPA4* (*FL-GFP-SPA4*), *FL-SPA4*, containing an N-terminal artificial nuclear localization sequence (*aNLS*) (*FL-GFP-NLS-SPA4*) and three *SPA4* deletion derivatives (Δkin , ΔNT , Δcc) without (left) or with an artificial *NLS* (right). All constructs are under the control of a dual 35S promoter and are fused to an N-terminal GFP epitope.

(b) Strategy to study *SPA4* domain function: The 35S:*GFP-SPA4* full-length and deletion constructs as well as the 35S:*GFP-NLS-SPA4* full-length and deletion constructs are expressed in *spa3 spa4* double mutants to investigate seedling development in light as well as *SPA*-regulated leaf size control.

spa3 spa4 double mutants display an enhanced de-etiolation phenotype with reduced hypocotyl length in FRc compared to wild-type or *spa3* single mutant seedlings (Laubinger and Hoecker, 2003). Therefore, transgenic T2 lines were screened under FRc conditions. The transgenic *spa3 spa4* lines carrying the Δcc deletion derivatives of *SPA4* showed no complementation. All lines investigated exhibited extremely short hypocotyls similar to the *spa3 spa4* mutant seedlings (Table 1, Figure 15 a, e). It was verified by immunoblot analysis of some the transgenic Δcc lines that the non-complementing lines indeed expressed the Δcc -GFP-*SPA4* deletion protein (Figure 18 & 19). The majority of the transgenic lines carrying *FL-GFP-SPA4*, Δkin or ΔNT deletion derivatives complemented the *spa3 spa4* mutant seedling phenotype in FRc (Table 1).

Table1: Complementation analysis of T2 seedlings carrying *FL-GFP-SPA4* or deletion constructs.

The *SPA4* constructs shown in Figure 14a were transformed into a *spa3 spa4* mutant background. Resulting T2 lines were grown under $0.4 \mu\text{mol m}^{-2} \text{s}^{-1}$ FRc, for three days. The number of individual transgenic T2 lines with long hypocotyls and the total number of transgenic T2 lines analyzed is given.

constructs transformed into <i>spa3 spa4</i>	FRc (rescued/ total)
<i>FL-GFP-SPA4</i>	41/50
<i>FL-GFP-NLS-SPA4</i>	17/25
$\Delta\text{NT-GFP-SPA4}$	22/25
$\Delta\text{NT-GFP-NLS-SPA4}$	30/37
$\Delta\text{kin-GFP-SPA4}$	26/36
$\Delta\text{kin-GFP-NLS-SPA4}$	36/58
$\Delta\text{cc-GFP-SPA4}$	0/20
$\Delta\text{cc-GFP-NLS-SPA4}$	0/11

The hypocotyl length of transgenic T3 seedlings expressing full-length *GFP-SPA4* (*FL-GFP-SPA4*), $\Delta\text{NT-GFP-SPA4}$ and $\Delta\text{kin-GFP-SPA4}$ was measured under various fluence rates in different light conditions (Figure 15, Supplemental Figure 3). Figure 15a shows the phenotype of FRc-grown transgenic *spa3 spa4* seedlings expressing various *GFP-SPA4* constructs. For each construct, two independent transgenic lines are presented. A fluence dose response curve in far-red light of three independent transgenic lines per complementing construct exhibited differences in complementation strength between the different *SPA4* derivatives (Figure 15b-e). All transgenic lines except $\Delta\text{cc-GFP-SPA4}$ exhibited a strong overcomplementing phenotype compared to the corresponding *spa3* mutant control or even wild-type seedlings (Figure 15b-e). The hypocotyl lengths of *FL-GFP-SPA4* and Δkin as well as one ΔNT line (2-9) were increased 1.5-2-fold compared to *spa3* and wild type in FRc ($5 \mu\text{mol m}^{-2} \text{s}^{-1}$) (Figure 15b-d). Two out of three homozygous $\Delta\text{NT-SPA4}$ transgenic lines displayed extremely elongated hypocotyls, which were 3-4-fold longer than the hypocotyls of *spa3* or wild-type seedlings (Figure 15c).

A similar effect was seen in the transgenic lines expressing the various *GFP-NLS-SPA4* constructs (Figure 16, Supplemental Figure 3). Among these lines, the *FL-GFP-NLS-SPA4* and the $\Delta\text{NT-GFP-NLS-SPA4}$ but not $\Delta\text{kin-GFP-NLS-SPA4}$ transgenic lines showed an even increased hypocotyl length compared to the respective transgenic lines without the artificial NLS (Figure 15b, c; Figure 16b, c). The hypocotyls of three independent *FL-GFP-NLS-SPA4* lines were 2-3-fold longer than the *spa3* and wild-type hypocotyls, whereas the hypocotyl length of two $\Delta\text{NT-}$

GFP-NLS-SPA4 lines was increased 5-fold compared to the wild type control in FRc ($5 \mu\text{mol m}^{-2} \text{s}^{-1}$) (Figure 16b,c). Thus, the SPA4 N-terminus is not required for SPA-regulated seedling development in light, while the coiled-coil domain is essential for this function.

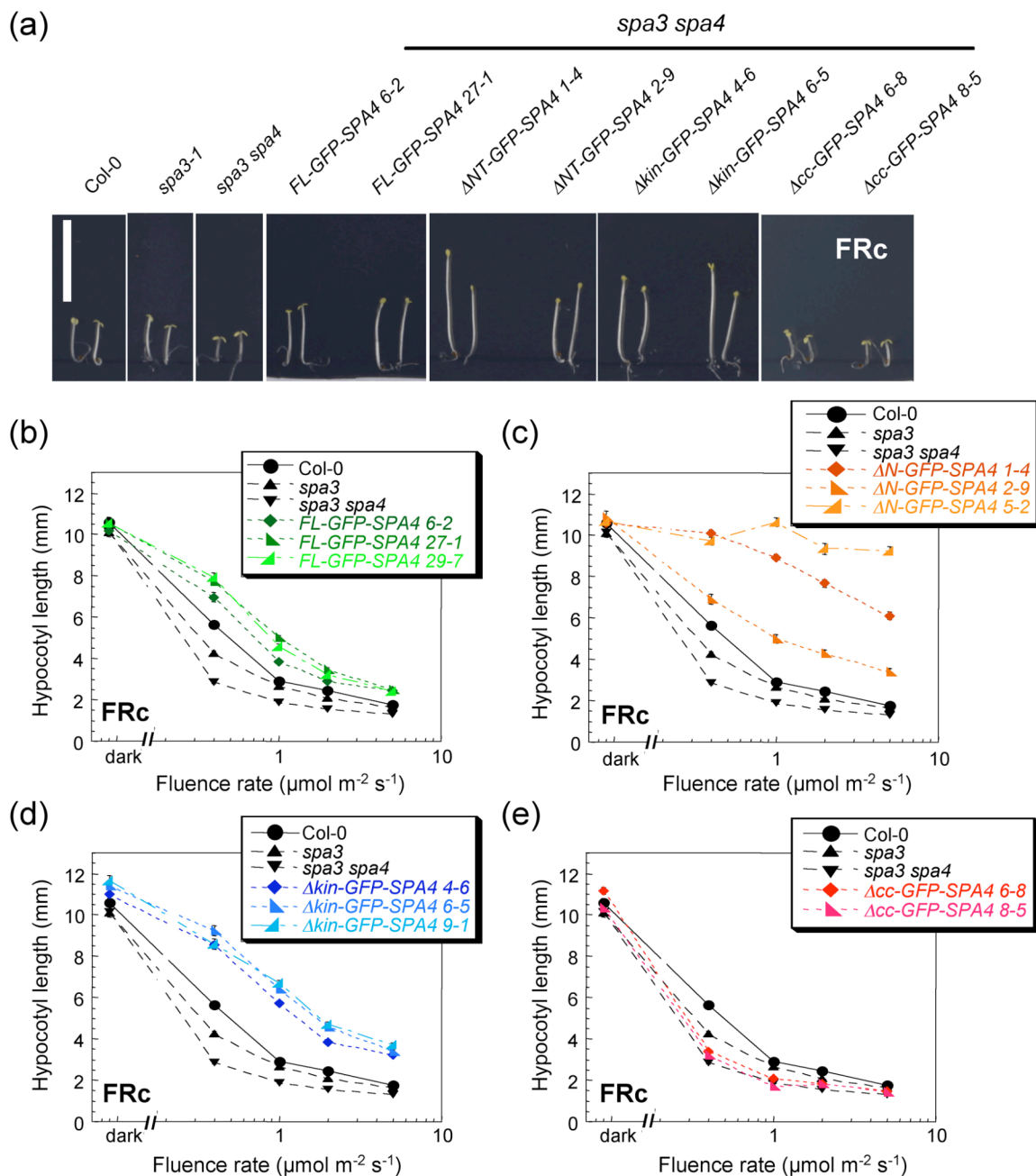


Figure 15. The SPA4 N-terminus is not required for SPA4 function in light-grown seedlings whereas the coiled-coil domain is essential.

(a) Visual phenotypes of transgenic *spa3 spa4* mutant seedlings expressing the *GFP-SPA4* full-length (FL) and *GFP-SPA4* deletion constructs shown in Fig 14 a. For each construct two independent lines are shown. Seedlings were grown in FRc ($0.4 \mu\text{mol m}^{-2} \text{s}^{-1}$) for 3 days. Wild-type (Col-0), *spa3* and *spa3 spa4* mutant seedlings are shown as controls. Scale bar: 10 mm.

(b-e) Hypocotyl lengths of seedlings grown under various fluence rates of FRc. Genotypes are the same as in (a). (b) FL, green (c) ΔNT, orange (d) Δkin, blue (e) Δcc, red. Per construct, 2-3 independent transgenic lines were analyzed ($n=30$). Error bars indicate the SEM.

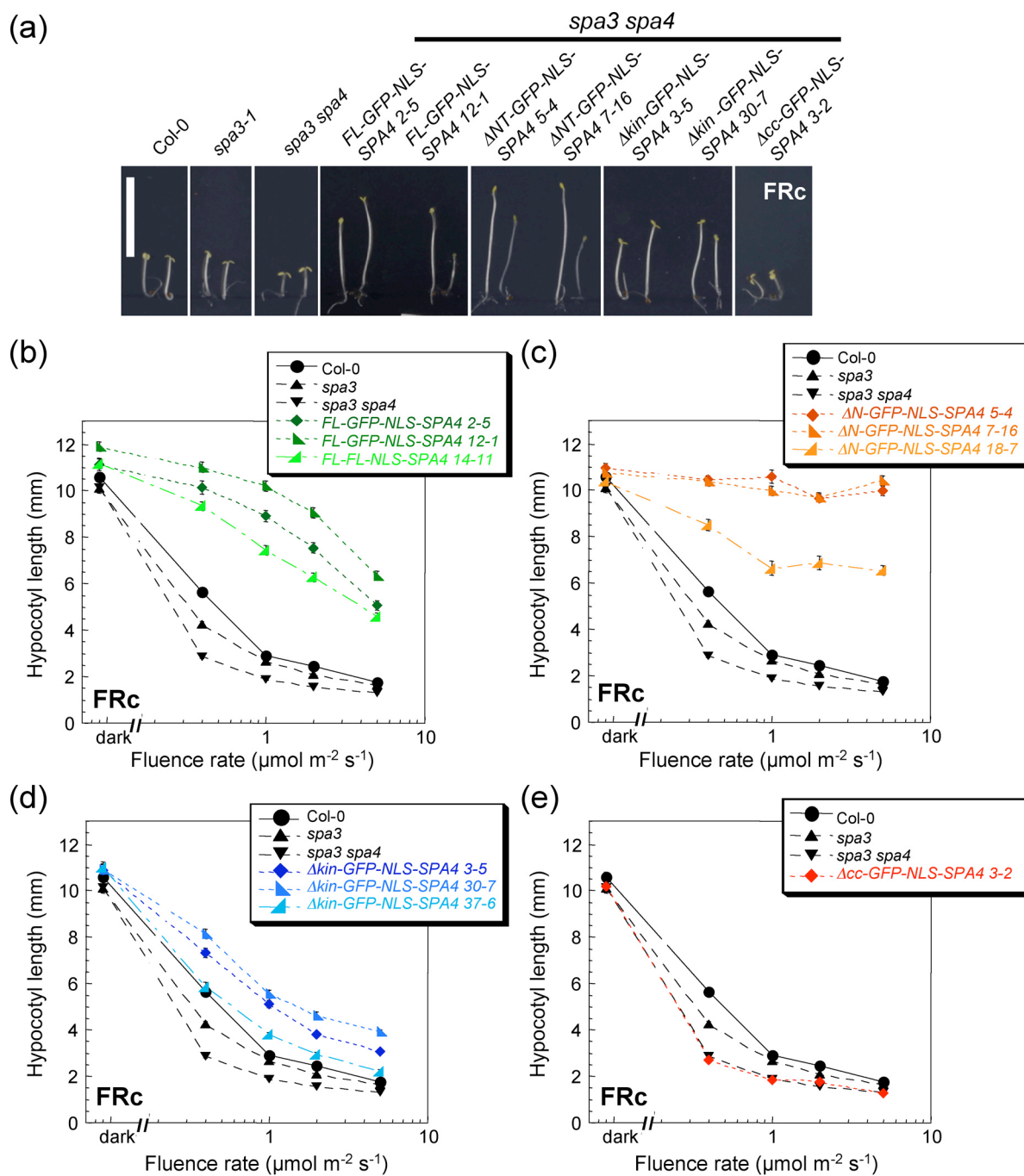


Figure 16. *FL-NLS-GFP-SPA4* and *ΔNT-NLS-GFP-SPA4* transgenic lines exhibit an extreme overcomplementation phenotype in FRc-grown seedlings.

(a) Visual phenotypes of transgenic *spa3 spa4* mutant seedlings expressing the *GFP-NLS-SPA4* full-length (FL) and deletion constructs shown in Fig 14 a. For each construct two independent lines are shown. Seedlings were grown in FRc ($0.4 \mu\text{mol m}^{-2} \text{s}^{-1}$) for 3 days. Wild-type (Col-0), *spa3* and *spa3 spa4* mutant seedlings are shown as controls. Scale bar: 10 mm.

(b-e) Hypocotyl lengths of seedlings grown under various fluence rates of FRc. Genotypes are the same as in (a). (b) FL, green (c) Δ NT, orange (d) Δ kin, blue (e) Δ cc, red. Per construct, 2-3 independent transgenic lines were analyzed ($n=30$). Error bars indicate the SEM.

Also under higher light conditions (FRC, $40 \mu\text{mol m}^{-2} \text{s}^{-1}$), when wild-type seedlings displayed an extremely short hypocotyl, the hypocotyl lengths of the *GFP-SPA4* transgenic lines showed different degrees of overcomplementation (Figure 17). The *FL-GFP-SPA4* as well as the Δkin and the *NLS- Δkin* transgenic seedlings were longer than the wild type (Figure 17b). The *FL-GFP-NLS-SPA4* lines showed almost 2-fold longer hypocotyls compared to the *FL-GFP-SPA4* lines without the artificial NLS (Figure 17b). The $\Delta\text{NT-SPA4}$ expressing lines exhibited even longer hypocotyls than all other transgenic lines. The hypocotyl lengths of two *NLS- $\Delta\text{NT-SPA4}$* expressing lines were almost as long in high FRC, as in darkness (Figure 17b, 16c). Furthermore, all investigated *GFP-SPA4* lines behaved similarly under various fluence rates of red light and blue light as well and displayed in part strong overcomplementation of the *spa3 spa4* seedling phenotype (Supplemental Figure 3). Hence, deletion of the kinase-like domain or the N-terminus of SPA4 did not impair SPA4 protein function regarding inhibition of photomorphogenesis in light-grown seedlings. Because the $\Delta\text{NT-GFP-SPA4}$ deletion constructs were able to complement the *spa3 spa4* mutant phenotype, no endogenous NLS seem to be essential for proper SPA4 function. When the complete N-terminus of SPA4 was deleted, the seedlings exhibited even longer hypocotyls than the corresponding transgenic lines containing *FL-SPA4* or *$\Delta\text{kin-SPA4}$* , suggesting an impaired responsiveness to light in these lines. This implies a function of the SPA4 N-terminus in regulating the level of SPA4 activity in controlling seedling photomorphogenesis.

Subsequently, GFP-SPA4 protein levels were determined in dark- and FRC-grown transgenic seedlings to investigate whether the altered complementation potency in the different transgenic lines is correlated to SPA4 protein abundance. Moreover, the question whether the $\Delta\text{NT-SPA4}$ protein levels are elevated in FRC similarly to the $\Delta\text{NT-SPA1}$ protein levels (Fittinghoff et al., 2006; Yang and Wang, 2006) was addressed by this approach.

GFP-SPA4 protein abundance was not altered in FRC when compared to dark-grown seedlings in any of the analyzed transgenic *GFP-SPA4* lines, likely due to use of the constitutive 35S promoter (Figure 18a-d). Line *$\Delta\text{NT-GFP-SPA4}$ 5-2* exhibited very high protein levels, which appears to be caused by the strong transcript level in this line (Figure 18a, c, e). However, in comparison to *FL-GFP-SPA4* the GFP-SPA4 protein levels were more abundant in the two other *$\Delta\text{NT-GFP-SPA4}$* lines (Figure 18

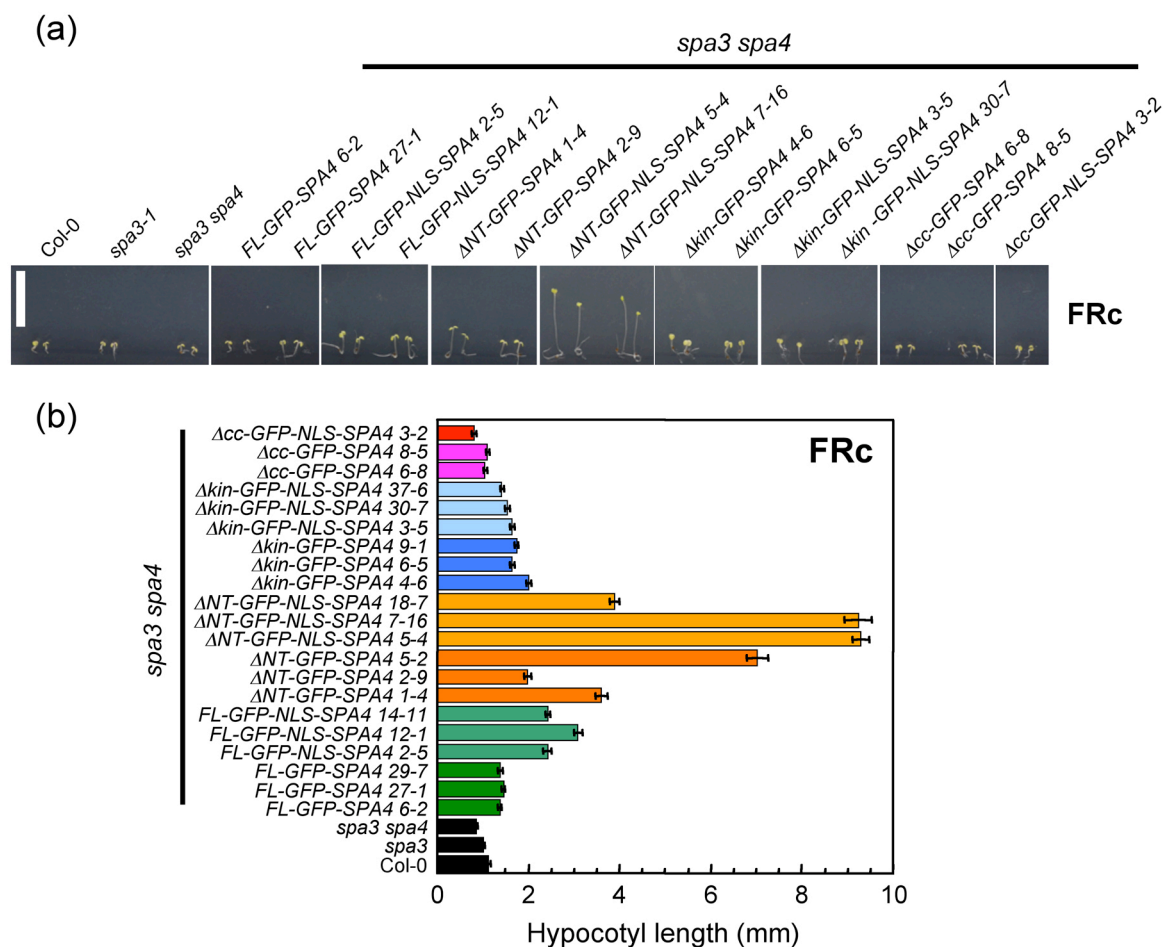


Figure 17. *GFP-SPA4* transgenic lines exhibit a strong overcomplementation phenotype in light-grown seedlings.

(a) Visual phenotypes of transgenic *spa3 spa4* mutant seedlings expressing the *GFP-SPA4* full-length (FL, green) and *SPA4* deletion constructs (Δ NT, orange; Δ kin, blue; Δ cc, red) shown in Fig 14 a. For each construct two independent lines are shown. Seedlings were grown in FRc (40 μ mol m⁻² s⁻¹) for 3 days. Wild-type (Col-0), *spa3* and *spa3 spa4* mutant seedlings are shown as controls. Scale bar: 10mm.

(b) Hypocotyl length of seedlings shown in (a). Per construct 2-3 independent transgenic lines were measured (n=30). Error bars indicate the SEM.

a, c). Quantification of Δ cc-GFP-SPA4 protein abundance revealed higher protein abundance in FRc, which reflects the higher transcript levels of Δ cc-GFP-SPA4 in FRc in these particular lines (Figure 18d). But when compared to Δ kin-GFP-SPA4, the GFP-SPA4 protein levels in the Δ cc-GFP-SPA4 lines were elevated, although the RNA levels in these lines were comparable (Figure 18b, d). Taken together, neither the transcript abundance of the *SPA4* full-length and deletion constructs nor the accumulation of the respective protein seemed to be regulated by light. Furthermore, the differences in protein levels observed between lines expressing distinct *GFP-SPA4* derivatives appeared to be caused mainly by different *SPA4* transcript levels in the respective transgenic lines. Nevertheless, the overall higher protein abundance of

Δcc -GFP-SPA4 suggests a role of the coiled-coil domain in regulation of SPA4 protein stability, as this cannot be explained by Δcc -GFP-SPA4 expression levels.

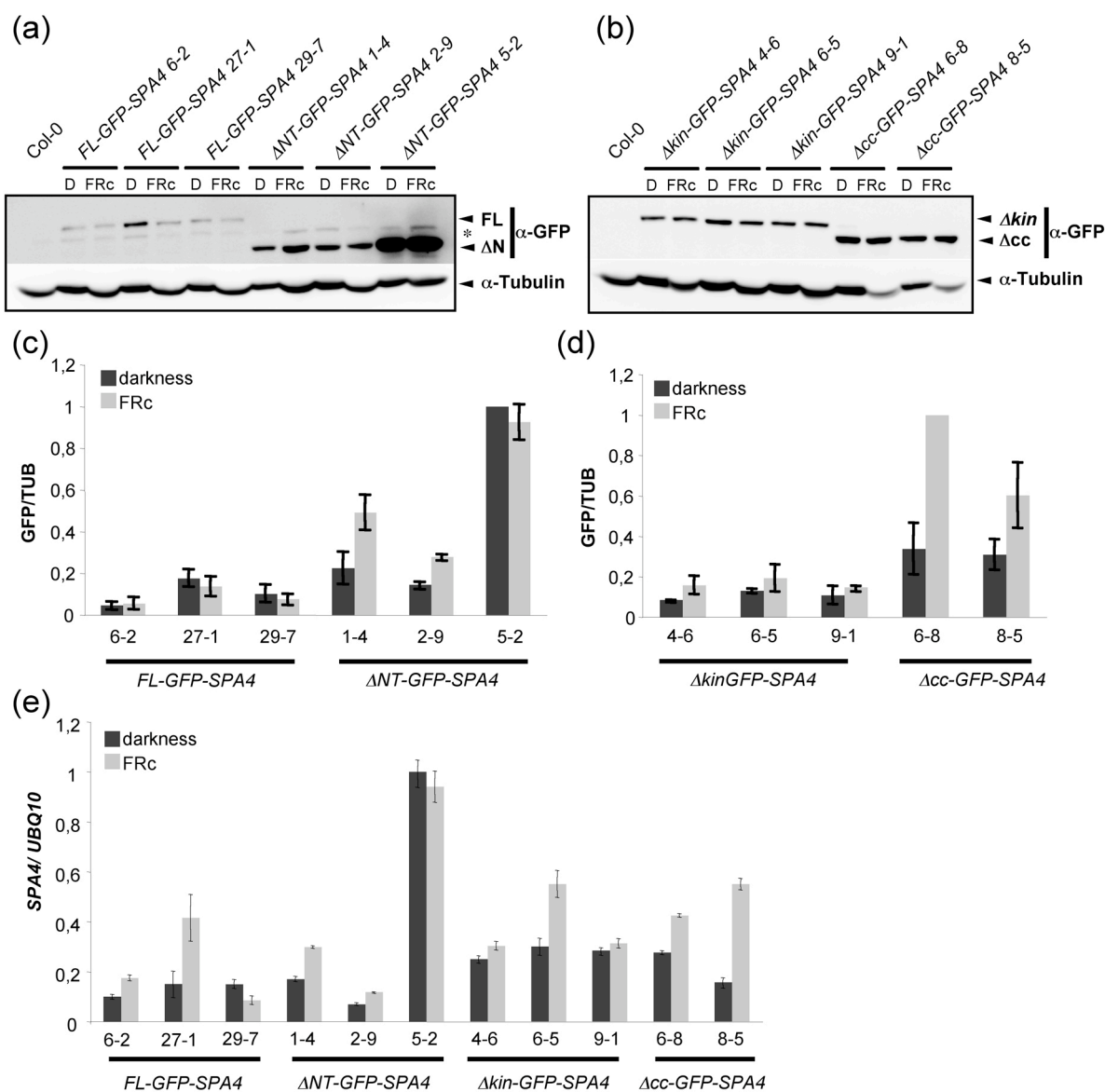


Figure 18. GFP-SPA4 protein accumulation is not affected by light.

(a-d) Immunodetection (a, b) and quantification (c, d) of GFP-SPA4 protein levels in 4-day-old *spa3 spa4* seedlings grown in darkness or FRc (3 $\mu\text{mol m}^{-2} \text{s}^{-1}$). GFP-SPA4 full-length (FL) and deletion derivatives (ΔNT , Δkin , Δcc) were expressed from a dual 35S promoter and detected using an α -GFP antibody. For each complementing construct three independent transgenic lines were analyzed. Per sample 40 μg protein extract was loaded. Tubulin levels were used as loading control. GFP/Tubulin levels were calibrated to that of the highest accumulating line, which was set to 1. Three (c) or two (d) technical replicates were used per sample. Error bars indicate the SEM. The asterisk indicates an unspecific signal detected by the α -GFP antibody.

(e) Transcript levels of *GFP-SPA4* in darkness or FRc in the lines shown in (a) and (b). Transcript levels were quantified relative to *UBQ10* and *SPA4/UBQ10* levels were calibrated to the highest expressing line, which was set to 1. Two technical replicates were used per sample. Error bars indicate the SEM.

There was also no significant difference in GFP-SPA4 protein abundance detected in the *GFP-NLS-SPA4* transgenic lines when comparing FRc- and dark-grown seedlings (Figure 19a-d). For quantification of protein levels only one technical replicate was used, but an independent experiment exhibited similar tendencies in GFP-SPA4 protein accumulation (data not shown). The elevated protein levels in the transgenic ΔNT -*GFP-NLS-SPA4* lines were due to increased transcript levels (Figure 19e), whereas the high protein levels in the Δcc -*GFP-NLS-SPA4* line 3-2 cannot be explained by elevated transcript abundance as the SPA4 mRNA levels in this line were only slightly increased compared to the *FL-GFP-SPA4* lines (Figure 19e). Δkin -*GFP-NLS-SPA4* line 37-6 showed nearly no detectable GFP-SPA4 protein because transcript abundance in this line was extremely low compared to the other ΔNT -*GFP-NLS-SPA4* transgenic lines (Figure 19b, c). Thus, GFP-NLS-SPA4 levels were not light-regulated.

Taken together, the differences of complementation strength in the various transgenic *GFP-SPA4* lines could mainly be explained by the differences in SPA4 mRNA levels and GFP-SPA4 protein levels. Yet, the fact that Δcc -*GFP-NLS-SPA4* 3-2 exhibited strongly increased GFP-SPA4 protein levels similar to the Δcc -*GFP-SPA4* lines suggest a general role of the coiled-coil domain in stability control of the SPA4 protein. An effect of the N-terminus on SPA4 stability was less noticeable in transgenic seedlings since the elevated ΔNT -*GFP-SPA4* and ΔNT -*GFP-NLS-SPA4* protein levels were mostly caused by higher abundance of the respective transgenes.

Microscopic localization studies of GFP-SPA4 in *spa3 spa4* seedlings expressing the different GFP-SPA4 or GFP-NLS-SPA4 proteins showed only weak GFP signals even in strong expressing lines like ΔNT -*GFP-SPA4* 5-2 and also no noticeable differences in nuclear and cytosolic GFP abundance were detectable (data not shown). Moreover, immunoblot analysis revealed the presence of free GFP in the protein samples of transgenic seedlings (data not shown). This made it impossible to obtain reliable data about cellular localization of GFP-SPA4 in the various transgenic GFP-SPA4 lines by fluorescence microscopy.

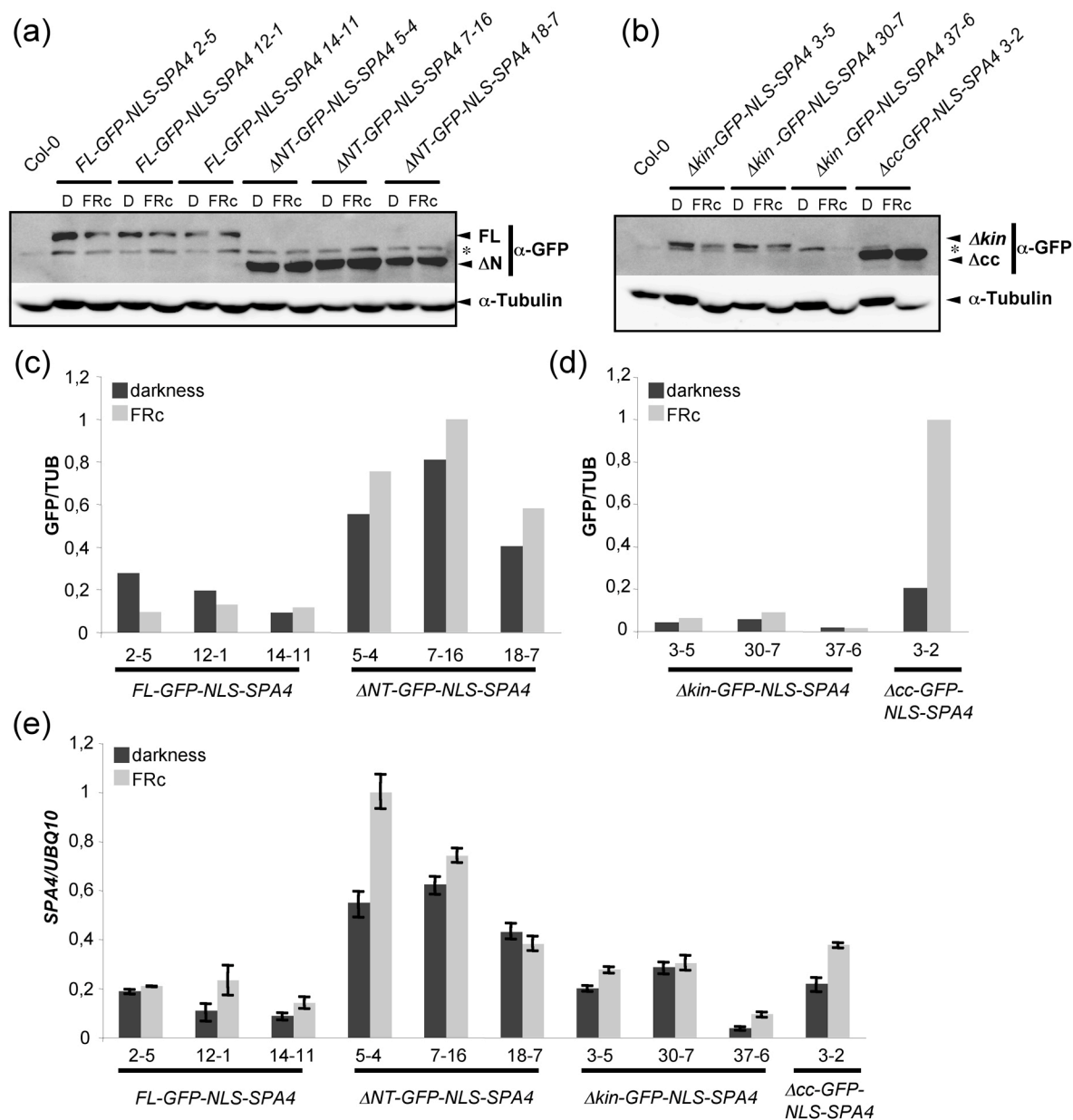


Figure 19. GFP-NLS-SPA4 protein accumulation is not affected by light.

(a-d) Immunodetection (a, b) and quantification (c, d) of GFP-NLS-SPA4 protein levels in 4-day-old *spa3 spa4* seedlings grown in darkness or FRc ($3 \mu\text{mol m}^{-2} \text{s}^{-1}$). GFP-NLS-SPA4 full-length (FL) and deletion derivatives were expressed from the 35S promoter and detected using an α -GFP antibody. For each construct, except for Δcc , three independent transgenic lines were analyzed. Per sample 40 μg protein extract was loaded. Tubulin levels were used as loading control. The asterisk indicates an unspecific signal detected by the α -GFP antibody. One replicate per sample was used for quantification (c, d).

(e) Transcript levels of *GFP-NLS-SPA4* in darkness or FRc in the lines shown in (a) and (b). Transcript levels were quantified relative to *UBQ10* and *SPA4/UBQ10* levels were calibrated to the highest expressing line, which was set to 1. Two technical replicates were used per sample. Error bars indicate the SEM.

II.3.2. Role of the SPA4 N-terminus in adult plant development

The analysis of various *spa* triple mutants suggested *SPA4* to be the major regulator of plant size (Laubinger et al., 2004; this study). To investigate the importance of the SPA4 N-terminal domain and the kinase-like domain in leaf growth control, the *spa3 spa4* double mutants, expressing *FL-SPA4* and deletion derivatives, were also analyzed regarding leaf size as *spa3 spa4* double mutant plants show a significant reduction in leaf size compared to *spa3* single mutants or wild-type plants (Laubinger et al., 2004; Fittinghoff et al., 2006).

The leaf phenotypes of two independent lines of *FL-GFP-SPA4*, ΔNT , Δkin and Δcc transgenic lines (without the artificial *NLS*) respectively, are presented in Figure 20a. Quantification of leaf length revealed that all investigated transgenic *GFP-SPA4* and *GFP-NLS-SPA4* lines except Δcc -*SPA4* fully complemented the leaf size phenotype of the parental *spa3 spa4* mutants (Figure 20b). Furthermore, in contrast to the results obtained from seedling analysis, there were no differences in leaf length detectable between the *FL-GFP-SPA4*, ΔNT , and Δkin transgenic lines with or without artificial *NLS*, except for ΔNT -*GFP-NLS-SPA4* 5-4, which exhibited extremely long leaves (Figure 20b). These results indicate that neither the kinase-like domain nor the complete N-terminus of SPA4 is required for SPA4-regulated leaf growth control and as well suggest that SPA4 activity is not increased in the ΔNT -*GFP-SPA4* lines in adult plant tissue.

Determination of GFP-SPA4 protein levels in 3-week-old long-day-grown transgenic lines expressing *GFP-SPA4* full-length or deletion derivatives with or without an *NLS* showed lower GFP-SPA4 protein abundance in *FL-SPA4* lines compared to the lines expressing the SPA4 deletion derivatives (Figure 21a). A reliable quantification of the GFP-SPA4 levels in leaves could not be obtained since the tubulin loading control did not show distinct signals. However, some prominent differences in GFP-SPA4 protein abundance were noticeable in the immunodetection (Figure 21a, b). Reduced transcript levels cannot explain the decreased FL-GFP-SPA4 protein levels since for instance *FL-GFP-SPA4* line 27-1 exhibited higher *SPA4* RNA levels than ΔNT -*GFP-SPA4* lines 1-4 and 2-9 (Figure 21a, c). The GFP-SPA4 protein was also less abundant in the *FL-GFP-NLS-SPA4* and the Δkin -*GFP-NLS-SPA4* lines than in the ΔNT -*GFP-NLS-SPA4* expressing transgenic lines (Figure 21b). The altered GFP-

SPA4 protein levels can only partially be explained by differences in transcript abundance, suggesting a de-stabilization of FL-GFP-SPA4 in Arabidopsis leaves, whereas the SPA4 protein lacking the complete N-terminus appears to be stabilized. This implies a function for the SPA4 N-terminus in controlling SPA4 protein abundance in adult plants.

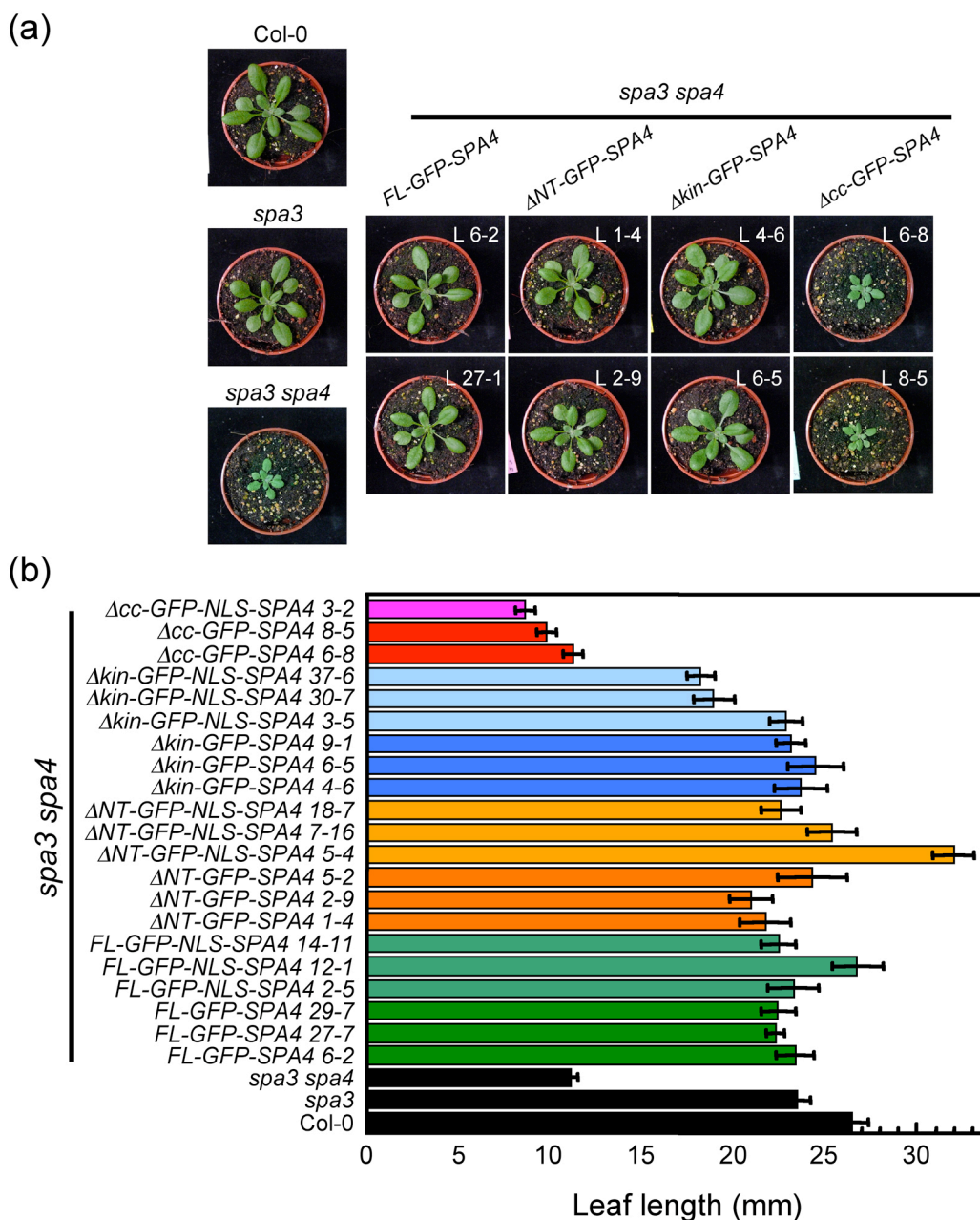


Figure 20. Plant size of transgenic *spa3 spa4* mutant plants expressing *FL-GFP-SPA4* and deletion constructs.

(a) Visual phenotype of transgenic *spa3 spa4* plants expressing *GFP-SPA4-FL* and *GFP-SPA4* deletion derivatives grown in LD for 21 days. For each construct 2 independent transgenic lines are shown. As controls, wild-type (Col-0), *spa3* and *spa3 spa4* double mutant plants are shown.

(b) Quantification of leaf length of the genotypes shown in (a) and *GFP-NLS-SPA4* expressing *spa3 spa4* lines. For each transgene 2-3 independent transgenic lines were analyzed. Error bars indicate the SEM.

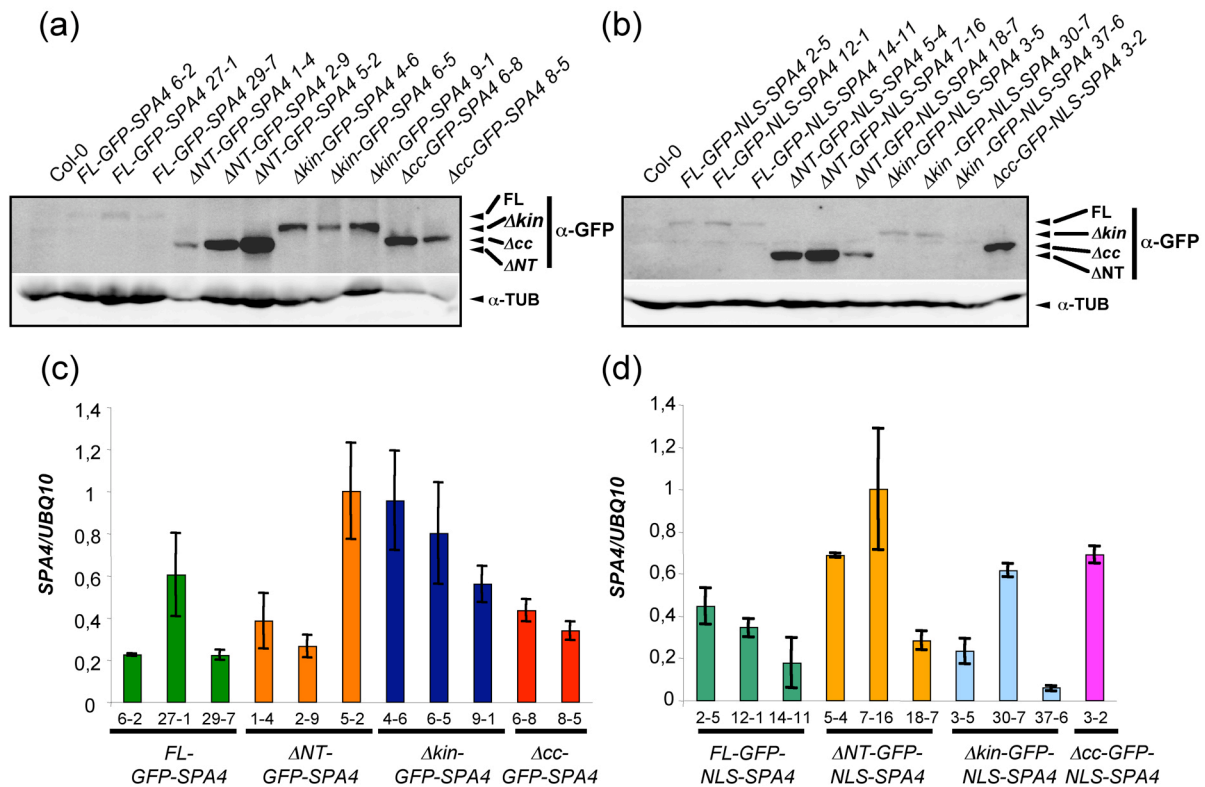


Figure 21. ΔNT -GFP-SPA4 accumulates to higher levels than FL-GFP-SPA4 in adult plants.

(a, b) Immunodetection of GFP-SPA4 (a) and GFP-NLS-SPA4 (b) protein levels 21-day-old transgenic plants grown under long-day conditions. GFP-SPA4 full-length (FL) and deletion derivatives (ΔNT , Δkin , Δacc) were detected using an α -GFP antibody. For each complementing construct 3 independent transgenic lines were analyzed. Per sample 60 μ g protein extract was loaded. Tubulin levels were used as loading control.

(c, d) Transcript levels of *GFP-SPA4* in the lines shown in (a) and (b). Transcript levels were quantified relative to *UBQ10* and *SPA4/UBQ10* levels were calibrated to that of the highest expressing line, which was set to 1, respectively. Per sample two biological replicates were used. Error bars indicate the SEM.

II.4. SPA1 structure function analysis

Previous reports have shown that SPA1 deletion proteins lacking the N-terminal domain including the kinase-like motif are more abundant than the full-length SPA1 protein in light-grown seedlings (Fittinghoff et al., 2006; Yang and Wang, 2006). Thus, it was tested whether the N-terminus is specifically involved in the light-mediated de-stabilization of the SPA1 protein (Balcerowicz et al., 2010) or leads to a general de-stabilization of SPA1 in dark- and light-grown seedlings. Moreover, SPA1 and SPA2 proteins are more abundant in dark- and light-grown *cop1* mutant seedlings (Zhu et al., 2008; Alexander Maier, unpublished), indicating that SPA

degradation is at least in part dependent on COP1. Therefore, SPA de-stabilization might also be dependent on SPA/COP1 interaction, which is mediated by the coiled-coil domains of both proteins (Hoecker and Quail, 2001; Laubinger and Hoecker, 2003; Laubinger et al., 2004).

II.4.1. Light-induced de-stabilization of SPA1 is dependent on the N-terminus and the coiled-coil domain

SPA1 protein levels were determined in transgenic *spa1* mutants expressing full-length *SPA1-HA* (*FL-SPA1-HA*), Δ *NT-SPA1-HA* or Δ *cc-SPA1-HA*, respectively, under the control of the endogenous *SPA1* promoter (Fittinghoff et al., 2006). Compared to *FL-SPA1-HA* protein levels both Δ *NT-SPA1-HA* and Δ *cc-SPA1-HA* proteins were much more abundant in FRC-grown seedlings, whereas in dark-grown seedlings deletion of the N-terminal domain or the coiled-coil domain of SPA1 had only a minor effect on SPA1-HA protein levels (Figure 22b, c). SPA1-HA protein levels in the transgenic lines carrying the Δ *NT-SPA1-HA* and Δ *cc-SPA1-HA* deletion derivatives were about 8-fold higher compared to the *FL-SPA1-HA* lines in FRC (Figure 22b, c). The elevated Δ *NT-SPA1-HA* protein levels in FRC could mainly be explained by the elevated SPA1 transcript levels in these lines (Figure 22d). However, *FL-SPA1-HA* transcripts were also increased in FRC-grown seedlings compared to darkness, but the protein levels of *FL-SPA1-HA* are more or less the same in darkness and FRC (Figure 22c, d), like it was seen for independent *pSPA1:SPA1-HA* lines before (Balcerowicz et al., 2010). The high abundance of Δ *cc-SPA1-HA*, especially in FRC, could not be explained by elevated transcript levels, as Δ *cc-SPA1-HA* RNA abundance was not altered by light (Figure 22c, d). These results indicate the importance of SPA-COP1 interaction in the light-regulated de-stabilization process of SPA1 since SPA1-COP1 interaction is abolished in the Δ *cc-SPA1-HA* lines, and further suggest a function for the SPA1 N-terminus in controlling SPA1 protein stability in the light.

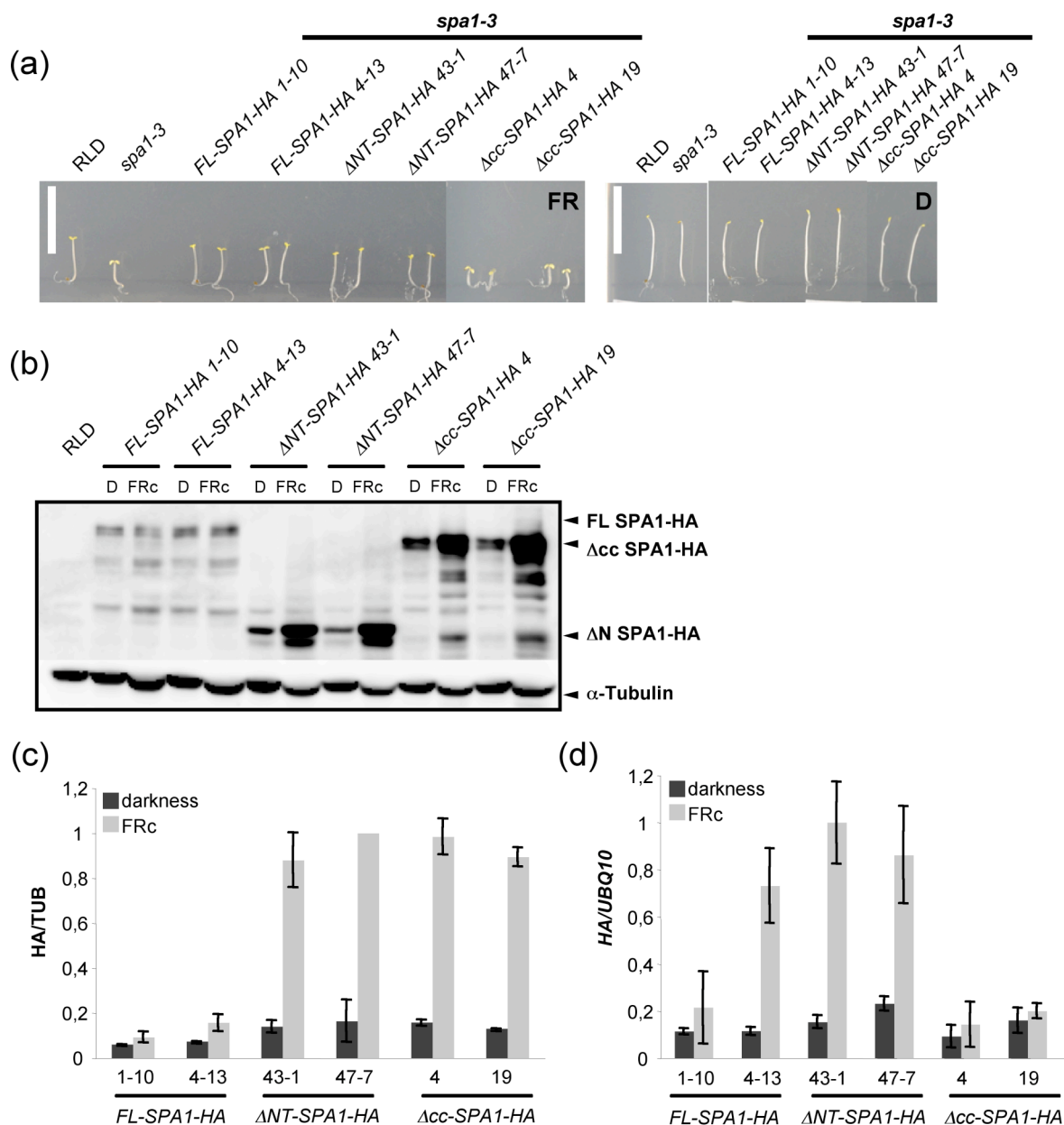


Figure 22. ΔN-SPA1 and Δcc-SPA1 protein levels increase strongly in FRc in contrast to FL-SPA1.

(a) Phenotypes of wild-type (RLD), *spa1-3* and transgenic *spa1-3* seedlings that were transformed with *FL-SPA1-HA*, *ΔNT-SPA1-HA* or *Δcc-SPA1-HA* grown in FRc (0.3 μmol m⁻² s⁻¹) or darkness for 4 days. For each construct two independent transgenic lines are shown.

(b) Immunodetection showing *FL-SPA1-HA*, *ΔNT-SPA1-HA* and *Δcc-SPA1-HA* protein levels of 4-d-old seedlings grown in darkness or FRc (0.3 μmol m⁻² s⁻¹). SPA1-HA was detected using anti-HA antibody. Two independent transgenic lines per construct were analyzed in the *spa1-3* background. 30 μg of protein extract was loaded per sample. Tubulin levels are shown as loading control.

(c) Quantification of *FL-SPA1-HA*, *ΔNT-SPA1-HA* and *Δcc-SPA1-HA* protein levels in darkness or FRc obtained from two biological replicates of the lines shown in (a). Protein levels were expressed relative to tubulin levels. HA/TUB values were calibrated to that of the highest-accumulating line, which was set to 1. Error bars indicate the SEM.

(d) Transcript levels of *FL-SPA1-HA*, *ΔNT-SPA1-HA* and *Δcc-SPA1-HA* in darkness or FRc in the lines shown in (a). Transcript levels were quantified relative to *UBQ10* and *HA/UBQ10* values were calibrated to that of the highest-accumulating line, which was set to 1. Two biological replicates were used per sample and each was analyzed in duplicate. Error bars indicate the SEM.

II.4.2. The SPA1 N-terminus partially contributes to seedling photomorphogenesis in a *spa* triple mutant background

To test whether the N-terminal domain of SPA1, which plays an important role in photoperiodic flowering time regulation (Kirsten Fittinghoff, PhD thesis, 2008), also contributes to plant size control, full-length *SPA1-HA* (*FL-SPA1-HA*), Δ *kin-SPA1-HA* and Δ *NT-SPA1-HA* deletion constructs (Fittinghoff et al., 2006) were transformed into a *spa1 spa3 spa4* triple mutant background. *spa1 spa3 spa4* mutant seedlings exhibit no altered seedling phenotype in darkness, but an extremely enhanced responsiveness even to low fluence rates of light (Laubinger et al., 2004). This makes them easy to distinguish from the corresponding *spa3 spa4* double mutant control which exhibits a less enhanced de-etiolation phenotype in light (Laubinger and Hoecker, 2003). Therefore, for each construct, 20-30 transgenic T2 lines, carrying *FL-SPA1-HA*, Δ *kin-SPA1-HA* or Δ *NT-SPA1-HA* constructs, respectively, were first investigated for complementation of the triple mutant seedling phenotype in FRc ($0.2 \mu\text{mol m}^{-2} \text{s}^{-1}$) (Table 2).

As it was shown before in the *spa1* mutant background, the *FL-SPA1-HA* as well as the Δ *kin-SPA1-HA* and Δ *NT-SPA1-HA* deletion derivatives were able to complement the loss of *SPA1* also in a *spa1 spa3 spa4* triple mutant background (Fittinghoff et al., 2006, Table 2). Surprisingly, measurement of hypocotyl length of transgenic T2 lines in FRc-grown seedlings revealed differences in complementation potency between *FL-SPA1-HA*, Δ *kin-SPA1-HA* and Δ *NT-SPA1-HA* transgenic lines (Table 2), which has not been observed in the *spa1* background (Fittinghoff et al., 2006; Figure 22a). To describe the variation in complementation strength of the different *SPA1-HA* constructs, individual T2 lines were classified according to hypocotyl length from Class I (no rescue) to Class V (hypocotyls longer than the wild type) (Table 2). While 15 out of 20 *FL-SPA1-HA* lines displayed strong overcomplementation by showing a hypocotyl that was even longer than the hypocotyl of Col-0 wild-type seedlings (Class V, Figure 23b), the extent of overcomplementation was lower in the Δ *kin-SPA1-HA* lines (Table 2, Figure 23b). Most analyzed transgenic Δ *kin-SPA1-HA* lines showed an increased hypocotyl length compared to the corresponding *spa3 spa4* double mutant control (Class IV). Nevertheless, the Δ *NT-SPA1-HA* transgenic lines were also capable to complement the *spa1 spa3 spa4* triple mutant phenotype, but to a minor extent than the Δ *kin-SPA1-HA* lines. Most analyzed Δ *NT-SPA1-HA* lines

exhibited a hypocotyl length comparable to the *spa3 spa4* mutant control (Class III, Figure 23b) or only partial complementation of the enhanced de-etiolation phenotype (Class II, Table 2).

Table 2: Complementation analysis of T2 seedlings carrying *FL-SPA1-HA* or deletion constructs.

FL-SPA1 cDNA and *SPA1* deletion derivatives were placed under the control of the *SPA1* endogenous 5' and 3' regulatory sequences and fused to a triple-*HA* tag. All constructs were transformed into a *spa1 spa3 spa4* mutant background. Resulting T2 lines were grown under $0.2 \mu\text{mol m}^{-2} \text{s}^{-1}$ FRc for three days. The number of individual transgenic T2 lines with long hypocotyls and the total number of analyzed transgenic T2 lines is given. Additionally, complementation strength of individual T2 lines was estimated by classifying individual T2 lines according to hypocotyl length of FRc-grown seedlings.

constructs transformed into <i>spa1 spa3 spa4</i>	FRc (rescued/total)	Class I no rescue (1.5-2 mm)	Class II partial rescue (2-4 mm)	Class III full rescue (4-7 mm)	Class IV over-complementation (8-9 mm)	Class V over-complementation (> 9 mm)
<i>FL-SPA1-HA</i>	20/20	0	1	1	3	15
<i>dkin-SPA1-HA</i>	21/23	2	1	3	12	5
<i>dNT-SPA1-HA</i>	17/30	13	7	7	3	0
control		hypocotyl length in FRc ($0.2 \mu\text{mol m}^{-2} \text{s}^{-1}$)				
WT (Col-0)					X (7-9 mm)	
<i>spa3 spa4</i>				X (4-7 mm)		
<i>spa1 spa3 spa4</i>		X (1.5-2 mm)				

For further analysis, T2 lines carrying one T-DNA insertion were selected for the generation of homozygous T3 lines. In case of *FL-SPA1-HA*, T2 line 8 (Class IV) and two Class V lines (12, 13) were selected. The homozygous *Δkin-SPA1-HA* T3 lines (3, 4, 8) were taken from Class IV, as Class V lines carried 2 insertions or T3 lines were not homozygous for the *SPA1* transgene. Two *ΔNT-SPA1-HA* lines (5, 6) were selected from Class II (partial rescue) and three T3 lines belonged to Class III (full rescue) because the three *ΔNT-SPA1-HA* lines showing overcomplementation carried two T-DNA insertions. Figure 23 shows the seedling phenotypes of the selected independent transgenic *spa1 spa3 spa4* mutant T3 lines carrying the *FL-SPA1-HA*, the *Δkin-SPA1-HA* and the *ΔNT-SPA1-HA* construct, respectively, grown in darkness (Figure 23a) or in $0.3 \mu\text{mol m}^{-2} \text{s}^{-1}$ FRc (Figure 23b). Quantification of the hypocotyl length in these lines again exhibited the different complementation potency of the individual *SPA1* constructs that were observed in the T2 generation. When grown in FRc, two out of three *FL-SPA1-HA* transgenic lines displayed a hypocotyl

length which was even longer than the wild type, whereas seedlings expressing Δkin -SPA1-HA were about as long as wild-type seedlings (Figure 23d). In contrast, none of the analyzed SPA1- ΔNT -HA lines showed overcomplementation, yet transgenic ΔNT lines had hypocotyls, which were as long as the *spa3 spa4* mutant control or exhibited partial rescue of the *spa* triple mutant seedling phenotype (Figure 23d). These results indicate that in a *spa* triple mutant background the N-terminal domain of SPA1 becomes more relevant for SPA1 function in the regulation of seedling development than in a *spa1* single mutant background. The importance of the SPA1 N-terminus might be covered by redundancy of the four SPAs in a *spa1* mutant background.

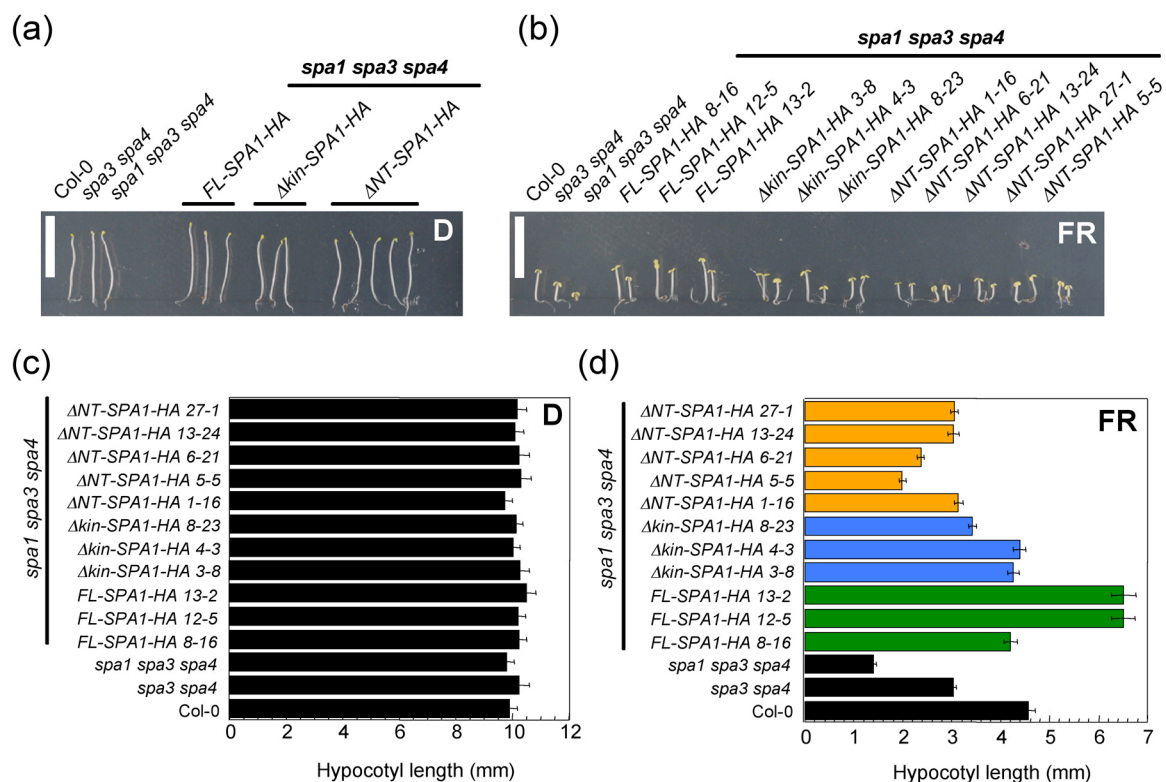


Figure 23. Seedling phenotype of transgenic *spa1 spa3 spa4* plants expressing FL-SPA1-HA or deletion constructs.

(a, b) Phenotypes of wild-type (Col-0), *spa3 spa4*, *spa1 spa3 spa4* mutants and transgenic *spa1 spa3 spa4* seedlings that were transformed with FL-SPA1-HA, ΔNT -SPA1-HA or Δkin -SPA1-HA grown in darkness (a) or FRc ($0.3 \mu\text{mol m}^{-2} \text{s}^{-1}$) (b) for 4 days. For each construct at least three independent transgenic lines are shown. Transgenic lines shown in (a) are arranged in the same order as in (b) (c, d) Quantification of hypocotyl lengths of seedlings shown in (a) and (b) grown in darkness (c) or FRc (d). In (d) SPA1-FL-HA lines are shown in green, orange bars represent ΔNT -SPA1-HA and blue bars show Δkin -SPA1-HA lines. Error bars indicate the SEM.

The role of the SPA1 N-terminus in the regulation of SPA1 full-length (FL) and SPA1 deletion protein stability was also analyzed in the *spa1 spa3 spa4* mutant background (Figure 24). The *spa* triple mutant plants expressing *FL-SPA1-HA* displayed elevated transcript levels in FRc, but mostly unchanged protein levels between seedlings grown in darkness or in FRc, similar to the FL-SPA1-HA levels observed in the *spa1* single mutant background (Figure 24a-e). Δ NT-SPA1-HA and Δ kin-SPA1-HA protein levels did not differ between seedlings grown in darkness or in FRc either when looking at the immunoblot analyses (Figure 24a and c). However, quantification revealed a to some extent higher SPA1 protein levels in FRc-grown seedlings in some *SPA1- Δ NT-HA* and *SPA1- Δ kin-HA* transgenic lines (Figure 24b and d). Also in darkness the SPA1-HA protein levels of most deletion derivatives were elevated at least 2-3-fold compared to FL-SPA1-HA, which is in part due to higher abundance of *Δ NT-SPA1-HA* and *Δ kin-SPA1-HA* transcripts (Figure 24b-e). However, the strong light-induced accumulation of Δ NT-SPA1-HA, which was seen in the transgenic lines in the *spa1* single mutant background, was abolished in the *spa1 spa3 spa4* mutant background (Figure 22, 24). The analysis of transcript and protein levels of the SPA1-HA lines has only been performed once so far using technical replicates, therefore an independent experiment has to be done to confirm these results.

Figure 24. Δ N-SPA1 and Δ kin-SPA1 protein levels are not differentially regulated by FR in a *spa1 spa3 spa4* mutant background. →

(a, c) Immunoblot showing FL-SPA1-HA, Δ NT-SPA1-HA and Δ kin-SPA1-HA protein levels of 4-d-old seedlings grown in darkness or FRc ($0.3 \mu\text{mol m}^{-2} \text{s}^{-1}$). SPA1-HA was detected using anti-HA antibody. At least three independent transgenic lines per construct were analyzed in the *spa1 spa3 spa4* background. Tubulin levels are shown as loading control.

(b, d) Quantification of FL-SPA1-HA, Δ NT-SPA1-HA and Δ kin-SPA1-HA protein levels in darkness or FRc of the lines shown in (a) and (b). Protein levels were expressed relative to tubulin levels. HA/TUB values were calibrated to that of the respective highest-accumulating line, which was set to 1. Three (b) or two (d) technical replicates were used per sample. Error bars indicate the SEM.

(e) Transcript levels of *FL-SPA1-HA*, *Δ NT-SPA1-HA* and *Δ kin SPA1-HA* in darkness or FRc in the lines shown in (a - d). Transcript levels were quantified relative to *UBQ10* and *HA/UBQ10* values were calibrated to that of the highest-accumulating line, which was set to 1. Two technical replicates were used per sample. Error bars indicate the SEM.

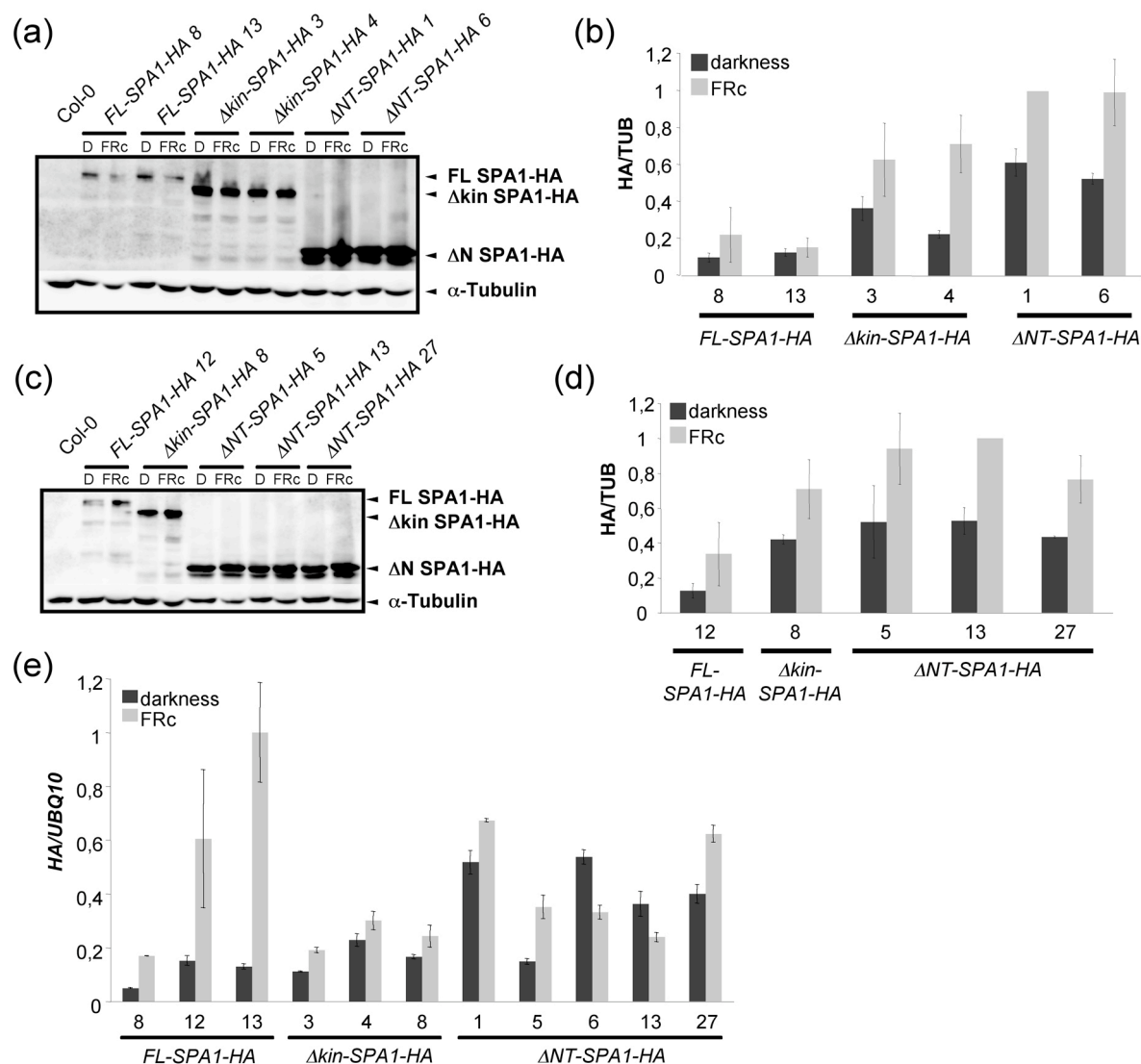


Figure 24. For description see previous page.

II.4.3. Complementation of ΔNT -SPA1 constructs in adult *spa* triple mutants

SPA1 contributes to leaf size control as it was shown recently that SPA1 acts in the phloem as well as the leaf mesophyll cells to regulate leaf growth (Ranjan et al., 2011). In order to investigate the role of the SPA1 N-terminus in SPA-regulated leaf growth control, the leaf length of 3-week-old FL-SPA1-HA, Δkin -SPA1-HA and ΔNT -SPA1-HA transgenic lines grown under long-day conditions was determined. Figure 25a shows the phenotype of wild type, *spa3 spa4*, *spa1 spa3 spa4* mutants and two independent transgenic homozygous SPA1-HA T3 lines for each construct. Quantification of the length of the longest leaf showed that almost all analyzed transgenic lines, had larger leaves than the parental *spa1 spa3 spa4* triple mutant,

which in most cases were also approximately 30% longer than those of the corresponding *spa3 spa4* double mutant control (Figure 25b). The *FL-SPA1-HA* line 12-5 exhibited only a weak complementation of the leaf size phenotype, possibly due to silencing of the *SPA1-HA* transgene. In contrast to the results obtained from the analysis of seedling photomorphogenesis, there were no significant differences in leaf length between *FL-SPA1-HA*, Δ *kin-SPA1-HA* and Δ *NT-SPA1-HA* transgenic lines. Taken together, these results suggest that the SPA1 N-terminus is not required for the regulation of leaf size in Arabidopsis.

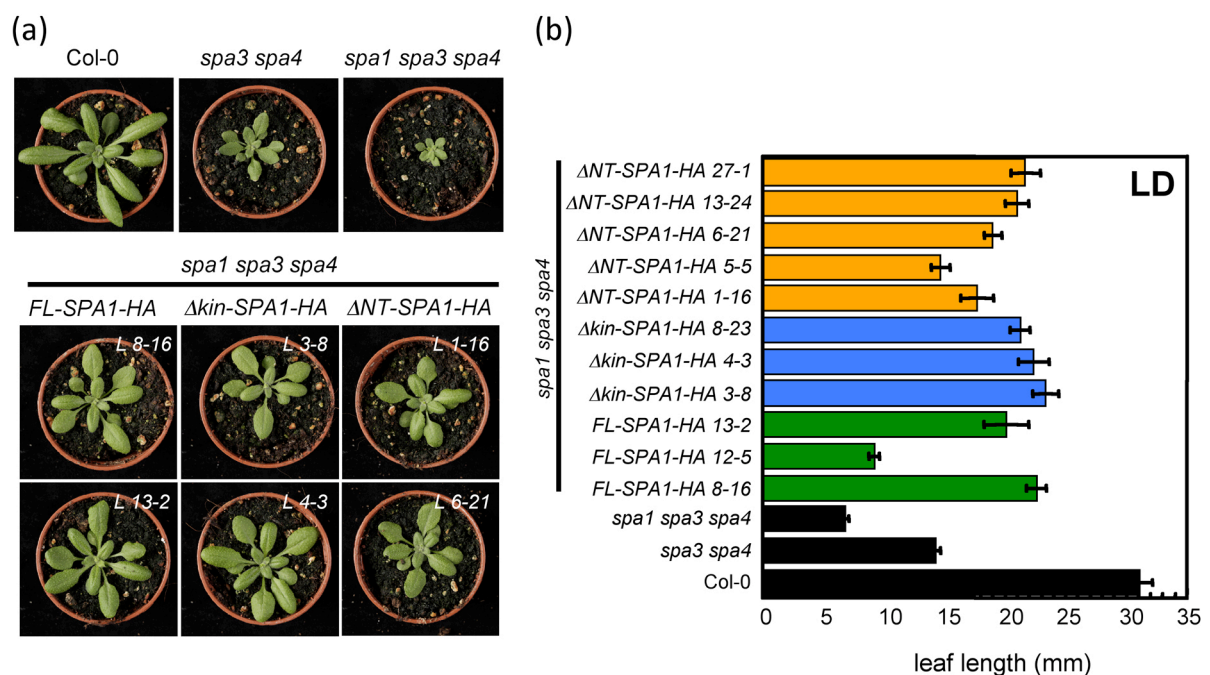


Figure 25. Plant size of transgenic *spa1 spa3 spa4* mutant plants expressing *SPA1-HA FL* and deletion constructs.

(a) Visual phenotype of transgenic *spa1 spa3 spa4* mutant plants expressing *SPA1-FL-HA* and *SPA1-HA* deletion derivatives grown in LD for 21 days. For each construct two independent transgenic lines are shown. As controls, wild-type (Col-0), *spa3 spa4* double and *spa1 spa3 spa4* triple mutant plants are shown.

(b) Quantification of leaf length of the genotypes shown in (a). For each transgene, at least three independent transgenic lines were analyzed. Error bars indicate the SEM.

II.5. Mapping of an *spa1* enhancer mutant

A number of regulators of light signal transduction like COP1 or SPA1 but also photoreceptors were identified using forward genetic screens by introducing random mutations into the plant genome and isolating the mutated gene via molecular markers (Deng et al., 1991; Hoecker et al., 1998; Chory et al., 1989a). The *spa1-3*

allele was obtained by an EMS mutagenesis in the RLD background which generated a premature stop codon in the first exon of the *SPA1* gene, thereby causing a decreased hypocotyl length of light-grown seedlings compared to wild-type seedlings (Hoecker et al., 1999). To identify further regulators of light signal transduction, an EMS mutagenesis of *spa1-3* mutant seeds was performed and thereafter a screening of M₂ seedlings for individuals that displayed enhancement or suppression of the *spa1* mutant phenotype in Rc was carried out (Nixdorf and Hoecker, 2010).

II.5.1. The *28g* locus shows an enhanced *spa1* mutant phenotype in light-grown seedlings but not in flowering time

One of the *spa1* enhancer mutants (named „*28g*“) obtained from the phenotypic screen of EMS-mutagenized *spa1-3* seeds showed a further reduced hypocotyl length compared to the *spa1* mutant when grown in light (Figure 26a, c). In red light ($0.3 \mu\text{mol m}^{-2} \text{s}^{-1}$) the hypocotyl length of *spa1 28g* double mutants was reduced two-fold compared to the hypocotyls of *spa1* single mutant seedlings (Figure 26c). The enhanced *spa1* phenotype was light-dependent because dark-grown *spa1 28g* seedlings were indistinguishable from *spa1* or wild-type seedlings (Figure 26a, b).

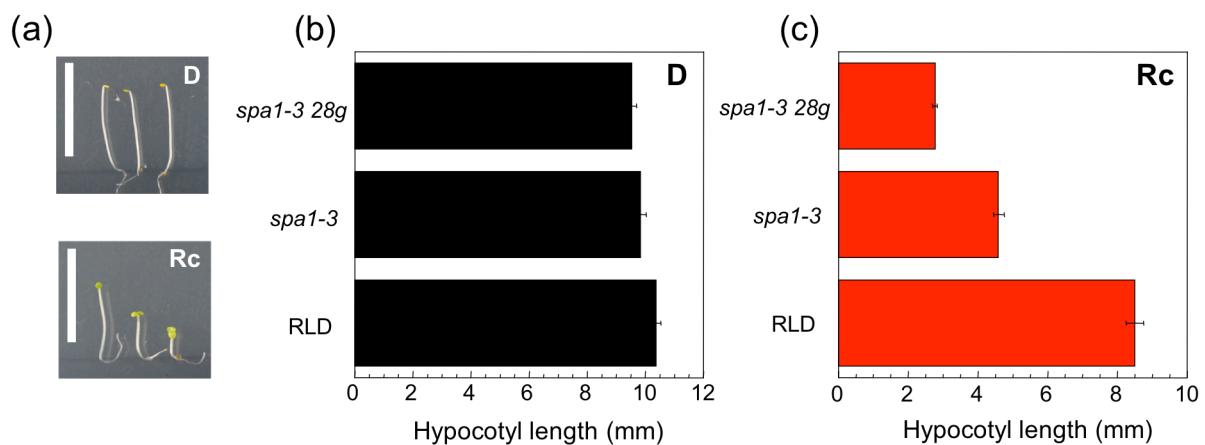


Figure 26. The *spa1 28g* double mutant shows an enhanced *spa1* mutant seedling phenotype in red light.

Visual phenotypes (a) and hypocotyl lengths of wild-type (RLD), *spa1-3* and *spa1-3 28g* seedlings grown for 4 days in darkness (b) and Rc ($0.3 \mu\text{mol m}^{-2} \text{s}^{-1}$) (c). Scale bar: 10 mm. Error bars indicate the SEM.

The flowering phenotype of the *spa1* mutant in SD was not enhanced by the additional mutation at the *28g* locus, but rather suppressed as the *spa1 28g* double mutants displayed a similar flowering time like the RLD wild-type control (Figure 27c, d). On the other hand, in long days the *spa1 28g* double mutant flowered even slightly later than the *spa1* single mutant or the RLD wild type (Figure 27a, b). Leaf size was comparable in *spa1*, *spa1 28g* and wild-type plants (data not shown). These results indicate that a mutation in the “28g” locus specifically enhances the *spa1* mutant phenotype in light-regulated seedling development, but rather suppresses the effect of a *SPA1* mutation in photoperiodic flowering time control.

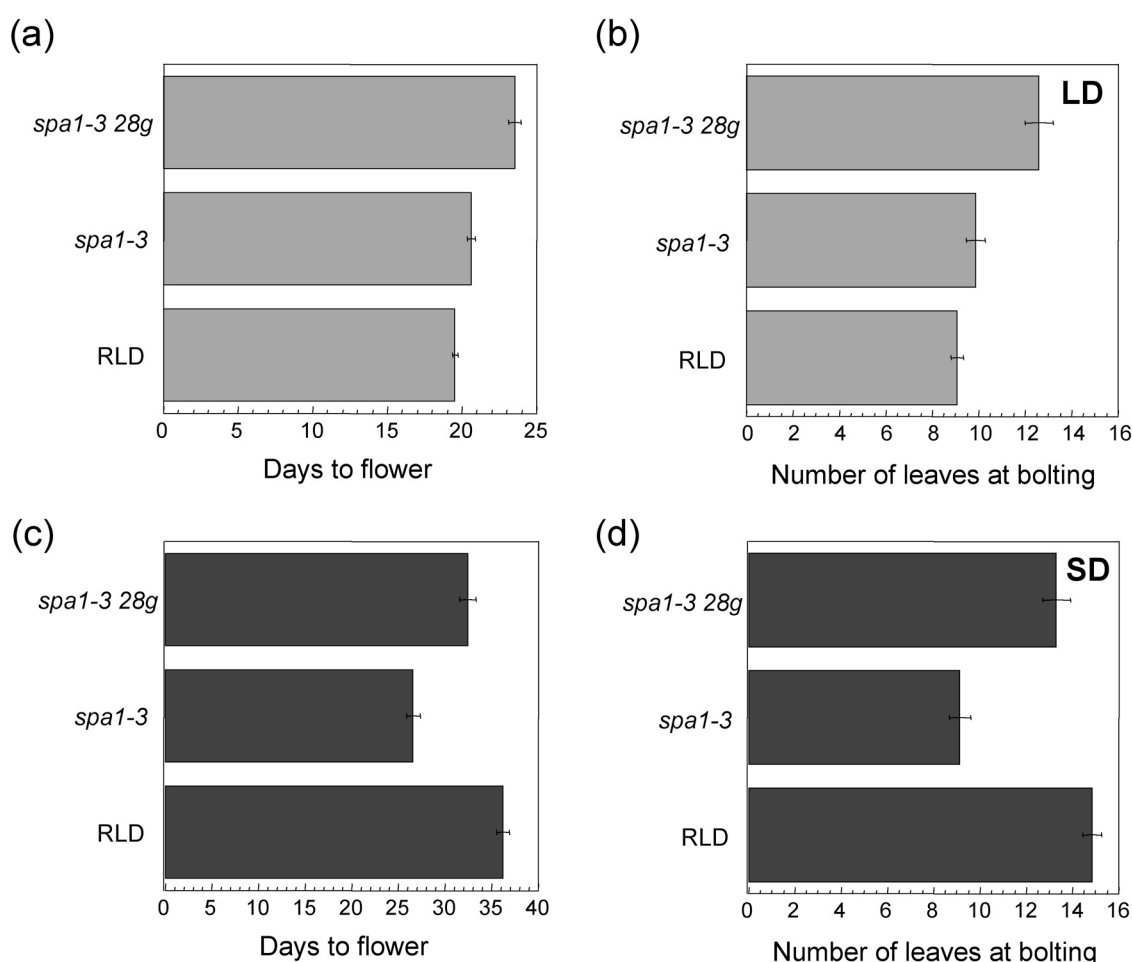


Figure 27. The *spa1 28g* double mutant shows no early flowering time phenotype in contrast to the *spa1* mutant.

Quantification of flowering time of wild-type (RLD), *spa1-3* and *spa1-3 28g* double mutant plants in LD (a, b) and SD (c, d). Plants were grown in LD (16 hour light/8 hour darkness) or SD (8 hour light/ 16 hour darkness) and flowering time was determined by counting days (a, c) or the number of rosette leaves at bolting (b, d). Error bars indicate the SEM.

II.5.2. Mapping of the *28g* locus

Using molecular markers, which can distinguish between Col and RLD ecotypes the *28g* locus was mapped to the top of chromosome 3 (Figure 28). The PCR-based SLP and CAPS markers used were taken from various databases (Monsanto Arabidopsis polymorphism and Ler sequence collection, Jander et al., 2002) or developed during this thesis. Since in contrast to Columbia (Col-0) or Landsberg *erecta* (Ler) sequences, the genome sequence of the RLD accession is not available, sequencing markers (SEQ) were created in addition. By amplifying random 1-2 kb fragments in a distinct region of chromosome 3 via PCR and subsequent sequencing of the fragments, single base pair exchanges between Col-0 and RLD could be identified. An overview of the molecular markers used in this thesis is presented in Table 6 in the Materials and Methods section. The position of the markers and the region off the *28g* locus is depicted in Figure 28.

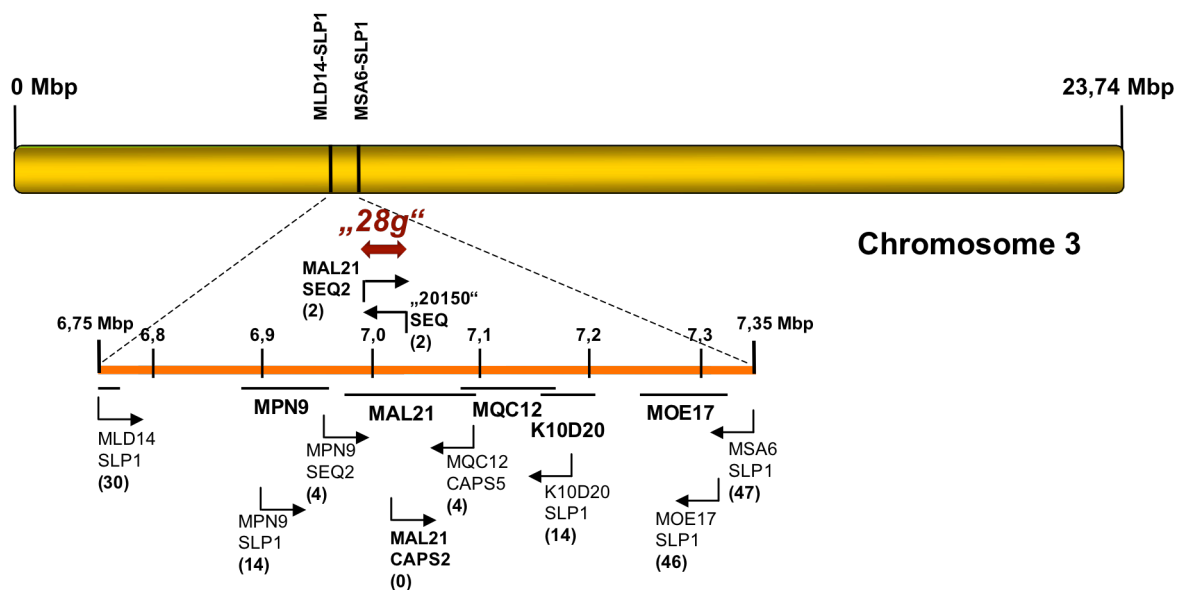


Figure 28. Mapping of the *28g* locus.

The *28g* locus (red arrow) was mapped to a 46 kb region on chromosome 3 between the markers MAL21-SEQ2 (BAC clone MAL21) and "20150"-SEQ (BAC clone MAL21) by using a mapping population consisting of around 4800 individual F2 plants. BAC clones are indicated in capital letters and numbers in brackets show number of recombination events detected by using the respective markers.

The first F2 mapping population (*spa1-3 28g* (RLD) x *spa1-7* (Col)) consisted of approximately 2300 F2 plants which were screened phenotypically for a *spa1 28g* mutant phenotype in Rc. Because of a very low recombination frequency in this particular area on chromosome 3, it was not possible to narrow down the region of

the *28g* locus as far as to identify the gene locus. Therefore, a second, ca. 2500 plants containing F2 mapping population was generated. Together with the remaining recombinants from the first mapping population and by developing new PCR markers it was possible to narrow down the putative region of the *28g* locus to a ca. 46 kb fragment on the top of chromosome 3. Database analyses revealed that in this region 16 annotated gene loci are present, mainly members of CYP705A type P450 cytochromes but also a Hexokinase-like protein (ATHXK4, AT3G20040) and an ubiquitin-conjugating E2 enzyme (AT3G20060) (Table 3).

Table 3: Possible candidates for the *28g* locus.

Overview about the gene loci which are present between the molecular markers MAL21-SEQ2 and “20150”-SEQ in the 46 kb region on chromosome 3, in which recombination events are still detectable.

Gene	Description	Marker
AT3G20030.1	F-box family protein; Identical to Putative F-box protein At3g20030 [Arabidopsis Thaliana] (GB:Q9LJZ8); similar to F-box family protein [Arabidopsis thaliana] (TAIR:AT5G60560.1); similar to hypothetical protein [Vitis vinifera] (GB:CAN77786.1); contains InterPro domain Cyclin-like F-box (InterPro:IPR001810); contains InterPro domain F-box associated type 1 (InterPro:IPR006527)	<u>MAL21-SEQ2</u>
AT3G20040.1	ATHXK4; ATP binding / hexokinase; Identical to Hexokinase-4 [Arabidopsis Thaliana] (GB:Q56XE8;GB:Q9LJZ7); similar to hexokinase, putative [Arabidopsis thaliana] (TAIR:AT1G50460.1); similar to unnamed protein product [Vitis vinifera] (GB:CAO16818.1); contains InterPro domain Hexokinase; (InterPro:IPR001312)	
AT3G20050.1	Encodes a putative cytoplasmic chaperonin that is similar to mouse Tcp-1 (t complex polypeptide 1).	
AT3G20060.1	Encodes one of two ubiquitin-conjugating enzymes belonging to the E2-C gene family (the other being UBC19). Transcript is always found in dividing cells, but also in other non-dividing cells. Protein is localized to the cytoplasm as well as to the nucleus.	
AT3G20060.2	Encodes one of two ubiquitin-conjugating enzymes belonging to the E2-C gene family (the other being UBC19). Transcript is always found in dividing cells, but also in other non-dividing cells. Protein is localized to the cytoplasm as well as to the nucleus.	
AT3G20070.1	Encodes a plant-specific protein of unknown function. Mutant embryos contain at most four small cells. The endosperm nucleoli are enlarged. Gene is expressed in siliques based on EST information.	
AT3G20070.2	Encodes a plant-specific protein of unknown function. Mutant embryos contain at most four small cells. The endosperm nucleoli are enlarged. Gene is expressed in siliques based on EST information.	
AT3G20075.1	a pseudogene with cytochrome P450 domain	
AT3G20080.1	member of CYP705A	
AT3G20080.2	member of CYP705A	
AT3G20080.3	member of CYP705A	
AT3G20083.1	a member of A-type cytochrome P450	

Gene	Description	Marker
AT3G20085.1	similarity to Retrotransposon - like protein (Copia-like retroelement pol polyprotein-like).	<u>MAL21-CAPS2</u>
AT3G20087.1	a cytochrome P450 pseudogene	
AT3G20090.1	member of CYP705A	
AT3G20100.1	member of CYP705A	
AT3G20110.1	member of CYP705A	
AT3G20120.1	member of CYP705A	
AT3G20120.2	member of CYP705A	
AT3G20130.1	member of CYP705A	
AT3G20130.2	member of CYP705A	
AT3G20140.1	member of CYP705A	
AT3G20150.1	kinesin motor family protein; similar to KINESIN-12B/PAKRP1L, microtubule motor/ plus-end-directed microtubule motor [Arabidopsis thaliana] (TAIR:AT3G23670.1); similar to hypothetical protein [Vitis vinifera] (GB:CAN75214.1); similar to unnamed protein product [Vitis vinifera] (GB:CAO38858.1); similar to kinesin related protein [Lycopersicon esculentum] (GB:AAO15358.1); contains InterPro domain Kinesin, motor region; (InterPro:IPR001752); contains InterPro domain Kinesin-related (InterPro:IPR010544)	<u>"20150"-SEQ</u>

III. Discussion

In plants, proper size and shape of lateral organs like leaves rely on a tight spatio-temporal organization of cell proliferation, differentiation and expansion. Furthermore, plant growth and final size is controlled by both genetic factors and environmental cues, which influence all three above-mentioned processes. Besides other external signals, light is an important factor controlling plant growth and morphogenesis. Mechanisms underlying light-regulated development include both transcriptional regulation and regulated protein degradation. Moreover, light signalling can influence other regulatory pathways such as phytohormone signalling. COP1/SPA complexes are central negative regulators of light signal transduction, whose functions as well as substrates in the control of seedling photomorphogenesis and photoperiodic flowering have already been characterized in detail. However, the roles of the SPA proteins and COP1 in the control of plant size control as well as their targets in this developmental process are unknown.

III.1. Role of COP1/SPA in Arabidopsis leaf size regulation

In *Arabidopsis thaliana*, a number of dwarfed mutants developing small leaves due to decreased cell number and/or cell size have been isolated (e.g. Horiguchi et al., 2006a; 2006b). Mutations causing dwarfed phenotypes have been linked to phytohormone signalling, cell-cycle coordination, translation- and proteolysis-controlling factors as well as stress responses (Krizek, 2009; Sugimoto-Shirasu and Roberts, 2003; Bögre et al., 2008). Adult *spa* quadruple mutants exhibit an extremely dwarfed phenotype similar to weak *cop1* mutants (McNellis et al., 1994a; Laubinger et al., 2004). To investigate the role of the COP1/SPA complex in plant growth in more detail, I performed a phenotypic analysis of *cop1* and *spa* mutants at cellular level. Fully developed leaves of *spa* triple mutants and *cop1* mutants exhibited severe growth defects. The reduced leaf area in these mutants was due to reduction of cell number and decreased size of epidermal cells as well as mesophyll cells (Figure 7 and 8). These results suggest that COP1/SPA-regulated leaf growth involves cell proliferation and cell growth control. Comparison of epidermal and mesophyll cell number and size in the various *spa* triple mutants further emphasized that SPA4 is the predominant factor in controlling leaf size (Figure 8).

Certain overexpression lines of known COP1/SPA targets exhibit a similar dwarfed phenotype like weak *cop1* or *spa* multiple mutants (Yoo et al., Onouchi et al., 2000; Yang et al., 2003). One approach to identify the COP1/SPA targets in leaf growth control was to investigate the genetic interaction between these factors and the SPAs or COP1, respectively. Mutations in *CO*, *FT* and *HFR1*, respectively, were not able to suppress the leaf size phenotype of *spa* mutants, suggesting that the small leaf phenotypes of *spa1 spa3 spa4* and *spa* quadruple mutants are independent of *CO*, *FT* and *HFR1* (Figure 9).

In contrast, *hy5* was able to partially suppress the leaf size phenotypes of *spa1 spa3 spa4* and *cop1* mutants, respectively (Figure 9). This indicates that *HY5* is involved in COP1/SPA-mediated leaf size regulation. *HY5* promotes the expression of many light-responsive genes and, furthermore, is important for the integration of light- and phytohormone signalling (Chattopadhyay et al., 1998; Cluis et al., 2004; Lau and Deng, 2010). Therefore, the previously reported elevated *HY5* protein levels may influence leaf size in *spa* and *cop1* mutants indirectly by altering the plants' gene expression profile or phytohormone signalling (Osterlund et al., 2000a; Saijo et al., 2003; Zhu et al., 2008; Nixdorf and Hoecker, 2010). Also *sth2* partially suppressed the *cop1* mutant leaf phenotype (Figure 9). *STH2* belongs to a clade of B-box containing genes of which some members have been implicated in light signal transduction (Datta et al., 2008b). Furthermore, a number of them, for instance CONSTANS LIKE 3 (*COL3*), *STH2* or *STH3*, are targets of COP1 and *col3*, *sth2* and *sth3* mutations repress the *cop1* mutant phenotype in various light-dependent processes (Indorf et al., 2007; Datta et al., 2006; 2007; 2008). An additional *sth3* mutation enhances the suppressing effect of *sth2* on *cop1* in seedling de-etiolation, pointing to redundancy within this transcription factor family (Datta et al., 2008). To test whether accumulation of these transcription factors has a significant impact on plant size, *cop1* (or *spa*) *hy5 sth col* higher-order multiple mutants would have to be examined. Since *STH2* and *STH3* were shown to regulate light responses like seedling de-etiolation and shade avoidance both independently from and in concert with *HY5* (Datta et al., 2007; 2008; Crocco et al., 2010), it is possible that this is also the case for plant growth control. Interestingly, via yeast-two-hybrid screens for protein-protein interaction between SPA4 and a transcription factor cDNA library a number of putative COP1/SPA targets including SALT TOLERANCE (*STO*), *STH2*, *STH3* and different *COL* proteins could be identified (Christian Falke, MSc thesis,

2009). If the abundance of these transcription factors was regulated by the SPA proteins as well, this would support the assumption that their accumulation and influence on gene expression indirectly contribute to the *cop1* and *spa* mutant phenotype.

Among the assumed COP1/SPA-interacting proteins identified by the above-mentioned yeast-two-hybrid screens were a number of growth-inhibitory class II TCP (TEOSINTE BRANCHED 1/CYCLOIDEA/PROLIFERATION CELL FACTOR 1)-type transcription factors (Aguilar-Martinez et al., 2007). Class II *TCPs* are thought to control temporal progression of leaf development by regulation of cell cycle genes such as *cyclin D3b* and furthermore, overexpression of some of these genes caused a reduction of leaf size (Nath et al., 2003; Li et al., 2005; Costa et al., 2005; Efroni et al., 2008; Palatnik et al., 2003; Schommer et al., 2008). However, altered expression of *TCP* genes often causes severe defects in leaf shape (Nath et al., 2003; Palatnik et al., 2003; Koyama et al., 2007), which is not the case for *spa* or *cop1* mutants (Figure 9 and 12), although *cop1* mutants seem to have rounder leaves compared to *spa1 spa3 spa4* mutants (data not shown). Here, a genetic approach using *cop1/spa tcp* multiple mutants could help to reveal a possible relationship between *COP1/SPA* and the *TCPs*.

The photoreceptor *phyB* is thought to act in mesophyll cells to control leaf size and *phyB* mutants display a reduced leaf size compared to wild type (Endo et al., 2005). *SPA1* has been shown to act in the mesophyll and in the phloem to regulate leaf size and moreover a *spa1* mutation suppresses the leaf size phenotype of the *phyB* mutant (Ranjan et al., 2011), suggesting that at least the mesophyll-specific action of *SPA1* appears to be downstream of *phyB*. *cop1 phyB* double mutants exhibited an increased leaf length compared to the *cop1* single mutant, but were still much smaller than *phyB* mutant plants (Figure 9). These findings imply that the *COP1/SPA* complex acts downstream of *phyB* at least in the mesophyll cells to control leaf size.

Many leaf size defects are caused by impaired phytohormone perception, accumulation and/or signalling and moreover the different phytohormones control developmental processes such as cell proliferation and cell growth by a complex network also in response to environmental cues (Busov et al., 2008; Wolters and Jürgens, 2009). Mutants with a deficiency in GA biosynthesis, content or response exhibit a semi-dwarfed or dwarfed stature (Fleet and Sun, 2005). The transcription-

repressing DELLA proteins have been shown to contribute to photomorphogenesis and restrain both cell proliferation and expansion rates in Arabidopsis leaves (Achard et al., 2007; 2009). However, exogenous application of GA₃ increased leaf length and plant height of *spa* triple and quadruple mutants, but could not restore the wild-type phenotype as seen in GA-deficient *ga1* mutants (Supplemental Figure 4). This indicates that GA-insensitivity is not the reason for the dwarfed phenotype of the *spa* mutants.

Auxin is important for the formation of leaf primordia and also for leaf growth, as it activates cell-cycle promoting transcription factors and thereby promotes cell proliferation in leaves (Hay et al., 2004; Wolters and Jürgens, 2009). This is consistent with the fact that mutants, which are impaired in auxin signalling such as *auxin resistant 1 (axr1)* are smaller than wild-type plants (Leyser et al., 1993). Interestingly, *hy5* mutants exhibit elevated auxin signalling because HY5 promotes the expression of some *INDOLE ACETIC ACID (IAA)* genes, which are negative regulators of auxin signalling (Cluis et al., 2004). Furthermore, recent studies showed that auxin response is reduced in *spa1 spa3 spa4* mutant leaves (Sebastian Rolauffs, unpublished). These findings suggest that the reduced cell number in *spa* mutants could be due to changes in auxin signalling and might thereby explain the partial suppression of the leaf size phenotype in *cop1* and *spa* triple mutants by the *hy5* mutation. Correlating auxin levels or response with cell number in *cop1/spa hy5* multiple mutants compared to wild type and *cop1* or *spa* mutants, respectively, could reveal a link between *COP1/SPA*-regulated leaf growth control and auxin signalling.

The growth-promoting brassinosteroids (BRs) have been shown to affect leaf size non-cell autonomously by their activity in the epidermis, whereas SPA1 was shown to act in the phloem and mesophyll cells to promote leaf growth, indicating that BR-regulated leaf growth is independent of COP1/SPA (Savaldi-Goldstein et al., 2007; Ranjan et al., 2011). Interestingly, *SPA4* as well as *SPA1* promoters have been shown to be active in the whole plant, but most prominently in the vascular tissue of Arabidopsis leaves, indicating that SPA4 might act in the same compartments as SPA1 to control leaf size (Kirsten Fittinghoff, PhD thesis, 2008).

The COP1/SPA complex might be involved in cell division control independently of phytohormone action, as COP1 has been shown to regulate protein levels of E2F transcription factors (E2FB and E2FC), which are important for cell cycle regulation in

light-mediated de-repression of shoot meristem activity (Lopez-Juez et al., 2008). Crossing dwarfed *spa* mutants to *cyclinB1;1:GUS* marker lines to visualize the G₂/M phase and thereby quantify cell division might allow to detect possible changes in cell proliferation activity in *spa* and *cop1* mutants.

Also cell expansion is impaired in *cop1* and *spa* triple mutants. In plants, cells can undergo DNA replication without cell division (endoreduplication), which results in nuclei of higher ploidy and is often associated with an increase in cell size (Sugimoto-Shirasu and Roberts, 2003). Determination of the DNA content in *spa* and *cop1* mutant nuclei could answer the question whether decreased ploidy levels are responsible for the reduced cell size in those mutants.

Environmental stress like drought can influence plant growth. Stomata regulate the uptake of CO₂ for photosynthesis and evaporation of water during transpiration. Their opening is regulated by internal and environmental signals like phytohormones (ABA), calcium, light, humidity and CO₂ (Schroeder et al., 2001). Some mutants exhibiting defects in stomata closure like the *snrk2.2/2.3/2.6* triple mutant show a dwarfed phenotype (Fujii and Zhu, 2009). COP1 has been shown to be a repressor of stomatal opening as stomata of *cop1* mutants are constitutively open in darkness (Mao et al., 2005). Additionally, COP1 and SPA proteins have been shown to repress stomatal differentiation in darkness (Kang et al., 2009). Whether SPA proteins are involved in stomata opening is not yet known, but constitutive opened stomata, leading to impaired photosynthesis, might be one explanation for the reduced plant size of *cop1* and *spa* mutants.

Plants, which show a constitutive defense response, often exhibit severe growth defects since sustained activation of biotic and abiotic stress responses is a metabolically expensive process (e.g. Tsutsui et al., 2009; Gou et al., 2009; Stokes and Richards, 2002). Therefore, one cannot exclude the possibility that the dwarfism of the *cop1* and *spa* mutant plants is a secondary effect of constitutive light signalling, caused by a massive loss of energy resources.

Taken together, *spa* triple mutants and *cop1* mutants exhibited severe defects in cell proliferation as well as cell expansion, resulting in a dwarfed plant size. During this study, the cause for the reduced cell number and size of *spa* and *cop1* mutants has not been revealed. Massive accumulation of transcription factors, which promote light signalling, might be one explanation. Defects in biosynthesis, accumulation or

signalling of various phytohormones might contribute to the reduced cell number and area of *spa* and *cop1* mutants. Further, *SPA4* was identified to be the main regulator in *COP1/SPA*-controlled leaf growth.

In this study it was shown that, in addition to its role in leaf size control, *SPA4* also contributes to photoperiodic flowering. Analysis of flowering time of *spa1 spa2 spa4* and *spa1 spa2 spa3* triple mutants showed that *SPA4*, but not *SPA3*, contributes to some extent to repress flowering in SD (Figure 6). There is evidence that the *SPA4* promoter, like the *SPA1* promoter, is strongly active in the vascular tissue of rosette leaves (Kirsten Fittinghoff, PhD thesis, 2008). Furthermore, latest studies revealed that *SPA1* acts in the phloem to regulate photoperiodic flowering (Ranjan et al., 2011). Taken together, *SPA4* contributes to flowering time control and can compensate to some extent for loss of *SPA1* function. However only *SPA1* is capable to repress early flowering in SD without the participation of the other *SPA* proteins.

III.2. SPA proteins are important but not essential for Arabidopsis development

In *Arabidopsis*, *COP1* and all four *SPA* proteins form a heterogeneous group of *COP1/SPA* complexes, consisting of a *COP1* homo-dimer and a *SPA* homo- or hetero-dimer (Zhu et al., 2008). The exact *SPA* protein compositions in these complexes are thought to vary depending on the abundance of individual *SPA* proteins in different tissues and light conditions as well as at distinct developmental stages (Zhu et al., 2008). This is consistent with the finding that the individual *SPA* proteins have partially redundant but also distinct functions at various developmental processes of the *Arabidopsis* life cycle. *spa* quadruple mutants exhibit an extreme constitutively photomorphogenic seedling phenotype in darkness and also a dwarfed plant size similar to weak *cop1* mutants (Laubinger et al., 2004; McNellis et al., 1994a). However, *cop1* null mutant alleles are lethal, indicating that *COP1*-dependent proteolysis is essential for *Arabidopsis* development and *SPA* function cannot compensate for a loss of *COP1* function (McNellis et al., 1994a).

In the previously characterized *spa* quadruple mutant, only *spa3-1* has been shown to be a null allele and in case of *spa2-1*, truncated *SPA2* protein was detected using a *SPA2*-specific antibody (Laubinger and Hoecker, 2003; Zhu et al, 2008). Thus, it is

possible that in a *spa* quadruple mutant residual *SPA* function is present and sufficient for the plants' survival. To test whether the *SPA* proteins are essential for *Arabidopsis* development similarly to *COP1* or whether *COP1* can compensate for a complete loss of *SPA* function, my aim was to generate a *spa* quadruple null mutant. To further dissect the distinct functions of the individual *SPA* genes, *spa* double and triple mutants containing the *spa* null mutant alleles were generated additionally. Phenotypic comparison between the newly generated *spa* multiple mutants and the previously studied *spa* mutants at the seedling as well as at the adult stage revealed no differences between the different mutants (Figure 12 and 13). These results suggest that *SPA* function is abolished in the not-null mutant alleles. This is consistent with the findings that the WD-repeat domain of *SPA1*, which is also absent in the previously characterized *spa* mutant alleles, is essential for *SPA1* function, as the protein-protein interaction with *COP1/SPA* targets like *HY5* and *HFR1* is mediated by the WD-repeat domain (Laubinger and Hoecker, 2003; Laubinger et al., 2004; Fittinghoff et al., 2006; Saijo et al., 2003; Yang et al., 2005b). *spa* quadruple null mutants - despite their severe phenotype - are viable, in contrast to *cop1* null mutants. This shows that *SPA* proteins are important but not essential for *Arabidopsis* development and *COP1* function is not completely dependent on *SPA* function. Indeed, *COP1* has *SPA*-independent functions in the regulation of UV-B signalling via *UVR8* and *HY5* (Oravec et al., 2006; Favory et al., 2009).

Besides the *COP1/SPA* complexes there are other *COP/DET/FUS* protein-containing complexes present in *Arabidopsis*, like the *COP9* signalosome (*CSN*) and the *CDD* complex. These complexes are thought to function collectively in ubiquitination- and proteasome-mediated protein degradation, and thereby regulate besides photomorphogenesis also the cell cycle, gene expression and DNA-repair (Yanagawa et al., 2004; Wei et al., 2008). Moreover, in *Arabidopsis*, the *COP1/SPA* complexes associate with a *CUL4-RBX1-DDB1*-based ubiquitin ligase (Chen et al., 2010). *CUL4-RBX1-DDB1* has been suggested to form a new group of E3 ligases involving the different *COP1/SPA* tetramers which are distinct from the previously described *RBX1-CUL4-CDD* complex, but work in concert with this complex to regulate seedling photomorphogenesis and photoperiodic induction of flowering (Chen et al., 2010; Figure 29). However, the specific mechanisms of the regulatory relationship between the *RBX1-CUL4-CDD* and the proposed *RBX1-CUL4-COP1-SPA* complexes are unknown.

Weak mutations in the CDD complex members *COP10* as well as *DET1* led to an enhancement of the *spa1 spa2 spa3* mutant seedling phenotype in darkness (Chen et al., 2010). In addition, a weak *det1* mutant allele showed strong synergistic genetic interaction with the *spa1* mutation in the control of photomorphogenesis during plant development, indicating that the COP1/SPA complexes and the CDD complex act together to regulate photomorphogenesis (Nixdorf and Hoecker, 2010).

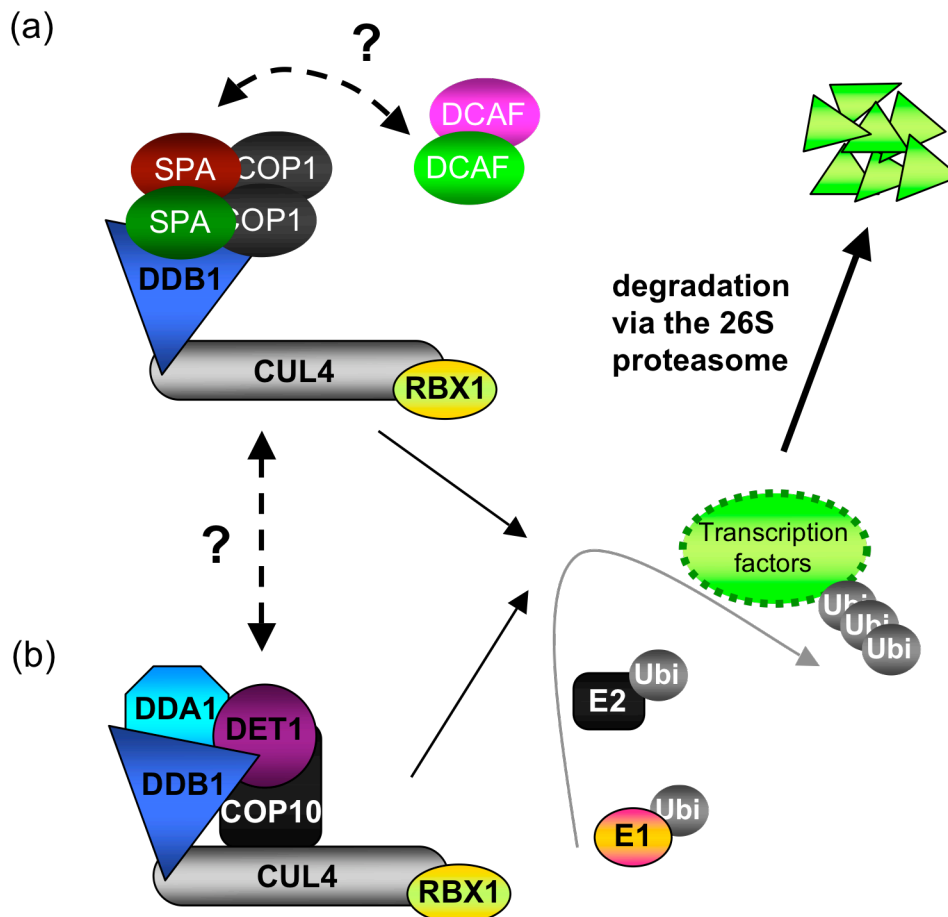


Figure 29. Potential model for the *COP1/SPA*-regulated proteolysis in light-regulated plant development.

(a) RBX1-CUL4-DDB1 likely interacts with COP1-SPA to form a new group of E3 ligases to target transcription factors for degradation via the 26S proteasome and thereby mediate light-regulation of plant development. In this CULLIN-based E3 ligase, the SPA proteins might be replaced by other DCAF proteins, depending on the signalling pathway, or COP1 may function without the SPA proteins. (b) RBX1-CUL4 and the CDD complex form a functional E3 ligase to repress photomorphogenesis. Dashed lines indicate possible regulatory relationships between the different assumed complex formations. E1 represents an ubiquitin (Ubi)-activating enzyme, and E2 represents an ubiquitin-conjugating enzyme. (Modified after Chen et al., 2010)

Loss-of-function mutations in any of the CSN genes, *COP1*, *COP10*, *DET1* or *DDB1* lead to lethality of the plants or cause severe developmental defects, whereas *spa*

quadruple mutants are extremely dwarfed, but do not show other severe aberrant phenotypes (McNellis et al., 1994a; Kwok et al., 1996; Schroeder et al., 2002; Laubinger et al., 2004; this study). These data suggest that *SPA* function is not essential for the survival of the plant. This is consistent with fact that in *Arabidopsis* a number of WD-40 proteins were identified as DDB1 and CUL4 associated factors (DCAFs), including DET1, COP10, COP1 and the SPA proteins, which are involved in numerous functions of plant development (Biedermann and Hellmann, 2011). The SPA proteins may act as substrate receptors that are specifically involved in particular photomorphogenesis responses and can be replaced by other DCAFs to regulate more basic developmental processes but not vice versa.

Nevertheless, the exact function of the SPA proteins within the COP1/SPA complexes remains to be elucidated. Due to the fact that SPA1 interacts with COP1/SPA targets like LAF1, HFR1, HY5, CO and phyA and that these proteins accumulate in *cop1* and *spa* mutants, it is likely that the SPA proteins are responsible for substrate recognition or specificity (Sajio et al., 2003; Seo et al., 2003; 2004; Yang et al., 2005a; Laubinger et al., 2006). Furthermore, it was shown that recombinant SPA1 alters the E3 ubiquitin ligase activity of COP1 *in vitro*, therefore the SPAs might be important for COP1 activity (Sajio et al., 2003; Seo et al., 2003). SPA proteins could also contribute to the light-dependent inactivation or de-stabilization of the COP1/SPA complexes, since it has been shown that SPA1 and SPA2 proteins are de-stabilized in light, whereas COP1 is relatively light-stable (Zhu et al., 2008; Balcerowicz et al., 2010).

III.3. Role of the SPA4 N-terminus in light-dependent seedling morphogenesis and plant size control

SPA as well as COP1 function is dependent on their respective coiled-coil and WD-repeat domains, which are essential for COP1-SPA and SPA-SPA interaction, as well as COP1/SPA-substrate interaction, respectively (Hoecker and Quail, 2001; Laubinger and Hoecker, 2003; Laubinger et al., 2004; Sajio et al., 2003; Yang et al., 2005a). A structure-function analysis of SPA1 revealed that the N-terminus, which contains the kinase-like domain of SPA1, is not necessary to rescue the *spa1* mutant phenotype of light-grown seedlings or the constitutive photomorphogenic seedling

phenotype of dark-grown *spa1 spa2 spa3* mutants (Fittinghoff et al., 2006; Yang and Wang, 2006). However, the early flowering phenotype of SD-grown *spa1* mutants could not be rescued by truncated versions of SPA1 lacking the kinase-like domain or the complete N-terminus (Kirsten Fittinghoff, PhD thesis, 2008), indicating that the N-terminus contributes to specific SPA1 function.

A comparable approach was applied to reveal the contribution of the SPA4 N-terminus to SPA4 function in light-dependent seedling development and also in leaf size control as SPA4 is the main regulator of adult Arabidopsis development (Laubinger et al., 2004; this study). Similar to the results observed in the studies using *pSPA1:SPA1-HA*, *FL-GFP-SPA4*, *ΔNT-GFP-SPA4* as well as *Δkin-GFP-SPA4*, but not the *Δcc-GFP-SPA4* constructs, were able to rescue the enhanced de-etiolated phenotype of the parental *spa3 spa4* mutant in FRc, suggesting that the N-terminus is dispensable for SPA4 function in the regulation of seedling photomorphogenesis. Furthermore, SPA4 function probably is not dependent on an NLS motif since also the GFP-SPA4 deletion protein lacking almost the complete N-terminal half in which a potential NLS would be expected was able to restore the *spa3 spa4* mutant hypocotyl phenotype (Figure 15). All complementing lines showed strong overcomplementation as transgenic seedlings carrying *FL-GFP-SPA4*, *ΔNT-GFP-SPA4* or *Δkin-GFP-SPA4* with or without the artificial NLS exhibited a hyper-etiolated seedling phenotype compared to wild type also at high light intensities (Figure 15-17). The overexpression phenotype could be due to the dual 35S promoter by which the different fusion proteins were expressed. It has been shown before that *35S:Myc-SPA1* transgenic plants showed an increased hypocotyl length compared to those of the control plants (Yang and Wang, 2006).

GFP-SPA4 transcript levels were not light-regulated, because of the 35S promoter and no differences in SPA4 protein abundance between dark- and FRc-grown seedlings were detected, indicating that neither FL-GFP-SPA4 protein nor the various SPA4 deletion proteins are differentially de-stabilized upon light exposure (Figure 18). The enhanced complementation strength of the *ΔNT-GFP-SPA4* protein compared to the FL-GFP-SPA4 protein could be explained by higher protein abundance in these lines, resulting from elevated transcript levels (Figure 17). However, *ΔNT-GFP-SPA4* line 2-9 exhibited relatively weak transcript abundance but higher protein levels than all FL-GFP-SPA4 lines, indicating that SPA4 lacking the N-

terminus might be more stable than the full-length protein. To test this hypothesis, *FL-GFP-SPA4* and Δ *NT-GFP-SPA4* lines exhibiting comparable transcript levels would have to be compared regarding GFP-SPA4 protein abundance. The non-complementing Δ *cc-GFP-SPA4* lines exhibited higher GFP-SPA4 protein accumulation, which was not due to elevated mRNA abundance. Δ *cc-GFP-SPA4* might be more stable because of an abolished protein-protein interaction between COP1 and SPA4 in these lines. Similar stabilizing effects were observed in Δ *cc-SPA1-HA* transgenic lines, though SPA1-HA stability is strongly light-regulated (Figure 22; for discussion, see section III.4). It is not known yet why elevated SPA4 protein abundance led to an extremely hyper-etiolated phenotype. Increased Δ *NT-SPA1* protein levels did not cause a hyper-etiolated phenotype compared to FL-SPA1, independent of the promoter driving the *SPA1* cDNA (Yang and Wang, 2006; Fittinghoff et al., 2006; this study). Because *35S:FL-Myc-SPA1* and *35S: Δ NT-Myc-SPA1* transgenic lines showed comparable seedling phenotypes, even though the Δ *NT-SPA1* protein accumulated to levels approximately 40-fold higher than FL-SPA1, it was suggested that the SPA1 N-terminus contributes to full activity of SPA1 (Yang and Wang, 2006). This might be the opposite for the function of the SPA4 N-terminus in seedling photomorphogenesis. In addition, it is notable that the sequence similarity of the N-terminal regions of *SPA1* and *SPA4* is low when compared to their highly homologous WD-repeat domains and that *SPA4* possess a shorter N-terminal extension than *SPA1* (Laubinger and Hoecker, 2003; Hoecker et al., 1999).

Noteworthy, it was shown that wild-type or *hfr1* mutant plants overexpressing *HFR1* exhibit an hypocotyl phenotype similar to wild type, whereas the deletion protein HFR1- Δ N105 expressing line was suggested to be a hyperactive gain-of-function mutant that functions constitutively even in darkness (Yang et al., 2003). In an independent report it was shown that an exaggerated light response of lines expressing a Δ *N-HFR1* deletion protein is probably caused by enhanced HFR1 protein stability and that tight control of HFR1 protein abundance is important for a normal de-etiolation response (Duek et al., 2004). It is possible that, in contrast to Δ *NT-SPA1*, the Δ *NT-SPA4* deletion protein is similarly hyperactive - at least in seedling de-etiolation responses - due to increased protein abundance or enhanced activity towards its target transcription factors.

Also in the *NLS-GFP-SPA4* transgenic lines, *SPA4* transcript levels and GFP-SPA4 protein abundance correlated with the hypocotyl length in the respective lines with

the exception of Δcc -GFP-NLS-SPA4 3-2, FL-SPA4 and ΔNT -SPA4 transgenic lines expressing GFP-SPA4 fusion proteins containing an artificial NLS showed an increased hypocotyl length compared to the corresponding lines without the NLS (Figure 15-17). These results cannot be explained by higher protein levels of GFP-NLS-SPA4, as the protein accumulation of the FL- and ΔNT -GFP-SPA4 and NLS-GFP-SPA4 transgenic lines were similar in direct comparison (Supplemental Figure 5). Higher nuclear abundance of the GFP-NLS-SPA4 protein might be an explanation for the enhanced hyper-etiolation of the FL-NLS-GFP-SPA4 lines because transient expression of FL-SPA4 in onion epidermal cells showed slightly increased nuclear GFP fluorescence (Supplemental Figure 6). Possibly, a higher concentration of FL-GFP-SPA4 molecules in the nucleus facilitates formation of COP1/SPA complexes. However, transient expression of ΔNT -, Δkin -, and Δcc -GFP-SPA4 with or without the artificial NLS showed that the GFP was detected in the nucleus as well as in the cytoplasm of onion epidermal cells in case of all SPA4 deletion derivatives (Supplemental Figure 7). Determination whether the differences in nuclear GFP-SPA4 protein abundance in the different lines correlate to their respective phenotype could answer this question. Still, immunoblot analysis of transgenic GFP-SPA4 expressing seedlings revealed an considerable amount of free GFP, which could be caused in course of protein extraction or by cleavage of the N-terminal GFP from the SPA4 protein (data not shown). Therefore, reliable localization studies of GFP-SPA4 in the transgenic lines were not possible. For unknown reasons the Δkin -GFP-NLS-SPA4 expressing lines complemented to the same extent as the Δkin -GFP-SPA4 lines without the artificial NLS.

The complementation analysis was performed in the *spa3 spa4* double mutant background. Therefore, it is possible that heterogeneous complexes with a ΔNT -SPA4 and a wild-type SPA1 molecule are sufficient to rescue the enhanced de-etiolated phenotype of the parental *spa3 spa4* mutant. Another possibility would be that the SPA4 N-terminus and its kinase-like domain are dispensable for SPA4 function in the control of seedling photomorphogenesis (Figure 30 and 33). An analysis of FL-SPA4 and ΔNT -SPA4 expressed in a true *spa* quadruple null mutant could confirm this hypothesis.

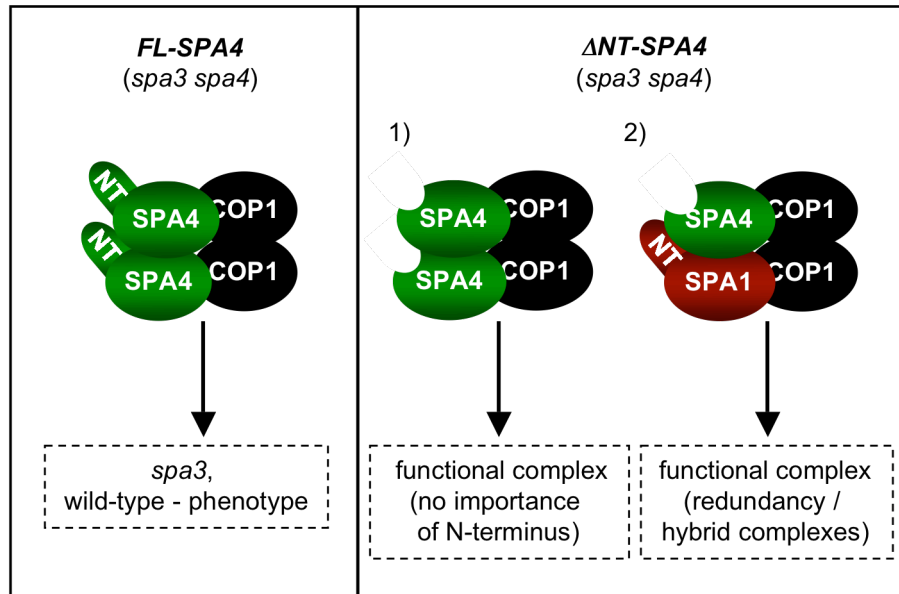


Figure 30. Model for the complementation of ΔNT -SPA4 of the *spa3 spa4* mutant leaf size and seedling photomorphogenesis.

- 1) The ΔNT -SPA4/COP1 complex is functional, therefore the N-terminus is dispensable for SPA4 function
- 2) ΔNT -SPA4 and wild-type SPA1 form a functional complex that compensate for the loss of the SPA4 N-terminus

In adult Arabidopsis plants, all *GFP-SPA4* transgenic lines except Δacc -*GFP-SPA4* were able to complement the leaf size phenotype of the *spa3 spa4* mutant to a similar degree independently from the presence of an NLS, indicating that the SPA4 N-terminus does not contribute to plant size control (Figure 20). FL-GFP-SPA4 protein abundance was reduced to a higher extent than could be solely caused by differences in transcript levels compared to the SPA4 deletion derivatives in 3-week old transgenic plants (Figure 21). These data suggest that in adult plant tissue the N-terminus contributes to SPA4 stability. To confirm this hypothesis, one would have to test whether the decrease of FL-GFP-SPA4 can be inhibited by blocking the proteasome because for SPA1 and SPA2 it has been shown that protein destabilization is mediated by the 26S proteasome (Balcerowicz et al., 2010).

Despite the higher abundance of ΔNT -GFP-SPA4 proteins, the ΔNT -SPA4 lines did not exhibit a stronger overcomplementing leaf phenotype compared to *FL-SPA4* (Figure 20, 21). This could be caused by a reduced activity of ΔNT -SPA4 compared to the FL-SPA4 protein in the regulation of leaf growth, as suggested for ΔNT -SPA1 in seedling photomorphogenesis, but in contrast to the data obtained by analysis of SPA4 function in seedling de-etiolation (Fittinghoff et al., 2006; Yang and Wang, 2006;

section II.4.1). This effect could be more obvious in adult plants since *SPA1* has only a minor function in leaf growth control compared to *SPA4* and potential Δ NT-*SPA4/SPA1-COP1* complexes formed in the *spa3 spa4* transgenic lines might be less functional in adult plant tissue compared to seedling stage, or less abundant as it was shown that *SPA3* and *SPA4* mRNAs accumulate to higher levels compared to *SPA1* in adult plants (Fittinghoff et al., 2006).

Taken together, Δ NT-*SPA4* constructs were able to complement the *spa* double mutant seedling phenotype as well as its reduced leaf size phenotype, indicating that the N-terminus does not contribute to *SPA4* function at these developmental stages or that functional Δ NT-*SPA4/SPA1-COP1* hybrid complexes are formed in this mutant background (Figure 30 and 33). The function of the *SPA4* N-terminus in photoperiodic flowering could not be determined because *spa3 spa4* mutants do not exhibit an early flowering phenotype due to presence of wild-type *SPA1* in this mutant (data not shown). The results from the GFP-*SPA4* protein analysis obtained in this study point to a function of the *SPA4* N-terminus in the control of *SPA4* protein de-stabilization in adult tissue, whereas its contribution to *SPA4* de-stabilization in seedlings was less evident (Figure 33). Therefore, the role of the N-terminus in regulation of *SPA4* protein stability requires further investigation.

III.4. The SPA1-N terminus and coiled-coil domain are involved in light-dependent SPA1 protein de-stabilization

Previous studies revealed that *SPA1* and *SPA2* proteins are de-stabilized by light, which resulted in reduced *SPA2* protein levels in light- compared to dark-grown seedlings and slightly reduced or unchanged *SPA1* protein levels in light- and dark grown seedlings since *SPA1* expression is strongly up-regulated by light, whereas the *SPA2* promoter is not light-induced (Fittinghoff et al., 2006; Balcerowicz et al., 2010). Because the integrity of the *COP1/SPA* complex is dependent on the presence of *COP1* as well as the *SPA* proteins and *COP1* protein levels are not altered by light, one mechanism to negatively regulate *COP1/SPA* complex activity in response to light could be the degradation of the *SPA* proteins (Zhu et al., 2008; Balcerowicz et al., 2010). Truncated *SPA1* protein lacking the N-terminal domain accumulated to higher levels in light-grown seedlings compared to the full-length

SPA1 protein, indicating that the SPA1 N-terminus is involved in de-stabilization of the protein (Fittinghoff et al., 2006; Yang and Wang, 2006).

In this study, it was shown that the N-terminus indeed is important for de-stabilization of SPA1 and that this process is strongly light-dependent (Figure 21). The extensive light-induced accumulation of Δ NT-SPA1-HA showed that, despite the fact that the N-terminus did not contribute to SPA1 function in controlling seedling photomorphogenesis in light-grown seedlings, it is particularly involved in light-dependent de-stabilization of the protein (Fittinghoff et al., 2006; Figure 22). Still, it remains unclear how the N-terminus contributes to SPA1 degradation. It is possible that the extended N-terminal domain of SPA1 contains sites for post-translational modifications like phosphorylation, ubiquitination or sumoylation, which could lead to the subsequent degradation of the protein via the 26S proteasome (Figure 31). Interestingly, compared to SPA1 and SPA2, SPA3 as well as SPA4 proteins lack an N-terminal extension, which might contribute to SPA de-stabilization (Laubinger and Hoecker, 2003). SPA4 appeared to be generally more stable, since GFP-SPA4 protein levels reflected the transcript levels also in light-grown seedlings (Figure 18 and 19). Though, it is possible that the GFP epitope might have a stabilizing effect on SPA4. Therefore, it remains to be tested whether also endogenous SPA3 and SPA4 proteins are de-stabilized in response to light.

In addition, the light-induced de-stabilization of SPA1 is likely dependent on the SPA1-COP1 interaction, because the Δ cc-SPA1-HA protein exhibited a massive light-dependent accumulation in the Δ cc-SPA1-HA transgenic seedlings (Figure 22 and 31). In these lines SPA1-COP1 interaction is disrupted, which suggests that COP1 is involved in the control of SPA1 protein stability. This is consistent with the fact that endogenous SPA1 and SPA2 protein levels are elevated in *cop1* mutants (Alexander Maier, unpublished). Furthermore, it was shown that the light-induced de-stabilization of SPA1 and SPA2 is mediated by the 26S proteasome (Balcerowicz et al., 2010). Even though the overall FL-SPA1 protein abundance is similar in dark- and light-grown seedlings, the seedlings exhibited photomorphogenesis in response to light, suggesting that light-induced SPA degradation is not the only mechanism by which COP1/SPA complex activity is reduced upon light perception. Also in dark-grown seedlings Δ NT-SPA1-HA and Δ cc-SPA1-HA protein levels were slightly

increased compared to full-length SPA1, indicating that in darkness SPA1 protein abundance has to be regulated as well (Figure 21).

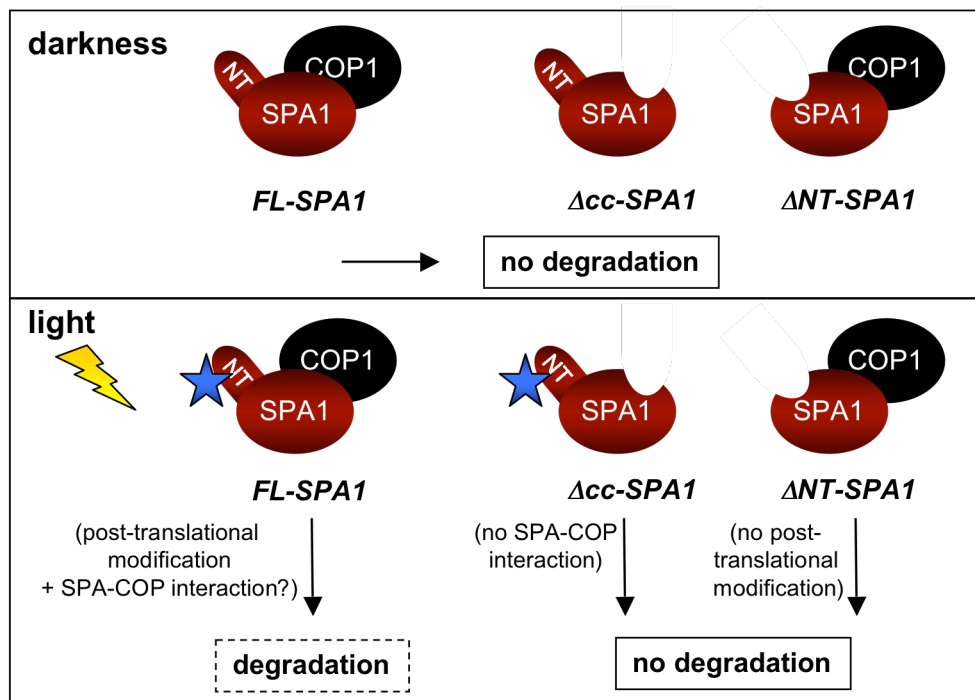


Figure 31. Model for light-dependent SPA1 de-stabilization

In darkness, SPA proteins are stable.

In the light, possible N-terminal modifications target SPA1 for degradation via the 26S proteasome, which is mediated by a COP1-dependent mechanism. Abolishing SPA1-COP1 interaction (Δcc -SPA1) and/or lack of binding sites for protein modification (ΔNT -SPA1) inhibit COP1-dependent de-stabilization of SPA1 in response to light.

III.5. The SPA1 N-terminus is of different importance in seedling photomorphogenesis and leaf size regulation in a spa triple mutant background

To investigate the role of the SPA1 N-terminus in plant size regulation, transgenic *spa1 spa3 spa4* mutants expressing full-length SPA1-HA, ΔNT -SPA1-HA or Δkin -SPA1-HA were analyzed. First, complementing lines were isolated by screening transgenic FRC-grown seedlings for rescue of the extremely enhanced photomorphogenesis phenotype of the *spa1 spa3 spa4* mutants. Surprisingly, in the *spa* triple mutant background the SPA1 N-terminus contributed to complementation strength of the transgenic lines, as most ΔNT -SPA1-HA lines exhibited shorter hypocotyls compared to Δkin -SPA1-HA or FL-SPA1-HA expressing lines (Figure 23;

Table 2), which was not the case in a *spa1* single mutant background (Fittinghoff et al., 2006). One explanation for this might be that in the *spa1* background wild-type *SPA2*, *SPA3* and *SPA4* are present, which enable formation of various additional COP1/SPA complexes to control seedling photomorphogenesis (Figure 32). In contrast, *spa1 spa3 spa4* mutants contain only wild-type *SPA2*, which has only a minor function in light-grown seedlings, and therefore the resulting Δ NT-SPA1/SPA2-COP1 complexes, as well as the Δ NT-SPA1/ Δ NT-SPA1-COP1 complexes, might be less efficient to regulate photomorphogenesis (Figure 32; Laubinger et al., 2004). However, also the truncated Δ NT-SPA1-HA protein was able to rescue the *spa1 spa3 spa4* mutant phenotype of light-grown seedlings. This further underlines that the N-terminus overall is not essential for SPA1 function in seedling photomorphogenesis.

When *FL-SPA1-HA* is expressed from the native *SPA1* promoter in a *spa1* single mutant background the transgenic seedlings do not exhibit an overcomplementation phenotype, in contrast to the results obtained with almost identical constructs in a *spa* triple mutant background (Fittinghoff et al., 2006; Figure 22; 23). This could also be explained by the fact that in a *spa1 spa3 spa4* mutant only wild-type *SPA2* is present. Therefore, mainly SPA1/SPA1-COP1 complexes are assembled in contrast to the different combinations, which are possible in a transgenic *spa1* single mutant expressing *FL-SPA1-HA* (Figure 32). The FL-SPA1/FL-SPA1-COP1 complex might be more efficient in controlling seedling photomorphogenesis than SPA1/SPA4-COP1 or SPA1/SPA3-COP1 complexes. This would also be consistent with the finding that *spa1* single mutants show a stronger seedling phenotype than *spa4* or *spa3* single mutants (Laubinger and Hoecker, 2003).

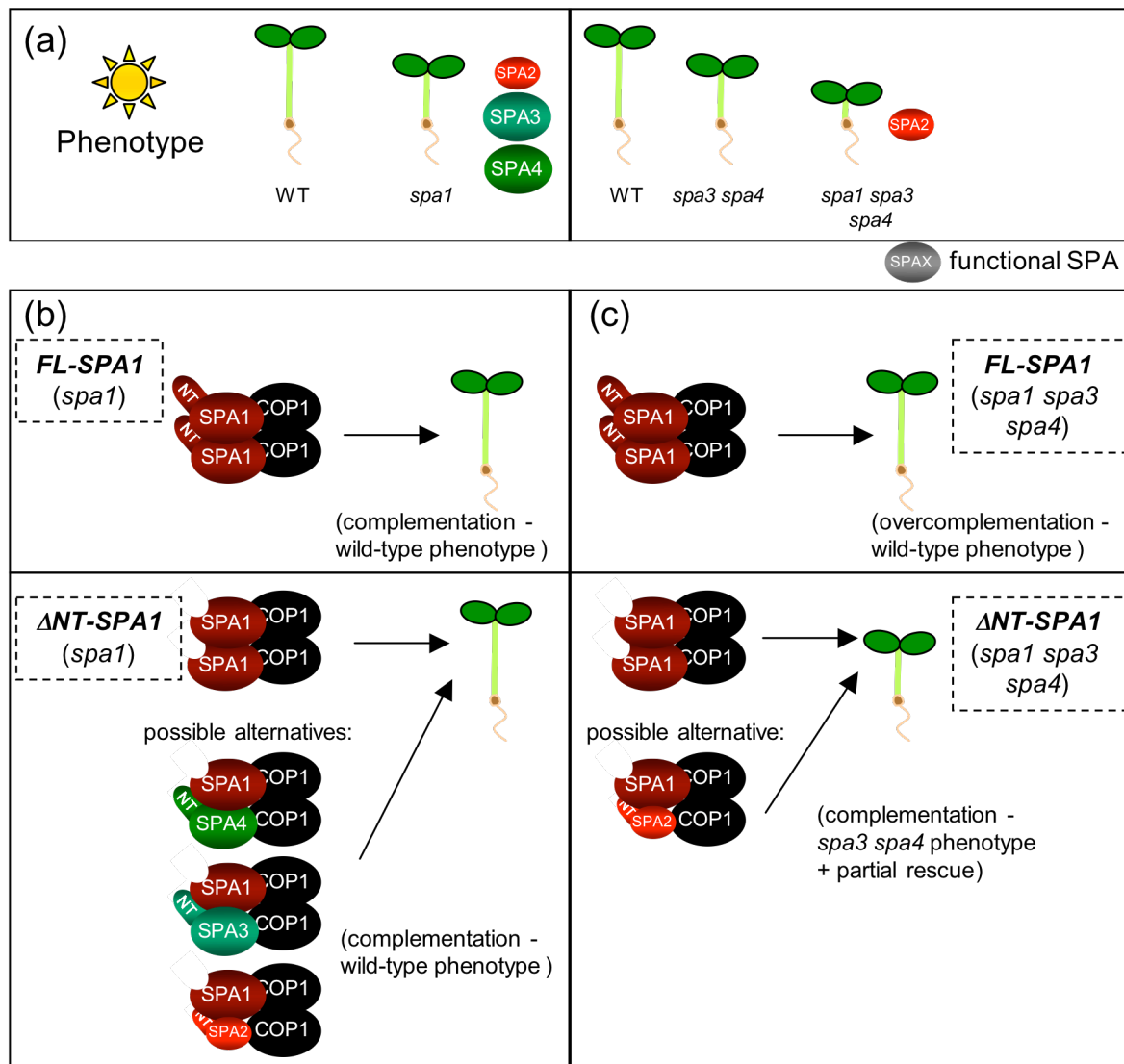


Figure 32. Model for the reduced complementation efficiency of $\Delta NT-SPA1$ in a *spa* triple mutant background.

(a) Schematic illustration of seedling phenotypes of wild type (WT), *spa1*, *spa3 spa4* and *spa1 spa3 spa4* mutants grown in the light. Ellipses indicate WT SPAs present in the analyzed mutant background.

(b) *SPA1* expression in the *spa1* mutant background: *FL-SPA1* is able to restore the WT phenotype. $\Delta NT-SPA1$ forms a functional complex with COP1 and/or other - endogenous - wild-type SPAs form functional complexes with $\Delta NT-SPA1$ and COP1, which contribute to the control of hypocotyl length.

(c) *SPA1* expression in the *spa1 spa3 spa4* mutant background: *FL-SPA1-HA* is able to rescue the *spa* triple mutant phenotype. Moreover, the *FL-SPA1-HA* transgenic lines display overcomplementation, possibly due to an overrepresentation of *SPA1/SPA1-COP1* complexes, as *SPA4-* and *SPA3-*containing COP1/*SPA* complexes are absent. $\Delta NT-SPA1$ forms a (partial) functional complex with COP1 and/or possible *SPA2/COP1* complexes are only partially able to contribute to rescue the *spa* triple mutant phenotype. Hence the complementation is in part incomplete.

Examination of *SPA1-HA* protein levels in the *FL-SPA1-HA*, $\Delta NT-SPA1-HA$ or $\Delta kin-SPA1-HA$ expressing *spa1 spa3 spa4* lines showed that truncated versions of *SPA1-HA* accumulated to higher levels compared to full-length *SPA1*, as it was shown

before for the *spa1* background (Figure 22 and 24). In case of ΔNT -SPA1-HA this could be due to increased transcript levels in these lines. Nevertheless, the protein accumulation patterns of the deletion proteins differed noticeably from those obtained in the *spa1* mutant background. FL-SPA1-HA exhibited the same RNA and protein levels like in the *spa1* mutant background in darkness and in FRc: strongly light-induced transcript accumulation and unchanged protein levels, indicating a light-dependent de-stabilization of full-length SPA1 also in the *spa1 spa3 spa4* background. In contrast, expression of the truncated SPA1 derivatives was not light-regulated and the protein accumulated strongly to similar levels in dark- and light-grown seedlings (Figure 24). This indicates that Δkin -SPA1-HA and ΔNT -SPA1-HA proteins are generally stabilized independent of light exposure. These results imply that SPA proteins might be involved in the light-induced de-stabilization of themselves, possibly in concert with COP1. Such a hypothetical negative feedback regulation could occur via autoubiquitination since SPA1 and SPA2 de-stabilization has been shown to depend at least partially on COP1 and the 26S proteasome (Zhu et al., 2008; Balcerowicz et al., 2010, Alexander Maier, unpublished).

Determination of leaf size of the FL-SPA1-HA, ΔNT -SPA1-HA and Δkin -SPA1-HA transgenic lines revealed that most SPA1 derivatives rescued the dwarfed phenotype of the parental *spa1 spa3 spa4* mutants to a similar extent, demonstrating that the N-terminus is completely dispensable for SPA1-regulated leaf size control (Figure 25). Unlike seedling photomorphogenesis, leaf growth is mainly regulated by SPA3 and especially SPA4 (Laubinger et al., 2004; this study). Thus, in adult *spa1 spa3 spa4* mutants expressing FL-SPA1-HA the overrepresentation of SPA1/SPA1-COP1 complexes might not have the same effect as proposed for the seedling stage. However, almost all transgenic SPA1-HA lines exhibited larger leaves compared to the *spa3 spa4* control (Figure 25). Since data concerning SPA1-HA transcript and protein levels are not yet available, it is not possible to draw any conclusions about possible correlations between transcript or protein abundance and the complementation of the respective SPA1-HA transgenic lines at this point.

Taken together, in contrast to photoperiodic flowering time control, the kinase-like domain-containing N-terminal part of SPA1 is dispensable for SPA1 function in seedling de-etiolation as well as leaf growth control (Figure 33). However, the SPA1

N-terminus is involved in light-induced SPA1 de-stabilization, but the mechanism how the N-terminus or the kinase-like domain reduce SPA1 protein stability remains unclear at this moment.

	<u>seedling</u>	<u>leaf growth</u>	<u>flowering time</u>	<u>protein de-stabilization</u>
				
SPA1 NT	dispensable (<i>spa1</i>) contributing (<i>spa1 spa3 spa4</i>)	dispensable (<i>spa1 spa3 spa4</i>)	necessary (<i>spa1</i>)	necessary (<i>spa1</i> ; <i>spa1 spa3 spa4</i>)
SPA4 NT	dispensable (<i>spa3 spa4</i>)	dispensable (<i>spa3 spa4</i>)	n.d.	dispensable in seedlings but necessary in leaves? (<i>spa3 spa4</i>)

Figure 33. Role of the SPA1 and SPA4 N-terminus in Arabidopsis development.

The SPA1 N-terminus is dispensable for seedling photomorphogenesis and leaf growth but necessary for photoperiodic flowering and SPA1 protein de-stabilization.

The SPA4 N-terminus is dispensable for seedling photomorphogenesis and leaf growth. Its function in flowering time could not be determined in a *spa3 spa4* mutant background because *spa3 spa4* mutants display the same flowering time phenotype as wild-type plants. The SPA4 N-terminus appears to regulate SPA4 protein stability at least in adult plants.

Mutant backgrounds used for analyses are indicated in brackets.

III.6. The 28g locus specifically enhances the spa1 mutant phenotype in seedling development

To identify new components in SPA-regulated light signal transduction, an EMS mutagenesis of *spa1-3* mutant seeds was performed and M2 seedlings were screened for individuals, whose phenotypes differed from the *spa1* mutant in the light (Nixdorf and Hoecker, 2010). A point mutation in the *28g* locus specifically enhanced the reduced hypocotyl length of *spa1* mutants in light-grown seedlings (Figure 25). This implies that the *28g* locus is a negatively acting factor in the regulation of photomorphogenesis. However, the early flowering phenotype of the *spa1* mutant in SD was suppressed by the mutation of the *28g* locus and also in LD an additional

mutation of *28g* caused a delay of flowering in the *spa1* mutant background (Figure 26). These findings indicate that the yet unknown gene at the *28g* locus is involved in light-dependent seedling growth control, but also impacts flowering time independently of day-length. The question whether the decrease in hypocotyl length in *spa1 28g* mutants is specifically dependent on *SPA1* or whether this gene has a general influence on hypocotyl growth and/or plant development can only be addressed by analyzing lines with a single mutation in the *28g* locus.

In the course of this thesis the *28g* locus was mapped to a region between 6991038 bp and 7031444 bp on the upper arm of chromosome 3. According to the TAIR database, in this particular region 16 loci are remaining as putative candidates for *28g* (Table 3). Most of the loci which are present in the residual 46 kb region between the markers MAL21-SEQ2 and 20150-SEQ encode members of the cytochrome P450 subfamily CYP705A. Plant P450s catalyze various oxygenation/hydroxylation reactions and are involved in a number of biochemical pathways to produce primary and secondary metabolites as well as plant hormones (Mizutani and Otha, 2010). The Arabidopsis genome contains 246 P450s, of which only 60 P450 genes have been characterized yet (Mizutani and Otha, 2010). For example, *DWF4/CYP90B1* and *ROT3/CYP90C1* are involved in Brassinosteroid biosynthesis and *dwf4* and *rot3* mutants exhibit defects in BR-dependent polar elongation of leaf cells (Choe et al., 1998; Kim et al., 1998).

At3g20060 encodes an ubiquitin-conjugating enzyme belonging to the *E2-C* gene family (*UBC19* and *UBC20*), which is thought to be specifically involved in cyclin B1 degradation and thus is important for cell-cycle control in Arabidopsis (Criqui et al., 2002).

At3g20040 encodes a hexokinase-like protein (*ATHXK4/ ATHKL2*), which has not been characterized yet. *Arabidopsis thaliana hexokinase 1 (HXK1)* is a glucose sensor, which regulates plant growth at different developmental stages. The *AtHXK1* null mutant *glucose insensitive 2 (gin2-1)* shows strong growth retardation as a result of reduced cell elongation and altered sensitivities to auxin and cytokinin (Moore et al., 2003). In contrast, *AtHKL1* is a negative effector of plant growth, as *hkl1-1* mutants exhibit an increase in hypocotyl length relative to Col-0 seedlings and is thought to affect seedling growth by mediating cross talk between glucose and phytohormone response pathways (Karve and Moore, 2009).

Since recombination events still occur between the last markers (MAL21-SEQ2 and 20150-SEQ), it is still possible to further narrow down the assumed region of the *28g* locus using additional molecular markers (Figure 27). Alternatively, sequencing of the remaining 46 kb region of *spa1-3* and the *spa1-3 28g* double mutant could reveal single basepair exchanges and possibly help to identify the point mutation that affects the function of the gene encoded by the *28g* locus. Subsequent isolation of the *28g* locus using complementation analysis and characterization of the corresponding gene could answer the question whether the phenotype of the *28g* mutant is dependent on a mutation of *SPA1* or whether the gene is involved in a signalling cascade independently of the *SPA1*-regulated photomorphogenesis pathway.

IV. Materials and Methods

IV.1. Materials

IV.1.1. Chemicals and antibiotics

All chemicals and antibiotics used were of analytical (p.a.) quality and obtained from following companies: Ambion (Austin, USA), Applied Biosystems (Darmstadt, Germany), Applichem (Darmstadt, Germany), Bio-Rad (München, Germany), Colgate-Palmolive (Hamburg, Germany), Duchefa (Haarlem, Netherlands), Difco (Detroit, USA), Fluka AG (Buchs, Switzerland), Gibco BRL (Eggenstein, Germany), Invitrogen (Karlsruhe, Germany), MBI Fermentas (St. Leon-Rot, Germany), Merck (Darmstadt, Germany), Roth (Karlsruhe, Germany), Santa Cruz Biotechnology (Santa Cruz, USA), Serva (Heidelberg, Germany) and Sigma-Aldrich (Deisenhofen, Germany).

IV.1.2. Enzymes, kits, antibodies and radioactivity

Enzymes for molecular biology were obtained from MBI-Fermentas (St. Leon-Rot, Germany), Clontech (Palo Alto, USA), Invitrogen (Karlsruhe, Germany), Roche (Grenzach, Germany) and Lonza Verviers (Potsdam, Germany).

The following kits were used according to manufacturers' instructions: QIAprep Spin Miniprep Kit, QIAquick Gel Extraction Kit, PCR Purification Kit, RNeasy Plant Mini Kit (all Qiagen GmbH, Hilden, Germany) and Megaprime DNA Labeling System (GE Healthcare, München, Germany).

For immunodetection α -GFP (Roche), α -tubulin (Sigma), α -mouse IgG-HRP (Sigma), α -HA (Roche) and α -rat IgG HRP (Santa Cruz Biotechnology) antibodies were used.

The α -[³²P]-dATP for RNA blot analysis was delivered from Hartmann Analytic GmbH (Braunschweig, Germany).

IV.1.3. Oligonucleotides

All oligonucleotides were synthesized by Invitrogen Life Technologies (Karlsruhe, Germany) or Metabion (Martinsried, Germany). Oligonucleotides used during this thesis are presented in Table 4.

Table 4: Sequence of oligonucleotides used in this study and their purpose.

Oligonucleotide	Sequence (5' to 3')	Application
Spa1-F6	CCAGTGCCTTGTGGTACCAAC	genotyping
Spa1-R3	GGTCCCCACTTCTTATTGTCCC	genotyping
LBB1	GCGTGGACCGCTTGCTGCATCT	genotyping
Spa2-F4600	GCAGTTAGCTATGCGAAGTTC	genotyping
Spa2-R6	GCAAACGCTTGAAACGAACAG	genotyping
Gabi-LB	CCCATTTGGACGTGAATGTAGACAC	genotyping
Spa3-F2	TTCGGA CTCTGGCTCTGATTCCTTG	genotyping
Spa3-R4	GTCCTCATTGATGGTCGACAAGTT	genotyping
SPA4 R11	TGAAGCAATAGAAACGAATCTCG	genotyping
SPA4 F11	TTAACGGTTGAGTTCGTTTTCC	genotyping
LB-SAIL	TAGCATCTGAATTCATAACCA	genotyping
spa1-100 WT R1	CATTCATAATACTATTCTCACCAGC	genotyping
spa1-100 WT F1	GATTTAAGGTATGGAGGCTGTAG	genotyping
SPA2 geno F2	GGGAAAATGTCTTTCCTGA	genotyping
SPA2 geno R2	AGCACGGCAAACCATCATA	genotyping
SPA4 geno F1	ggtcaagaagcttctctctg	genotyping
SPA4 geno R1	TCATCATCAAGTCCTCCAAG	genotyping
FISH1 GENO1	CTGGGAATGGCGAAATCAAG	genotyping
co-SAIL F	ACGACATAGGTAGTGGAGAGAACAAC	genotyping
co-SAIL R	ATCCACAAGGTTTAGATACTCATCAC	genotyping
JH2295 (FT-R1)	TAAGCTCAATGATATTCCCCTACA	genotyping
JH2296 (FT-F1)	CAGGTTCAAAACAAGCCAAGA	genotyping
HFR geno F1	ttaggatgaatcggaggagt	genotyping
HFR geno R1	ttgctgtagcttacgcatct	genotyping
HFR geno R2	ggtacgagttgctgtagcttacg	genotyping
hy5-f1	GTTTGGAGGAGAAGCTGTCCG	genotyping
hy5-r1	caaaagcattgacgttgag	genotyping
LBA1	TGGTTCACGTAGTGGGCCATCG	genotyping
SPA2-TF2	CTTCTTCGTTCCACCGCCTCTGTTG	mutant screen
SPA2-TR2	TTCAACTCACTGGTCCTCAGCACAC	mutant screen
SPA4-TF1	CGTGGTATTGTGGTCATCGTCCTCA	mutant screen
SPA4-TR2	TAAAGACCGACCCGTCTCTGATGGA	mutant screen
FISH1	CTGGGAATGGCGAAATCAAGGCATC	mutant screen
FISH2	CAGTCATAGCCGAATAGCCTCTCCA	mutant screen
SPA2 RT F1	CATTGAAAGGGAAGGGAGTT	RT-PCR
SPA2 RT R5	TCACACTGAAATTGGCTCAGC	RT-PCR
SPA4 RT F4	CGTGTGGTCTCTTTATGTAATCA	RT-PCR
SPA4 RT R3	gaggagacagggcagaatag	RT-PCR
SPA4 dkin F3	AGCTCGAGAGAACCTAGAGAGAATTTGGAAG	SPA4 cloning
SPA4 dcc F3	ATCAACTCGGCATTGAGTTGTAACGGTAGA	SPA4 cloning
SPA4 dNT F3	GATTATGTCGAACCTAGAGAGAATTTGGAAG	SPA4 cloning
SPA4 dkin R3	AGGTTCTCTCGAGCTACCAATCTCTCGAGAC	SPA4 cloning
SPA4 dcc R3	CAATGCCGAGTTGATAAACTCACTTTGTAG	SPA4 cloning
SPA4 dNT R3	AGTTTCGACATAATCAATGTGAGACAAAGACTT	SPA4 cloning
XmaI SPA4 F	CTGACCCGGGATGAAGGTTCTTCAGAATCT	SPA4 cloning
SPA4 NotI R (ohne Stop)	AGCTGCGGCCGCTACCATCTCCAAAATCTTGAT	SPA4 cloning
attB1 SPA4 F1	GGGGACAAGTTTGTACAAAAAAGCAGGCTGGATGAAG GGTCTTCAGAATC	SPA4 cloning

Oligonucleotide	Sequence (5' to 3')	Application
attB1 aNLS F1	GGGGACAAGTTTGTACAAAAAAGCAGGCTGGATGCCT AAGAAGAAGAGAAAG	SPA4 cloning
attB2 SPA4 R1	GGGGACCACTTTGTACAAGAAAGCTGGGTGTACCATC TCCAAAATCTTGATATTG	SPA4 cloning
Apal NLS XmaI F	CTAgggcccatgcctaagaagaagagaaaggttgaggaccgggAAG	SPA4 cloning
XmaI NLS Apal R	CTTcccgggtcctccaacctttctcttcttaggcattggcccTAG	SPA4 cloning
colony aNLS F1	tgctaagaagaagagaaaggttg	SPA4 cloning
pMDC 43 S4 F5	agtagacgatgcctcgcagt	Realtime-PCR
pMDC 43 S4 R5	agctgggtgtaccatctcca	Realtime-PCR
HA F1 RT	GGCCGCTTACCCATATGAC	Realtime-PCR
HA R1 RT	GGTAAGCGTAATCCGGAACG	Realtime-PCR
UBQ10 F3	CACACTCCACTTGGTCTTGCCT	Realtime-PCR
UBQ10 R3	TGGTCTTTCCGGTGAGAGTCTTCA	Realtime-PCR
MLD14-SLP1 F	CACTGCATTGTTGTGGAAAAAGATG	mapping 28g
MLD14-SLP1 R	CTCTTTCAAATGGTGAAGCAGTAAC	mapping 28g
MPN9-SLP1 F	AAGATTCATTGCTTAATCGAAATGT	mapping 28g
MPN9-SLP1 R	AAAAAGGTTTTCTAATGTAAAGAAGTA	mapping 28g
MPN9-SEQ2 F	cccatgcagaagagaaaagc	mapping 28g
MPN9-SEQ2 R	atgtttgagacgctgtcacg	mapping 28g
MAL21-SEQ2 F	CGTGGATCCATCTATAAAGGAGTT	mapping 28g
MAL21-SEQ2 R	ccgtctatttaagcagccttat	mapping 28g
MAL21-CAPS2 F	AGCATCGAGGAAAAATCCACTTG	mapping 28g
MAL21-CAPS2 R	CTTCGGGAGTCCATTGGTTA	mapping 28g
20150-SEQ F	ttcgtcgtctcccatttc	mapping 28g
20150-SEQ R	ATCCTCAAGCATCGAACCAG	mapping 28g
MQC12-CAPS5 F	agtgtatacaacaaatgttaacgtg	mapping 28g
MQC12-CAPS R	agatccctcccacatgc	mapping 28g
K10D20 SLP1 F	gtatcaatgtatgtatcatgtttcca	mapping 28g
K10D20 SLP1 R	tgtacttgattgtacaaaacactg	mapping 28g
MOE17-SLP1 F	CTGGGGTGTCTCACAGGAT	mapping 28g
MOE17-SLP1 R	TGAATTCGGGTTCAAGATTGT	mapping 28g
MSA6-SLP1 F	CTCCTCCTGCTGGTTTTGAG	mapping 28g
MSA6-SLP1 R	CGTTGGAGGTGGTCTTAGGT	mapping 28g

IV.1.4. Bacterial strains

For standard cloning, *Escherichia coli* strain *DH5 α* was used. For gateway cloning of destination vectors, the *ccdB* gene resistant *Escherichia coli* strain *DB3.1* (Invitrogen) was used. For plant transformation, *Agrobacterium tumefaciens* strain *GV3101* (*pMP90RK*) was used.

IV.1.5. Cloning vectors

For standard clonings, pBluescript KS (pBS; Stratagene, La Jolla, USA) was used. Entry vector pDONR207 (GentR) (Invitrogen) was used for BP reaction and

destination vector pMDC43 (HygR) (Curtis and Grossniklaus, 2003) was used for LR reaction for the SPA4 structure function analysis.

A modified binary vector pJHA 212 (spectinomycin resistance gene; kanamycin resistance gene *npt* was replaced by the hygromycin resistance gene *hpt*) was used for *Agrobacterium* transformation of SPA1-HA FL and deletion constructs in the *spa1 spa3 spa4* background.

IV.1.6. Plant lines

To create a *spa* null quadruple mutant, *spa1-100 spa3-1* double mutants were crossed with *spa2-2 spa4-3* double mutants. *spa2-1* and *spa4-3* mutant alleles were isolated in the course of this thesis from a T-DNA insertion line library (C. Koncz, MPIZ, Cologne; Rios et al., 2002). The *spa1-100* allele was derived from the Syngenta Arabidopsis Insertion Library (SAIL) T-DNA insertion mutant population (Sessions et al., 2002), carries a T-DNA insertion in the second exon and likely presents a *spa1* null allele (Yang et al., 2005). The *spa3-1* allele was also isolated from the SAIL T-DNA collection and carries a T-DNA insertion in its first intron (Laubinger and Hoecker, 2003).

The previous available *spa1-7* allele was obtained from the SALK T-DNA insertion library (Alonso et al., 2003) and was confirmed to carry a T-DNA insertion in the third exon at position 2638 bp after the ATG of *SPA1* (Fittinghoff et al., 2006). *spa2-1* carries a T-DNA insertion in the last intron of *SPA2* at position 4008 bp after the presumed start codon (Laubinger et al., 2004) and was obtained from the GABI-KAT T-DNA collection (Rosso et al., 2003). In *spa4-1* (SAIL-collection), two T-DNAs are inserted head-to-head 3' to the codon for D⁶⁴⁰ of SPA4, apparently causing a deletion of the following 31 nucleotides (Laubinger and Hoecker, 2003).

For mapping of the EMS mutant *28g* locus, the F₂ generation of a cross between a *spa1-7* single mutant (Col-0 background) and a *spa1-3 28g* double mutant (RLD background) was used. The *spa1-3* mutant allele was derived from an EMS mutagenesis and carries a single base pair substitution that leads to a premature stop codon in the first exon (Hoecker et al., 1999).

The transgenic *spa1-3* lines, carrying *SPA1-FL-HA*, *SPA1-ΔNT* and *SPA1-Δcc* constructs were generated and phenotypically characterized by Kirsten Fittinghoff (Fittinghoff et al., 2006).

The mutant *hy5* allele used for crossing into a *spa1 spa3 spa4* background was obtained from SALK (SALK_096651), (Alonso et al., 2003), carries a T-DNA insertion and was determined to be a null allele (Ruckle et al., 2007).

The *cop1-4 hy5-215* double mutant and the corresponding *hy5-215* single mutant (Oyama et al., 1997) were provided by Roman Ulm, University Freiburg.

All further used mutants were described previously. Table 5 shows an overview about all Arabidopsis lines used in this study.

Table 5: Overview of all plant lines used in this study.

Designation (genotype), accession, type of mutation causing the respective mutation and references are presented.

Genotype	Accession	Mutation	References
wild type	RLD		
<i>spa1-3</i>	RLD	EMS	Hoecker et al., 1998
<i>spa1-3 28g</i>	RLD	EMS	U. Hoecker
<i>spa1-7 x spa1-3 28g F1</i>	Col-0/RLD	T-DNA/EMS	(1) M. Nixdorf, University Düsseldorf; (2) this study
<i>spa1-7 x spa1-3 28g F2</i>	Col-0/RLD	T-DNA/EMS	this study
<i>spa1-7 x spa1-3 28g F3</i>	Col-0/RLD	T-DNA/EMS	this study
<i>spa1-3 FL-SPA1-HA</i>	RLD	EMS	Fittinghoff et al., 2006
<i>spa1-3 dNT-SPA1-HA</i>	RLD	EMS	Fittinghoff et al., 2006
<i>spa1-3 dkin-SPA1-HA</i>	RLD	EMS	Fittinghoff et al., 2006
<i>spa1-3 dcc-SPA1-HA</i>	RLD	EMS	Fittinghoff et al., 2006
wild type	Ler		
<i>ga1-3</i>	Ler	fast neutron bombardement	Sun et al., 1992
<i>gai</i>	Ler	X-ray	Koornneef et al., 1985
wild type	Col-0		
<i>spa1-7</i>	Col-0	T-DNA (SALK-collection)	Fittinghoff et al., 2006
<i>spa2-1</i>	Col-0	T-DNA (GABI-KAT-collection)	Laubinger et al., 2004
<i>spa3-1</i>	Col-0	T-DNA (SAIL-collection)	Laubinger and Hoecker, 2003
<i>spa4-1</i>	Col-0	T-DNA (SAIL-collection)	Laubinger and Hoecker, 2003
<i>spa1-7 spa2-1</i>	Col-0	T-DNA	Laubinger et al., 2004
<i>spa3-1 spa4-1</i>	Col-0	T-DNA	Laubinger and Hoecker, 2003
<i>spa2-1 spa3-1 spa4-1</i>	Col-0	T-DNA	U. Hoecker
<i>spa1-7 spa3-1 spa4-1</i>	Col-0	T-DNA	U. Hoecker
<i>spa1-7 spa2-1 spa4-1</i>	Col-0	T-DNA	P. Fackendahl, 2005
<i>spa1-7 spa2-1 spa3-1</i>	Col-0	T-DNA	P. Fackendahl, 2005
<i>spa1-7 spa2-1 spa3-1 spa4-1</i>	Col-0	T-DNA	P. Fackendahl, 2005
<i>spa1-100</i>	Col-0	T-DNA (SAIL-collection)	Yang et al., 2005
<i>spa2-2</i>	Col-0	T-DNA (C. Koncz, MPIZ)	C. Koncz, MPI Cologne; this study

Genotype	Accession	Mutation	References
<i>spa4-3</i>	Col-0	T-DNA (C. Koncz, MPIZ)	C. Koncz, MPI Cologne; this study
<i>spa1-100 spa2-2</i>	Col-0	T-DNA	this study
<i>spa3-1 spa4-3</i>	Col-0	T-DNA	this study
<i>spa2-2 spa3-1 spa4-3</i>	Col-0	T-DNA	this study
<i>spa1-100 spa3-1 spa4-3</i>	Col-0	T-DNA	this study
<i>spa1-100 spa2-2 spa4-3</i>	Col-0	T-DNA	this study
<i>spa1-100 spa2-2 spa3-1</i>	Col-0	T-DNA	this study
<i>spa1-100 spa2-2 spa3-1 spa4-3</i>	Col-0	T-DNA	this study
<i>spa3 spa4 FL-GFP-SPA4</i>	Col-0	T-DNA	this study
<i>spa3 spa4 FL-GFP-NLS-SPA4</i>	Col-0	T-DNA	this study
<i>spa3 spa4 dNT-GFP-SPA4</i>	Col-0	T-DNA	this study
<i>spa3 spa4 dNT-GFP-NLS-SPA4</i>	Col-0	T-DNA	this study
<i>spa3 spa4 dkin-GFP-SPA4</i>	Col-0	T-DNA	this study
<i>spa3 spa4 dkin-GFP-NLS-SPA4</i>	Col-0	T-DNA	this study
<i>spa3 spa4 dcc-GFP-SPA4</i>	Col-0	T-DNA	this study
<i>spa3 spa4 dcc-GFP-NLS-SPA4</i>	Col-0	T-DNA	this study
<i>spa1 spa3 spa4 FL-SPA1-HA</i>	Col-0	T-DNA	K. Fittinghoff, University Cologne
<i>spa1 spa3 spa4 dkin-SPA1-HA</i>	Col-0	T-DNA	K. Fittinghoff, University Cologne
<i>spa1 spa3 spa4 dNT-SPA1-HA</i>	Col-0	T-DNA	K. Fittinghoff, University Cologne
<i>co-SAIL (co-10)</i>	Col-0	T-DNA (SAIL-collection)	G.Coupland, MPIZ Cologne; Laubinger et al., 2004
<i>ft-10</i>	Col-0	T-DNA (GABI-KAT-collection)	Yoo et al., 2005
<i>ft-10 spa1-7 spa2-1 spa3-1 spa4-1</i>	Col-0	T-DNA	this study
<i>phyB-9</i>	Col-0	EMS	Rösler et al., 2007
<i>cop1-4</i>	Col-0	EMS	McNellis et al., 1994
<i>cop1-6</i>	Col-0	EMS	McNellis et al., 1994
<i>cop1-6 phyB-9</i>	Col-0	EMS	Boccalandro et al., 2004
<i>cop1-4 sth2-1</i>	Col-0	EMS/T-DNA (SALK-collection)	Datta et al., 2007
<i>hy5-215</i>	Col-0	EMS	Oyama et al., 1997
<i>cop1-4 hy5-215</i>	Col-0	EMS	R. Ulm, unpublished
<i>hy5-SALK</i>	Col-0	T-DNA (SALK-collection)	Ruckle et al., 2007
<i>hy5-SALK spa1-7 spa3-1 spa4-1</i>	Col-0	T-DNA	this study
<i>hfr1-101 (formerly rsf1)</i>	Col-0	T-DNA (SALK-collection)	Fankhauser and Chory, 2000; Spiegelman et al., 2000
<i>hfr1-101 spa1-7 spa3-1 spa4-1</i>	Col-0	T-DNA	this study

IV.2. Work with *Arabidopsis thaliana*

IV.2.1. Seed sterilization

For sterile growth of *Arabidopsis* on MS-plates, seeds were surface sterilized. For liquid sterilization, seeds were immersed with 10% Klorix (Colgate-Palmolive,

Hamburg, Germany) and 0.03% Triton-X-100 for 8 minutes and washed three times with sterile water before plating them on 1xMS medium. Liquid sterilization was applied when seedlings were used for hypocotyl length measurements.

For dry seed sterilization, aliquots of seeds were incubated with chlorine gas for approximately 4 hours and subsequently were evaporated for 2 hours. To produce chlorine gas, 80 ml of sodium hypochlorite was mixed with 2.5 ml of concentrated hydrochloric acid in an exsicator. Dry seed sterilization was applied for phenotypic screens of transgenic T2 and T3 lines and for protein as well as RNA isolation.

IV.2.2. Plant growth

Arabidopsis seeds were stratified in 4°C for three days in water supplemented with 0.1% agarose. Seeds were normally sown in a substrate mixture containing three parts soil and one part Vermiculit. In the greenhouse, plants were grown under long-day conditions with 16 hours light and 8 hours darkness and a relative humidity of approximately 40%. The temperature was kept at 21°C during light period and was reduced to 18°C during darkness.

To determine flowering time or leaf size in controlled conditions, seeds were sown on soil and plants were grown in a randomized fashion in LD (16 hours light/ 8 hours darkness) or in SD (8 hours light/ 16 hours darkness) at constant 21°C and a relative humidity of 60%. Light sources were fluorescent tubes (OSRAM, Lumilux, cool white) and light intensity was approximately $110 \mu\text{mol m}^{-2} \text{s}^{-1}$.

To determine whether the plants were responsive to GA, all lines were GA treated (100 μM GA₃) for 3 days at 4°C, then sowed on soil. Plants were sprayed with 100 μM GA₃ every 2-3 days starting one week after sowing.

For seedling analysis, seeds were sown on sterile MS plates and stratified in 4°C for 4 days, followed by a 3-hour white-light treatment at 21°C to induce germination. Afterwards plates were transferred either to darkness or kept in the dark for 21 hours at 21°C and were then exposed to continuous far-red light (FRc), red light (Rc) or blue light (Bc) respectively for three days at 21°C. Light conditions were generated using LED light sources (Quantum Devices, Barneveld, WI, USA).

IV.2.3. Measurement of hypocotyl length

To determine hypocotyl length, 4-day-old seedlings were pressed lengthwise on MS plates containing 1% agar and were subsequently documented with a digital camera. Measurements of hypocotyl length were conducted on digital images via NIH Image

Software (Bethesda, USA). 20-30 hypocotyls were measured per genotype. Statistical analyses were performed via KaleidaGraph 3.6 (Synergy Software) software program.

IV.2.4. Quantification of leaf size

Leaf length was determined by measuring the lengths of the longest leaf (including petiole) of 3-week-old long-day grown plants. Leaf area was determined after taking pictures of flattened leaf blades (leaf 3) with a digital camera. Measurements of leaf area were conducted subsequently via NIH Image Software and statistical analyses were performed via KaleidaGraph 3.6 software. Per genotype at least 10 leaves were analyzed.

IV.2.5. Determination of flowering time

Time of flowering under SD or LD conditions was determined by counting the numbers of true leaves at that day when the first inflorescence was visible by eye. Additionally, number of days to flower from the day of sowing was determined. 10-15 plants were analyzed for each genotype. Statistical analyses were made using KaleidaGraph 3.6 software.

IV.2.6. Microscopy of Arabidopsis leaves

a) Quantification of palisade cells in *Arabidopsis thaliana* leaves

For estimating palisade cell size and number from Arabidopsis leaves, leaf 3 of a 4-week-old LD-grown plant was placed into a microcentrifuge tube and immersed in 0.1% Triton-X-100, followed by centrifugation at 10000 g for 1 min at room temperature to sediment the chloroplasts (Horiguchi et al., 2006). The leaves were placed on a glass slide, covered with a cover slide and analyzed under a light microscope (LEICA-DRME). Images were taken using a high resolution KY-F70 3-CCD JVC camera and DISKUS software (DISKUS, Technisches Büro Hilgers, Königswinter). Palisade cells in the sub-epidermal layer at the tip of the leaf blade between the mid-vein and the leaf margin were examined in 10 leaves per genotype. To determine the cell area, 20 palisade cells from each leaf were measured using ImageJ software (NIH, USA). Total number of palisade cells, was calculated from the number of cells counted in a given area (0.16 μm^2) and total leaf blade area. Statistical analysis was performed using KaleidaGraph 3.6 (Synergy Software) software program.

b) Quantification of epidermal cells in *Arabidopsis thaliana* leaves

To estimate epidermal cell size and number from *Arabidopsis* leaves, leaf 3 of a 4-week-old long day grown plant was fixed onto a glass slide covered with sticky tape. Next, the adaxial epidermis was coated with a thin layer of Collodium and air-dried for approximately 15 min. Then the Collodium imprint was carefully peeled off with fine forceps and placed in a drop of water onto a glass slide, covered with a cover slide and analyzed under a light microscope. Images were taken as described in a). Adaxial epidermal cells at the tip of the leaf blade between the mid-vein and the leaf margin were examined in 10 leaves per genotype. To determine the cell area, 30 epidermal cells from each leaf were measured using ImageJ software (NIH, USA). Total number of epidermal cells, was calculated from the number of cells counted in a given area ($0.16 \mu\text{m}^2$) and total leaf blade area. Statistical analysis was performed using KaleidaGraph 3.6 software.

IV.2.7. Screening of transgenic plants

T1 seeds from *GFP-SPA4* transgenic lines in the *spa3 spa4* mutant background as well as from *SPA1-HA* transgenic lines in the *spa1 spa3 spa4* mutant background were screened on 1xMS plates containing 1% sucrose and 20mg/L hygromycin (Invitrogen). First complementation analysis was performed by phenotypic analysis of hypocotyl length in FRc (0.2 or $0.4 \mu\text{mol m}^{-2} \text{s}^{-1}$). Number of insertion sites was estimated by segregation ratio of transgenic T2 lines on hygromycin plates. At least two independent transgenic lines per complementing construct were propagated to obtain homozygous T3 lines. These lines or progenies of these lines were used for detailed phenotypic characterization and immunoblot analysis.

IV.2.8. Screening of an *Arabidopsis* T-DNA insertion mutant collection

Screening of the Koncz T-DNA collection for *spa2* and *spa4* null mutant alleles was performed according to the protocol established by G. Rios and B. Hertel at the MPIZ, Cologne (Rios et al., 2002).

IV.2.9. Molecular mapping

spa1-3 seeds were mutagenized with EMS and M_2 seedlings were screened under $0.05 \mu\text{mol m}^{-2} \text{s}^{-1}$ Rc for altered photomorphogenesis compared to the parental *spa1-3* genotype (Nixdorf and Hoecker, 2010). For genomic mapping of the *28g* mutation, *spa1-3 28g* double mutants (RLD background) were crossed with *spa1-7* mutant plants (Col-0 background). The segregating F_2 progeny derived from this cross was

screened for the double mutant seedling phenotype under $0.3 \mu\text{mol m}^{-2} \text{s}^{-1}$ Rc. Polymorphic molecular markers were created via the Monsanto Arabidopsis polymorphism and Ler sequence collection (Jander et al., 2002). Molecular markers used in this study are presented in Table 6.

Table 6: Molecular markers used for mapping of the 28g locus

Markers used for mapping of the 28g locus, position and type of the polymorphism as well as restriction enzymes used for detection of the CAPS polymorphism are presented.

Marker	Position on chromosome 3	Indel size/ substitution (Col-0/ RLD)	Enzyme (CAPS marker) / fragment size (bp)
MLD14-SPL1	6748172	18/-18	
MPN9-SLP1	6901594	-10/10	
MPN9-SEQ2	6957387	C/T	
MAL21-SEQ2	6991038	T/C	
MAL21-CAPS2	7015410	G/T	Col-0: CfoI (142 + 138/ 280)
"20150"-SEQ	7031444	G/C	
MQC12-CAPS5	7094256	T/A	RLD: SspI (259/ 150 + 109)
K10D20-SLP1	7180940	28/-28	
MOE17-SPL1	7319249	15/-15	
MSA6-SLP1	7354431	54/-54	

IV.3. Molecular biology methods

IV.3.1. Standard molecular biology methods

Standard molecular biology methods, like nucleic acid precipitation, DNA gel-electrophoresis and staining of DNA Fragments, were performed according to protocols described in Sambrook and Russel (2001).

IV.3.2. Cloning

Conventional DNA cloning was performed using standard protocols (Sambrook and Russel, 2001). Gateway cloning (BP and LR reaction) was done according to manufactures' protocol (Invitrogen). For details of cloning strategies, see section IV.5.

IV.3.3. Bacterial transformation and plasmid isolation

Escherichia coli competent cells were transformed by heat shock method and subsequently plated on selective media and kept at 37°C overnight. Plasmid DNA from *E. coli* was isolated via the Qiagen Plasmid Mini Kit (Qiagen) according to manufactures' instructions.

Agrobacterium tumefaciens cells were transformed via electroporation and then plated on selective media and incubated at 28°C for two days.

IV.3.4. Sequence Analyses

Correctness of PCR-generated cloned DNA fragments was determined by restriction digestion with appropriate restriction enzymes followed by sequencing (GATC, Konstanz, Germany). Sequence alignment analysis and also construct design were performed using Vector NTI-suite software (Invitrogen) and Lasergene (DNASTAR, Madison, USA). PCR primers were designed using Primer3 software (Whitehead Institute for Biomedical Research).

IV.3.5. Transient transformation

For localization studies, GFP-SPA4 fusions were transiently expressed in onion epidermal cells via biolistic transformation. As control, a ds-red construct was co-expressed to highlight the transformed cells.

a) Preparation of microcarriers: 30 mg of gold particles (1 µm, Bio-Rad, Hercules, USA) were placed in a reaction tube, incubated for 15 min with 1 ml 70% ethanol and centrifuged for 15 sec at 400 rpm. The supernatant was discarded and the gold particles were washed 2x with 1 ml sterile water and subsequently resuspended in 1 ml of sterile water. After sonification for 3 sec (Branson Sonifier 250, USA), 50 µl aliquots were prepared while vortexing, frozen in liquid nitrogen and stored at -80 °C.

b) DNA coating of the microcarriers: for two shots, 600 ng of each plasmid was used. H₂O, 20 µl 2.5 M CaCl₂, 8 µl 0.1 M spermidine and 10 µl gold particles were added while vortexing to a final volume of 50 µl. The mixture was vortexed for 10 min and the gold particles were pelleted by centrifugation (5 sec, 10 000 rpm). The supernatant was removed carefully and the gold particles were washed with 100 µl 70% ethanol, centrifuged for 5 sec at 10 000 rpm and washed again with 40 µl 100% ethanol. Finally, the microcarriers were resuspended in 24 µl 100% ethanol and sonificated for 3 sec to deagglomerate the particles.

c) Particle bombardment: per shot, 10 µl of the coated microcarriers were pipetted onto a macrocarrier (Bio-Rad) and dried until the ethanol evaporated. The particle bombardment was performed with the Biolistic Particle Delivery System (Bio-Rad, Hercules, USA) according to manufacturers instructions. Bombardment conditions used were: 900psi, rupture disk and vacuum 26mm Hg. Prior to analysis, samples were kept in darkness for 24 h.

IV.3.6. Fluorescence microscopy

Localization of the GFP-SPA4 fusion proteins was assayed via fluorescence microscopy using a Leica DMRE microscope and epifluorescence optics. Images were taken using a KY-F70 3-CCD JVC camera and DISKUS software.

IV.3.7. Plant transformation

Agrobacterium-mediated transformation of flowering Arabidopsis plants was performed using floral-dip method as described previously (Clough and Bent, 1998).

IV.3.8. Genomic DNA preparation

For high-throughput DNA analysis (e.g. for screening segregating F2 lines of crossings or testing of F2 mapping population) approximately 10-15 seedlings or one 0.5 x 0.5 cm piece of an Arabidopsis leaf per line were transferred to 8 tube strips (compatible to Qiagen TissueLyser) containing a 5 mm stainless steel bead. Then, 300 µl extraction buffer (50mM Tris/HCl pH 7.2, 300mM NaCl, 10% Sucrose) were added and disrupted in the Tissue Lyser at 30 Hz for 3 min. 1µl of tissue suspension was used as template for a 20 µl PCR reaction.

Standard genomic DNA preparation from Arabidopsis seedlings or leaves was performed as described previously (Edwards et al., 1991).

IV.3.9. RNA isolation

For RT-PCR, REALTIME-PCR and RNA blot analyses; total RNA from Arabidopsis seedlings or leaves was isolated using the RNeasy Plant Mini Kit (Qiagen) according to the manufacturers' protocol.

IV.3.10. Transcript analysis by RT-PCR

To analyze the *spa2-2* or *spa4-3* mutant alleles via RT-PCR, total RNA from three homozygous lines per mutant was isolated. One µg of RNA was treated with RNase-free DNase I (MBI Fermentas), according to the manufacturers' instruction. Subsequently, cDNAs were synthesized using an oligo-dT primer and RevertAid H Minus M-MuLV Reverse Transcriptase (MBI Fermentas). For PCR, 1.5 µl cDNA was used as template. *SPA2* and *SPA4* cDNA-specific primers were used respectively. As a control *SPA3* specific primers were used.

IV.3.11. Transcript analysis by REALTIME-PCR

For transcript analysis of *GFP-SPA4* and *SPA1-HA* transgenic lines, RNA isolation and cDNA synthesis was performed as described before. Transcript levels were

determined by quantitative PCR using an Applied Biosystems 7300 realtime PCR system with 1.5 μ l cDNA in a 25 μ l reaction containing POWER SYBR Green pre-mix (Applied Biosystems) and gene-specific primers. One to two biological replicates were used per sample, and each was analyzed in duplicate. The results were analyzed by the $\Delta\Delta C_t$ method using *UBQ10* for normalization.

IV.3.12. RNA blot analysis

To analyze *SPA2* or *SPA4* transcript levels in the *spa2-2* or *spa4-3* mutant alleles respectively, Total RNA was isolated from 4-day-old dark-grown seedlings that had been transferred to Rc ($30 \mu\text{mol m}^{-2} \text{s}^{-1}$) for two hours. 10 μ g of total RNA was separated by standard glyoxal gel electrophoresis (Ambion), blotted onto nylon membranes (Hybond-N, GE Healthcare) using a Turbo blotter (Schleicher und Schüll) and immobilized by UV-crosslinking. Membranes were hybridized with *SPA2*- or *SPA4*-specific, ^{32}P -labelled probes comprising the complete respective ORF. Radioactive labelled probes were obtained using the Mega Prime Labelling Kit (Amersham, GE) according to manufacturers' instructions. After over-night hybridization with specific probes in 10 ml hybridization buffer (250mM Na_2HPO_4 , 7% (w/v) SDS, 1% (w/v) BSA and 2.5 mM EDTA, pH 7.2) at 65°C, the membranes were washed once with 2x SSC, 0.1% SDS, once with 0.5x SSC, 0.1% SDS and once with 0.1x SSC, 0.1% SDS at 65°C for 30min each. Exposition to phosphorimager plates (FLA-7000, Fuji) was carried out for 4 days for *SPA* signals. *SPA* signals were normalized to the signal of *18S rRNA*.

IV.3.13. Preparation of DNA Probes for RNA blot analysis

SPA2 and *SPA4* specific DNA probes were obtained by PCR amplification via *SPA2*-Sall-R and *SPA2*-RI-F from a *SPA2* pJET plasmid and via *SPA4*-BamHI and *SPA4*-RI-F primers from a cTopo*SPA4* plasmid, respectively. The *18S rRNA* probe was obtained by restriction digestion of a pP055 plasmid via BamHI and EcoRI. All probes were purified by gel elution and 25 ng of DNA was used for labelling of the respective DNA probes.

IV.4. Biochemical methods

IV.4.1. Total protein isolation from Arabidopsis

Approximately 200 mg of tissue (seedling or leaf) were snap-frozen in liquid nitrogen, ground to a fine powder and resuspended in protein extraction buffer (50 mM Tris pH 7.5, 150 mM NaCl, 1 mM EDTA, 10% glycerol, 1 mM DTT, 1% protease inhibitor cocktail (Sigma), 0,1% Nonidet, 1 mM PMSF for GFP-SPA4 protein analysis; 50 mM Tris pH 7.5, 150 mM NaCl, 1 mM EDTA, 10% glycerol, 5 mM DTT, 1% protease inhibitor cocktail (Sigma), 10 μ M MG132, 1% Triton-X-100 for SPA1-HA protein analysis) in the ratio 150 μ l per 100 mg tissue. The mixture was centrifuged at 14000 rpm and 4°C for 50 min (SPA4) or 12 min (SPA1). The supernatant was supplemented with 5x Laemmli buffer (310mM Tris/HCl pH 6,8, 10% (w/v) SDS, 50% (v/v) Glycerol; 0,5% (w/v) Brom-phenol-blue, 500 mM DTT) (Laemmli et al., 1970) and incubated at 100°C for 8 min (SPA4) or at 96°C for 5 min (SPA1). Protein concentration was determined using the Bradford assay (Bio-Rad). Except for SPA1-HA protein analysis in the *spa1 spa3 spa4* mutant background, all experiments were performed at least twice using one or two biological replicates per sample.

IV.4.2. SDS-polyacrylamidegelelectrophoresis (SDS-PAGE)

Protein samples were separated by SDS-PAGE (7,5% acryamid concentration of separating gel) and blotted onto nitrocellulose membranes using a semidry blotting system (CTI, Taunusstein) and Towbin transfer buffer (96 mM Glycin, 10 mM Tris, 10% (v/v) Methanol) for 2 1/2 h at 0,6 mA/cm². Per sample 30 μ g (SPA1-HA), 40 μ g (GFP-SPA4, 4-d-old seedlings) or 60 μ g (GFP-SPA4, 3-week-old plants) of total protein was used, respectively.

IV.4.3. Immunoblot analysis

After transfer, membranes were blocked using Roti-Block (Roth) and incubated with the respective primary antibody followed by horseradish peroxidase (HRP)-conjugated secondary antibody, with subsequent visualization on a LAS-4000 mini-image-analyzer (Fuji). Signal intensities were quantified using Multi-Gauge software (Fuji). Commercial available antibodies used were α -GFP (Roche), α -tubulin (Sigma), α -mouse IgG-HRP (Sigma), α -HA (Roche) and α -rat IgG HRP (Santa Cruz Biotechnology).

IV.5. Cloning strategies

IV.5.1. Construction of 35S:GFP-SPA4 full-length and deletion constructs

To generate 35S:GFP-SPA4 and 35S:GFP-NLS-SPA4 and their respective deletion derivatives SPA4- Δ NT, Δ kin and Δ cc, several cloning steps were performed. First, a Topo-cSPA4 vector was used as template for amplification of SPA4 full-length (FL) cDNA using XmaI-SPA4F (with ATG) and SPA4-NotIR (without stop) primers and Pfu polymerase (MBI Fermentas) for subsequent PCR purification and restriction digestion with XmaI (Cfr9I) and NotI (both MBI Fermentas). The digested SPA4-FL PCR product was ligated into a modified pBluescript (pBS KS; Stratagene) plasmid carrying 5' and 3' regulatory sequences of SPA4 (provided by Kirsten Fittinghoff, PhD thesis, 2008) using T4 Ligase (MBI Fermentas). Positive clones were selected using colony PCR, appropriate restriction analysis and subsequent sequencing.

For cloning NLS-SPA4-FL, an artificial SV40 NLS (modified after Matsushita et al., 2003) was obtained by annealing two oligonucleotides (ApaI-NLS-XmaI-F and XmaI-NLS-ApaI-R) encoding the amino acid residues (MPKKKRKEGG) and carrying ApaI and XmaI recognition sites at 60°C for 20 min. NLS sequence was digested with ApaI and XmaI and ligated into previously generated SPA4-FL pBS vector. Positive clones were identified as described before.

Next the SPA4-FL cDNA as well as the NLS-SPA4-FL cDNA were amplified from the respective vectors with sequence-specific primers containing attached attB1 site to forward primer and attB2 site to reverse primer. The purified PCR product was cloned into pDONR207 entry vector through BP reaction (Invitrogen) following manufacturers' instruction. After sequencing SPA4-FL and NLS-SPA4-FL were cloned from the before created entry vector into a pMDC43 destination vector (Curtis and Grossniklaus, 2003) using LR reaction (Invitrogen) according to manufacturers' instruction (Figure 34).

Following verification of correct insertion via sequencing, plasmid clones carrying 35S:GFP-SPA4-FL or 35S:GFP-NLS-SPA4-FL respectively were selected for Agrobacterium GV3101-mediated transformation of *spa3 spa4* mutant plants (Clough and Bent, 1998).

Construction of the Δ NT, Δ kin and Δ cc deletion derivatives of SPA4 was performed via overlapping PCR (modified after Horton et al., 1989 and Warrens et al., 1997). In Δ NT-SPA4, 234 aa after bp 105, in Δ kin-SPA4, 122 aa after bp 442 and in Δ cc-SPA4

152 aa were deleted 807 bp after the ATG. Initially, six different PCR products were amplified using the Topo-cSPA4 plasmid as a template and various primer combinations (see below). The primers are designed so that the ends of the products contain complementary sequences. Next, two appropriate PCR products were mixed for each construct and used as templates for a PCR reaction with external primers, as these PCR products, when mixed, denatured and reannealed, having matching sequences at their 3' ends that overlap and can act as primers for each other (Horten et al., 1989) to generate the wanted deletion derivatives.

To obtain *SPA4-ΔNT*, first two PCR products were generated using XmaI-SPA4-F and ΔN-R3 (fragment 1) and ΔN-F3 and SPA4-NotI-R (4) respectively. For generation of the *SPA4-Δkin* construct, the following primer combinations were used for the first round of PCR: XmaI-SPA4-F + Δkin-R3 (2) and Δkin-F3 + SPA4-NotI-R (5). For *SPA4-Δcc*, XmaI-SPA4-F + Δcc-R3 (3) and Δcc-F3 + SPA4-NotI-R (6) primer combinations were used. PCR products were checked on an agarose gel for correct fragment size and purified via gel extraction. For *SPA4-ΔNT* 5 μl of purified PCR products (1) and (4), for *SPA4-Δkin*, PCR products (2) and (5) and for *SPA4-Δcc*, PCR products (3) and (6) were mixed and used as template for the second round of PCR using XmaI-SPA4-F and SPA4-NotI-R primers to obtain the respective deletion fragments of SPA4 cDNA. The resulting PCR products were purified, digested with XmaI and NotI and ligated into pBS (see cloning of *SPA4-FL* constructs).

All subsequent cloning steps were performed as described for the generation of the *SPA4-FL* vector. Furthermore, for every SPA4 deletion derivative, a respective artificial NLS-containing construct was generated in addition.

All SPA4 deletion constructs were verified via sequencing and transformed into *spa3 spa4* mutant plants by *Agrobacterium*-mediated floral dip transformation as well.

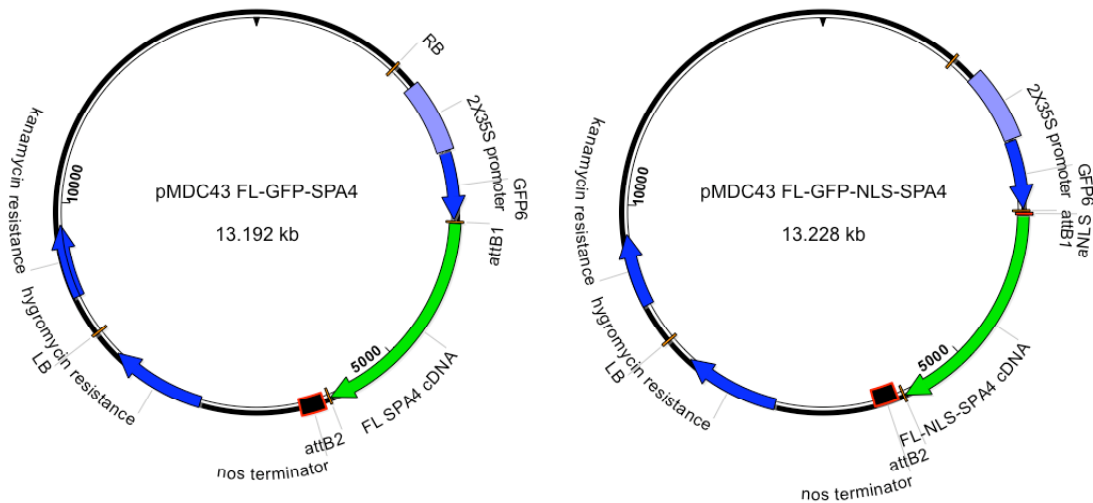


Figure 34. *FL-GFP-SPA4* and *FL-GFP-NLS-SPA4* constructs.

SPA4 cDNA is depicted in green, N-terminal *GFP* fusion is depicted in blue and the dual 35S promoter is displayed in violet. The *FL-GFP-NLS-SPA4* construct contains an artificial NLS between *GFP*- and *SPA4* cDNAs, depicted in red. The pMDC43 vectors carry kanamycin and hygromycin resistance genes. *SPA4* deletion constructs are not presented.

IV.5.2. Constructs for *SPA1* structure-function analysis

Generation of *FL-SPA1-HA*, ΔNT -*SPA1-HA*, Δkin -*SPA1-HA* and Δcc -*SPA1-HA* constructs was performed by K. Fittinghoff as described previously (Fittinghoff et al., 2006, supplementary experimental procedures). For experiments in the *spa1-3* mutant background, *SPA1* constructs in pPZP211 (Hajdukiewicz et al., 1994) were used (Fittinghoff et al., 2006).

For analysis of *SPA1-HA* in the *spa1 spa3 spa4* mutant background, the respective *SPA1* promoter:cDNA fusions had to be subcloned in a modified pJHA212 vector (Figure 35) carrying Hygromycin instead of Kanamycin resistance as the *spa1-7* T-DNA mutant allele carries Kanamycin resistance and *spa3-1* and *spa4-1* alleles carry BASTA resistance (Fittinghoff et al., 2006; Laubinger and Hoecker, 2003). Cloning of *pSPA1:SPA1-HA* from pPZP211 into pJHA212 was performed by restriction cloning via XmaI (Cfr9I) sites (Expression vectors were provided by K. Fittinghoff).

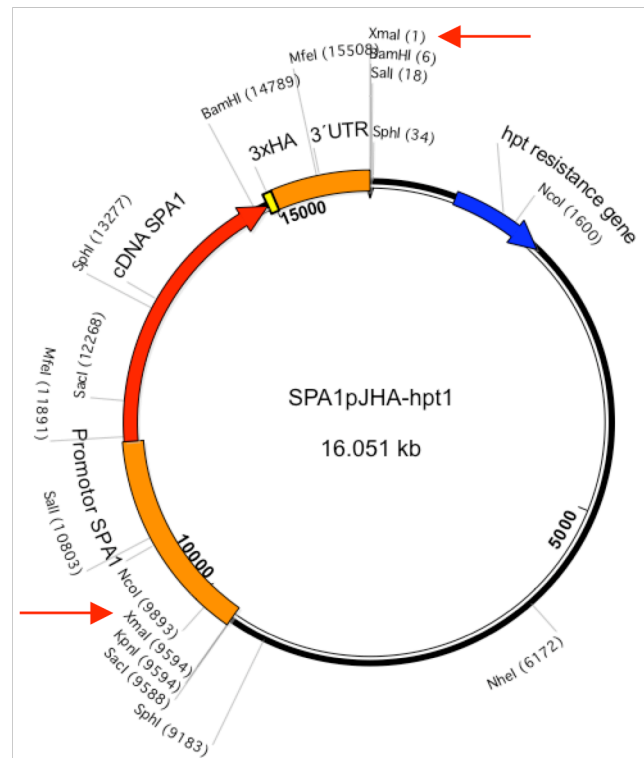
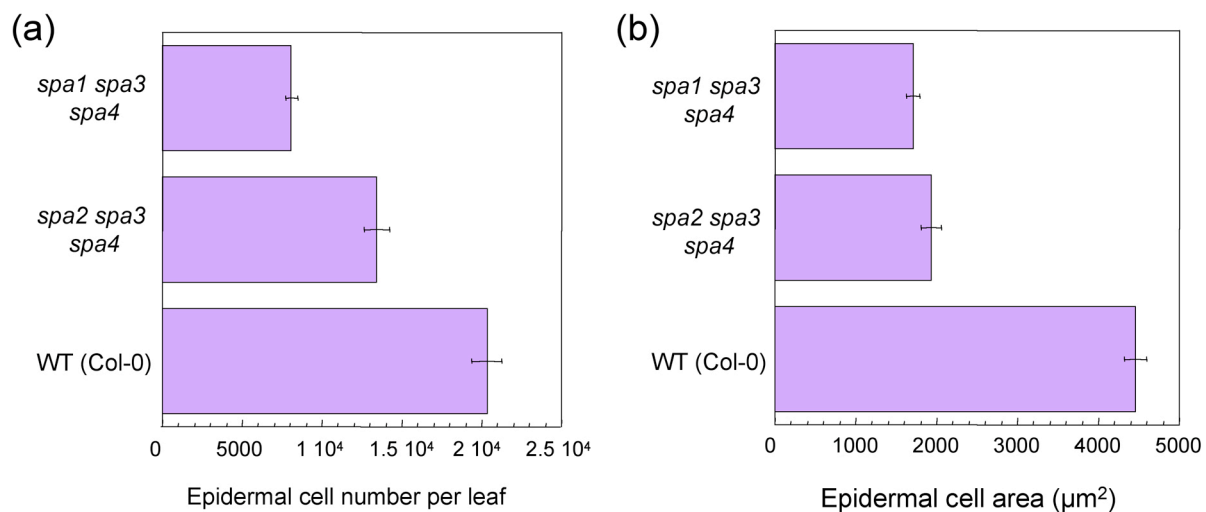


Figure 35. Schematic presentation of the *FL-SPA1-HA* construct.

5' and 3' regulatory sequences are highlighted in orange and *SPA1* coding sequence of *SPA1* is depicted in red. The C-terminal 3xHA sequence is shown in yellow. *SPA1* deletion constructs are not shown. Red arrows indicate XmaI (Cfr9I) restriction sites used for cloning. The pJHA vector carries a hygromycin resistance gene (*hpt*).

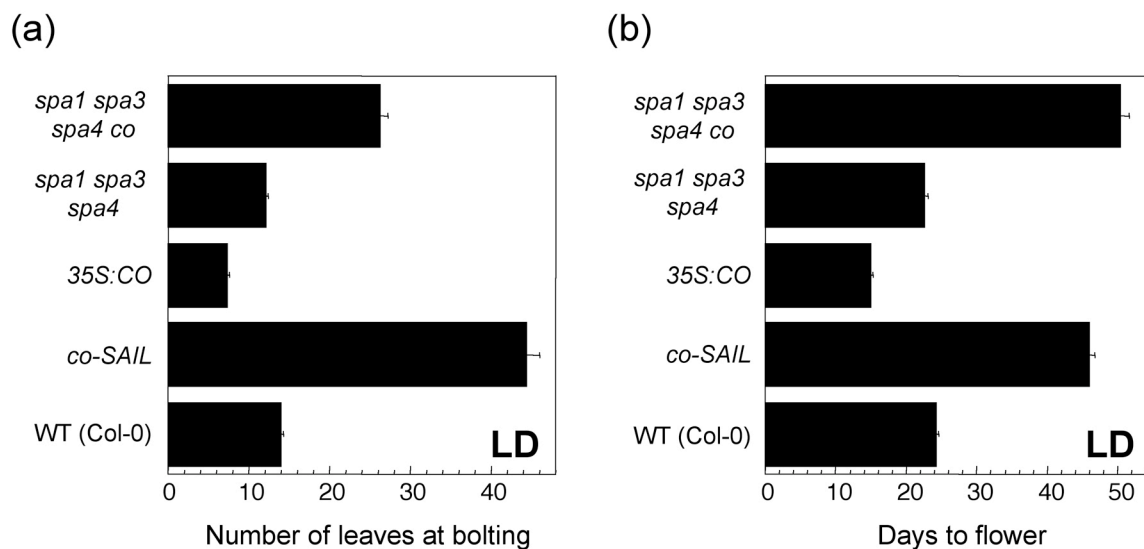
V. Supplement



Supplemental Figure 1. Decreased cell number and cell size in epidermal tissue of *spa* and *cop1* mutants.

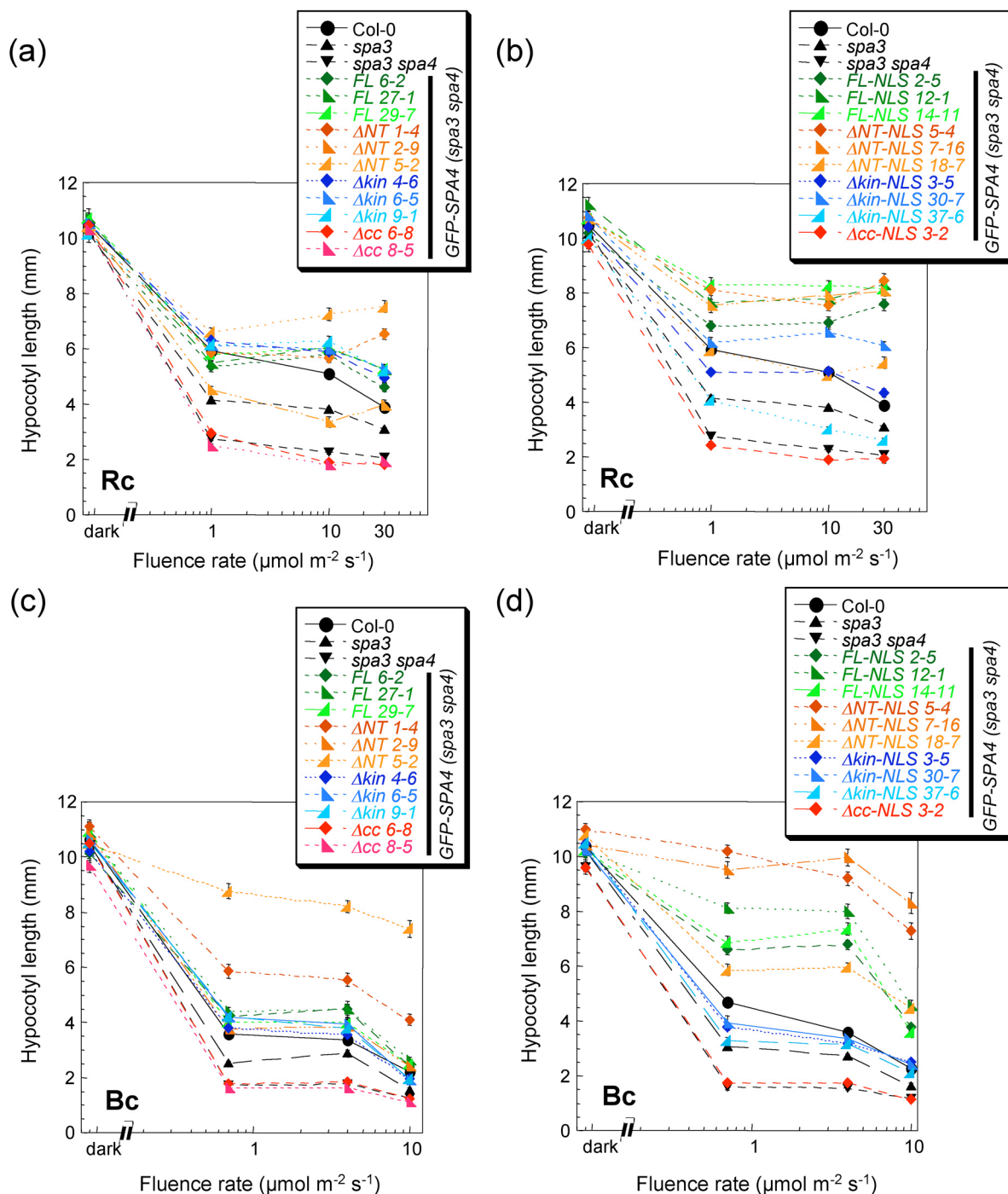
(a) Quantification of average epidermal cell number per leaf of 4-week old wild-type (Col-0), *cop1*, *spa2 spa3 spa4* and *spa1 spa3 spa4* mutants grown in LD. Error bars indicate the SEM.

(b) Quantification of average epidermal cell size of the genotypes listed in (a). Error bars indicate the SEM.



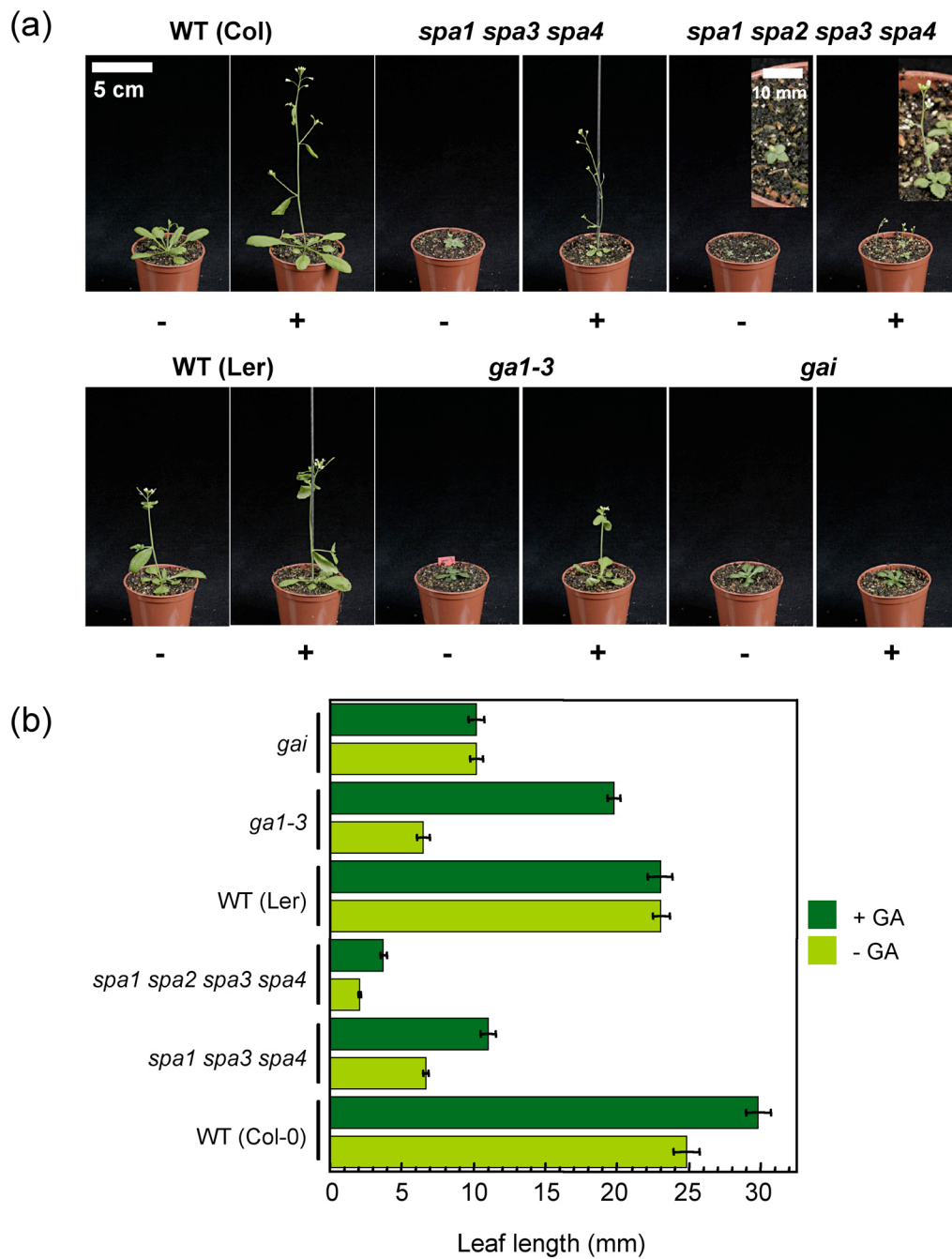
Supplemental Figure 2. Flowering time of *spa1 spa3 spa4 co* mutants.

Flowering time of wild type (Col-0), *35S:CO* lines, *co-SAIL*, *spa1 spa3 spa4* triple and *spa1 spa3 spa4 co* quadruple mutants, grown in LD. Flowering was determined by counting the number of rosette leaves at bolting (a) and the days to flower (b). Error bars indicate the SEM.



Supplemental Figure 3. SPA4 full-length (FL), ΔNT and Δkin deletion derivatives complement the *spa3 spa4* mutant phenotype in light-grown seedlings under various light conditions.

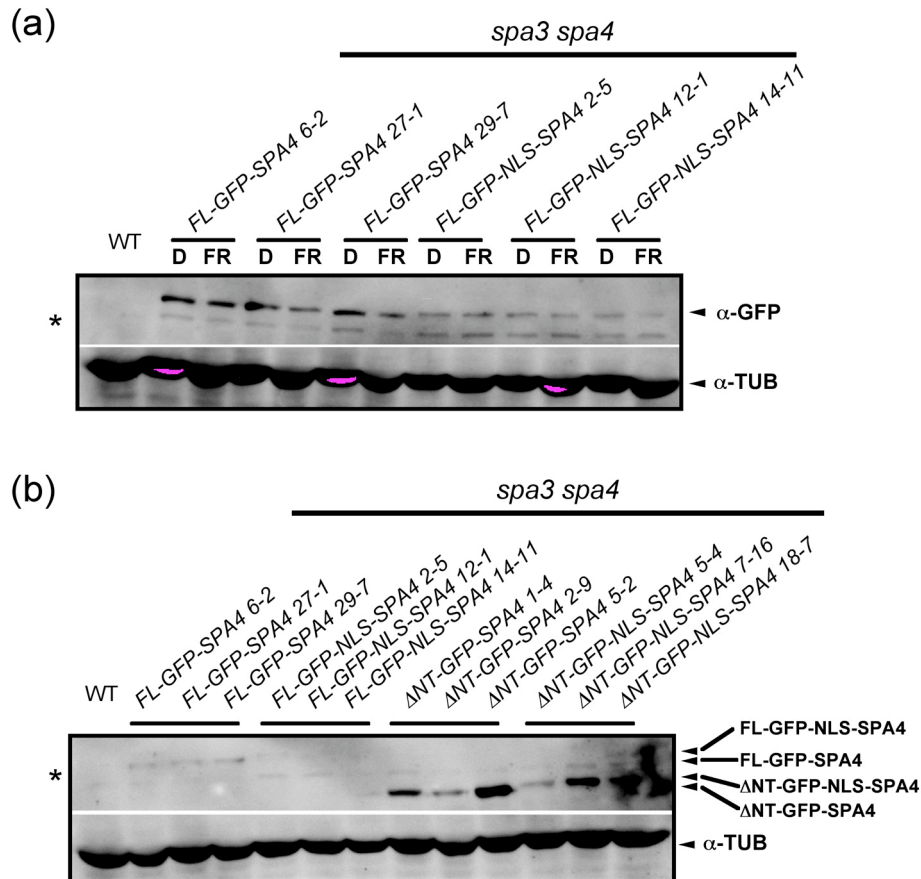
Hypocotyl length of seedlings grown under various fluence rates of Rc (a,b) or Bc (c,d). Transgenes were present in the *spa3 spa4* mutant background. Transgenic lines and colour code like in Figure 15 and 16. Wild-type (Col-0), *spa3* and *spa3 spa4* mutant seedlings are shown as controls. Transgenic lines without artificial NLS are shown in (a) and (c). Panel (c) and (d) show transgenic lines containing an additional N-terminal artificial nuclear localization sequence (NLS). For each complementing construct, three independent transgenic lines are shown. Error bars indicate the SEM ($n=30$).



Supplemental Figure 4. Effect of GA₃ on *spa* mutants.

(a) Visual phenotypes of 4-week old LD-grown *spa* triple, *spa* quadruple, GA-deficient (*gai1*) GA-insensitive (*gai*) mutants and the respective wild type (WT) controls. Plants were treated with water (-) or GA₃ (+)

(b) Quantification of the leaf length of genotypes shown in (a). Plants were 3 weeks old. Error bars indicate the SEM.

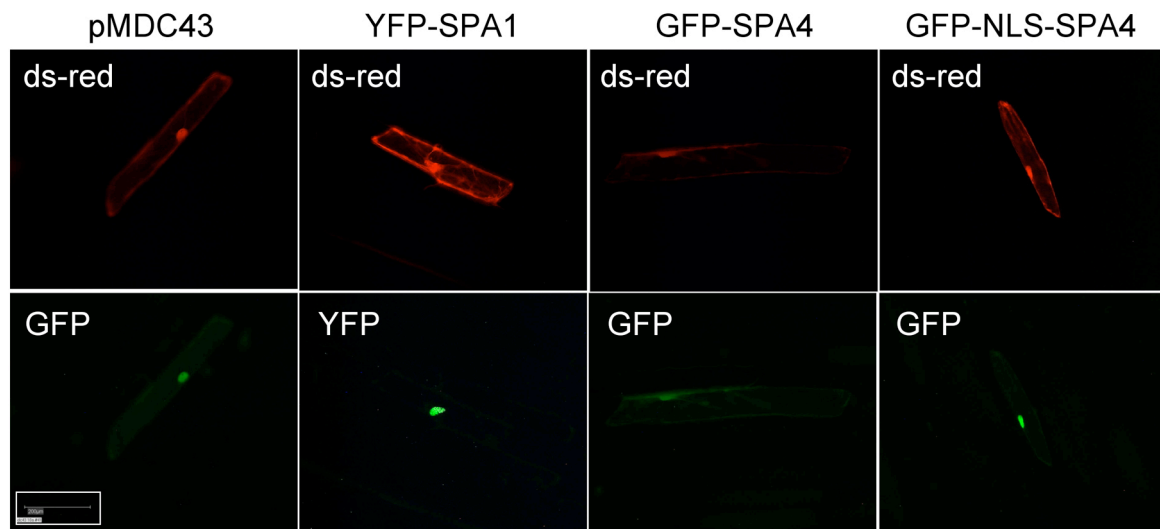


Supplemental Figure 5. GFP-NLS-SPA4 proteins do not accumulate to higher levels compared to GFP-SPA4.

(a) Immunoblot analysis of *FL-GFP-SPA4* and *FL-GFP-NLS-SPA4* expressing *spa3 spa4* mutant seedlings grown in darkness or FRc ($3 \mu\text{mol m}^{-2} \text{s}^{-1}$) for 4 days. For each constructs three independent transgenic lines were analyzed. GFP-SPA4 fusion proteins were detected using an α -GFP antibody. Tubulin levels were used as loading control.

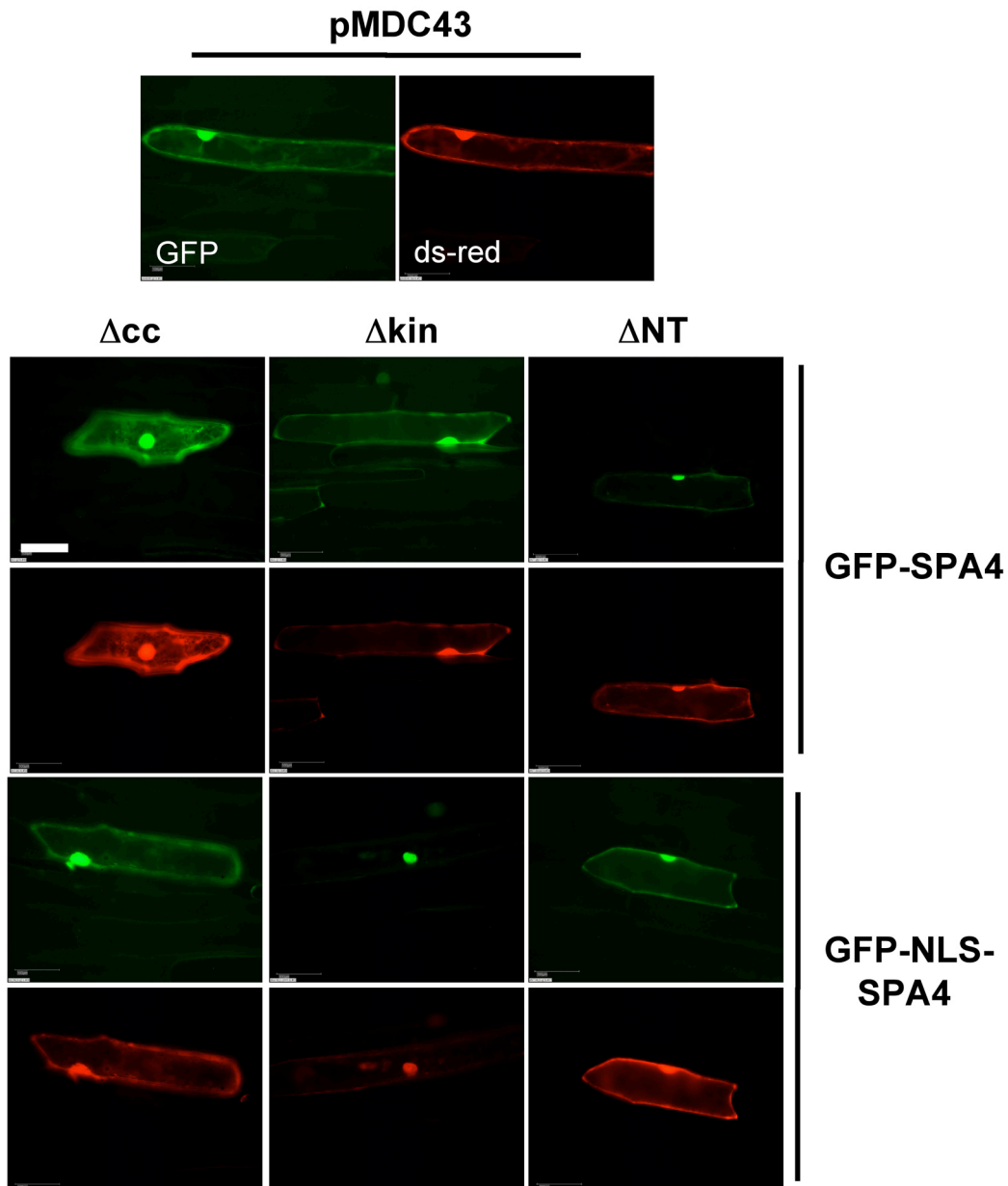
(b) Immunoblot analysis of GFP-SPA4 protein levels in 4-day-old *spa3 spa4* mutant seedlings grown in FRc ($3 \mu\text{mol m}^{-2} \text{s}^{-1}$). *FL-GFP-SPA4*, *FL-GFP-NLS-SPA4*, Δ NT-GFP-SPA4 and Δ NT-GFP-NLS-SPA4 deletion derivatives were expressed from a dual 35S promoter and detected using an α -GFP antibody. Tubulin levels were used as loading control. For each constructs three independent transgenic lines were analyzed.

Asterisks indicate an unspecific signal detected by the α -GFP antibody.



Supplemental Figure 6. Localization of FL-GFP-SPA4 and FL-GFP-NLS-SPA4 fusion proteins.

GFP-SPA4 and GFP-NLS-SPA4 fusion proteins were transiently expressed in onion epidermal cells. Ds-red was used as a marker for successfully transfected cells. YFP-SPA1 and pMDC43 were used as positive and negative controls, respectively. Magnification is the same in all images. Bar = 100 μ m



Supplemental Figure 7. Cellular localization of transiently expressed SPA4 deletion derivatives fused to GFP.

ΔNT -GFP-SPA4, Δkin -GFP-SPA4 and Δcc -GFP-SPA4 fusion proteins without or with artificial NLS were transiently expressed in onion epidermal cells. Ds-red was used as marker for successfully transfected cells. pMDC43 empty vector is shown as control. Magnification is the same in all images. Bar = 100 μm .

VI. References

- Abe, M., Kobayashi, Y., Yamamoto, S., Daimon, Y., Yamaguchi, A., Ikeda, Y., Ichinoki, H., Notaguchi, M., Goto, K., and Araki, T. (2005). FD, a bZIP protein mediating signals from the floral pathway integrator FT at the shoot apex. *Science* **309**, 1052-1056.
- Achard, P., Liao, L., Jiang, C., Desnos, T., Bartlett, J., Fu, X., and Harberd, N.P. (2007). DELLAs contribute to plant photomorphogenesis. *Plant Physiol* **143**, 1163-1172.
- Achard, P., Gusti, A., Cheminant, S., Alioua, M., Dhondt, S., Coppens, F., Beemster, G.T., and Genschik, P. (2009). Gibberellin signaling controls cell proliferation rate in Arabidopsis. *Curr Biol* **19**, 1188-1193.
- Achard, P., Cheng, H., De Grauwe, L., Decat, J., Schoutteten, H., Moritz, T., Van Der Straeten, D., Peng, J., and Harberd, N.P. (2006). Integration of plant responses to environmentally activated phytohormonal signals. *Science* **311**, 91-94.
- Aguilar-Martinez, J.A., Poza-Carrion, C., and Cubas, P. (2007). Arabidopsis BRANCHED1 acts as an integrator of branching signals within axillary buds. *Plant Cell* **19**, 458-472.
- Ahmad, M., and Cashmore, A.R. (1993). *HY4* gene of *A. thaliana* encodes a protein with characteristics of a blue-light photoreceptor. *Nature* **366**, 162-166.
- Ahmad, M., Lin, C., and Cashmore, A.R. (1995). Mutations throughout an Arabidopsis blue-light photoreceptor impair blue-light-responsive anthocyanin accumulation and inhibition of hypocotyl elongation. *Plant J* **8**, 653-658.
- Ahmad, M., Jarillo, J.A., and Cashmore, A.R. (1998). Chimeric proteins between cry1 and cry2 Arabidopsis blue light photoreceptors indicate overlapping functions and varying protein stability. *Plant Cell* **10**, 197-207.
- Al-Sady, B., Kikis, E.A., Monte, E., and Quail, P.H. (2008). Mechanistic duality of transcription factor function in phytochrome signaling. *Proc Natl Acad Sci U S A* **105**, 2232-2237.
- Al-Sady, B., Ni, W., Kircher, S., Schafer, E., and Quail, P.H. (2006). Photoactivated phytochrome induces rapid PIF3 phosphorylation prior to proteasome-mediated degradation. *Mol Cell* **23**, 439-446.
- Alabadi, D., and Blazquez, M.A. (2008). Integration of light and hormone signals. *Plant Signal Behav* **3**, 448-449.
- Alonso, J.M., Stepanova, A.N., Lisse, T.J., Kim, C.J., Chen, H., Shinn, P., Stevenson, D.K., Zimmerman, J., Barajas, P., Cheuk, R., Gadriab, C., Heller, C., Jeske, A., Koesema, E., Meyers, C.C., Parker, H., Prednis, L., Ansari, Y., Choy, N., Deen, H., Geralt, M., Hazari, N., Hom, E., Karnes, M., Mulholland, C., Ndubaku, R., Schmidt, I., Guzman, P., Aguilar-Henonin, L., Schmid, M., Weigel, D., Carter, D.E., Marchand, T., Risseuw, E., Brogden, D., Zeko, A., Crosby, W.L., Berry, C.C., and Ecker, J.R. (2003). Genome-wide insertional mutagenesis of Arabidopsis thaliana. *Science* **301**, 653-657.
- Amasino, R. (2010). Seasonal and developmental timing of flowering. *Plant J* **61**, 1001-1013.
- An, H., Roussot, C., Suarez-Lopez, P., Corbesier, L., Vincent, C., Pineiro, M., Hepworth, S., Mouradov, A., Justin, S., Turnbull, C., and Coupland, G. (2004). CONSTANS acts in the phloem to regulate a systemic signal that induces photoperiodic flowering of Arabidopsis. *Development* **131**, 3615-3626.
- Anastasiou, E., Kenz, S., Gerstung, M., MacLean, D., Timmer, J., Fleck, C., and Lenhard, M. (2007). Control of plant organ size by KLUH/CYP78A5-dependent intercellular signaling. *Dev Cell* **13**, 843-856.
- Bai, Y., Falk, S., Schnittger, A., Jakoby, M.J., and Hulskamp, M. (2010). Tissue layer specific regulation of leaf length and width in Arabidopsis as revealed by the cell autonomous action of ANGUSTIFOLIA. *Plant J* **61**, 191-199.
- Balcerowicz, M., Fittinghoff, K., Wirthmueller, L., Maier, A., Fackendahl, P., Fiene, G., Koncz, C., and Hoecker, U. (2010). Light-exposure of Arabidopsis seedlings causes

- rapid de-stabilization as well as selective post-translational inactivation of the repressor of photomorphogenesis SPA2. *Plant J.* **65**, 712-723
- Ballesteros, M.L., Bolle, C., Lois, L.M., Moore, J.M., Vielle-Calzada, J.P., Grossniklaus, U., and Chua, N.H.** (2001). LAF1, a MYB transcription activator for phytochrome A signaling. *Genes Dev* **15**, 2613-2625.
- Bauer, D., Viczian, A., Kircher, S., Nobis, T., Nitschke, R., Kunkel, T., Panigrahi, K.C., Adam, E., Fejes, E., Schafer, E., and Nagy, F.** (2004). Constitutive photomorphogenesis 1 and multiple photoreceptors control degradation of phytochrome interacting factor 3, a transcription factor required for light signaling in *Arabidopsis*. *Plant Cell* **16**, 1433-1445.
- Berna, G., Robles, P., and Micol, J.L.** (1999). A mutational analysis of leaf morphogenesis in *Arabidopsis thaliana*. *Genetics* **152**, 729-742.
- Bernhardt, A., Lechner, E., Hano, P., Schade, V., Dieterle, M., Anders, M., Dubin, M.J., Benvenuto, G., Bowler, C., Genschik, P., and Hellmann, H.** (2006). CUL4 associates with DDB1 and DET1 and its downregulation affects diverse aspects of development in *Arabidopsis thaliana*. *Plant J* **47**, 591-603.
- Biedermann, S., and Hellmann, H.** (2011). WD40 and CUL4-based E3 ligases: lubricating all aspects of life. *Trends Plant Sci* **16**, 38-46.
- Bishop, G.J., and Koncz, C.** (2002). Brassinosteroids and plant steroid hormone signaling. *Plant Cell* **14 Suppl**, S97-110.
- Boccalandro, H.E., Rossi, M.C., Saijo, Y., Deng, X.W., and Casal, J.J.** (2004). Promotion of photomorphogenesis by COP1. *Plant Mol Biol* **56**, 905-915.
- Bogre, L., Magyar, Z., and Lopez-Juez, E.** (2008). New clues to organ size control in plants. *Genome Biol* **9**, 226.
- Braun, N., Wyrzykowska, J., Muller, P., David, K., Couch, D., Perrot-Rechenmann, C., and Fleming, A.J.** (2008). Conditional repression of AUXIN BINDING PROTEIN1 reveals that it coordinates cell division and cell expansion during postembryonic shoot development in *Arabidopsis* and tobacco. *Plant Cell* **20**, 2746-2762.
- Briggs, W.R., and Christie, J.M.** (2002). Phototropins 1 and 2: versatile plant blue-light receptors. *Trends Plant Sci* **7**, 204-210.
- Busov, V.B., Brunner, A.M., and Strauss, S.H.** (2008). Genes for control of plant stature and form. *New Phytol* **177**, 589-607.
- Carabelli, M., Possenti, M., Sessa, G., Ciolfi, A., Sassi, M., Morelli, G., and Ruberti, I.** (2007). Canopy shade causes a rapid and transient arrest in leaf development through auxin-induced cytokinin oxidase activity. *Genes Dev* **21**, 1863-1868.
- Cashmore, A.R., Jarillo, J.A., Wu, Y.J., and Liu, D.M.** (1999). Cryptochromes: Blue light receptors for plants and animals. *Science* **284**, 760-765.
- Chattopadhyay, S., Ang, L.H., Puente, P., Deng, X.W., and Wei, N.** (1998). *Arabidopsis* bZIP protein HY5 directly interacts with light-responsive promoters in mediating light control of gene expression. *Plant Cell* **10**, 673-683.
- Chen, H., and Xiong, L.** (2008). Role of HY5 in abscisic acid response in seeds and seedlings. *Plant Signal Behav* **3**, 986-988.
- Chen, H., Huang, X., Gusmaroli, G., Terzaghi, W., Lau, O.S., Yanagawa, Y., Zhang, Y., Li, J., Lee, J.H., Zhu, D., and Deng, X.W.** (2010). *Arabidopsis* CULLIN4-damaged DNA binding protein 1 interacts with CONSTITUTIVELY PHOTOMORPHOGENIC1-SUPPRESSOR OF PHYA complexes to regulate photomorphogenesis and flowering time. *Plant Cell* **22**, 108-123.
- Chen, H., Shen, Y., Tang, X., Yu, L., Wang, J., Guo, L., Zhang, Y., Zhang, H., Feng, S., Strickland, E., Zheng, N., and Deng, X.W.** (2006). *Arabidopsis* CULLIN4 Forms an E3 Ubiquitin Ligase with RBX1 and the CDD Complex in Mediating Light Control of Development. *Plant Cell* **18**, 1991-2004.
- Chen, M., Chory, J., and Fankhauser, C.** (2004). Light signal transduction in higher plants. *Annu Rev Genet* **38**, 87-117.
- Choe, S., Dilkes, B.P., Fujioka, S., Takatsuto, S., Sakurai, A., and Feldmann, K.A.** (1998). The DWF4 gene of *Arabidopsis* encodes a cytochrome P450 that mediates

- multiple 22 α -hydroxylation steps in brassinosteroid biosynthesis. *Plant Cell* **10**, 231-243.
- Chory, J., Peto, C., Feinbaum, R., Pratt, L., and Ausubel, F.** (1989a). *Arabidopsis thaliana* mutant that develops as a light-grown plant in the absence of light. *Cell* **58**, 991-999.
- Chory, J., Peto, C.A., Ashbaugh, M., Saganich, R., Pratt, L., and Ausubel, F.** (1989b). Different Roles for Phytochrome in Etiolated and Green Plants Deduced from Characterization of *Arabidopsis thaliana* Mutants. *Plant Cell* **1**, 867-880.
- Clack, T., Mathews, S., and Sharrock, R.A.** (1994). The phytochrome apoprotein family in *Arabidopsis* is encoded by five genes: the sequences and expression of PHYD and PHYE. *Plant Mol Biol* **25**, 413-427.
- Clough, S.J., and Bent, A.F.** (1998). Floral dip: a simplified method for *Agrobacterium*-mediated transformation of *Arabidopsis thaliana*. *Plant J* **16**, 735-743.
- Clouse, S.D., and Sasse, J.M.** (1998). Brassinosteroids: Essential regulators of plant growth and development. *Annu Rev Plant Physiol Plant Mol Biol* **49**, 427-451.
- Cluis, C.P., Mouchel, C.F., and Hardtke, C.S.** (2004). The *Arabidopsis* transcription factor HY5 integrates light and hormone signaling pathways. *Plant J* **38**, 332-347.
- Conlon, I., and Raff, M.** (1999). Size control in animal development. *Cell* **96**, 235-244.
- Cookson, S.J., and Granier, C.** (2006). A dynamic analysis of the shade-induced plasticity in *Arabidopsis thaliana* rosette leaf development reveals new components of the shade-adaptative response. *Ann Bot* **97**, 443-452.
- Cookson, S.J., Van Lijsebettens, M., and Granier, C.** (2005). Correlation between leaf growth variables suggest intrinsic and early controls of leaf size in *Arabidopsis thaliana*. *Plant Cell and Environment* **28**, 1355-1366.
- Cookson, S.J., Chenu, K., and Granier, C.** (2007). Day length affects the dynamics of leaf expansion and cellular development in *Arabidopsis thaliana* partially through floral transition timing. *Ann Bot* **99**, 703-711.
- Corbesier, L., Vincent, C., Jang, S., Fornara, F., Fan, Q., Searle, I., Giakountis, A., Farrona, S., Gissot, L., Turnbull, C., and Coupland, G.** (2007). FT protein movement contributes to long-distance signaling in floral induction of *Arabidopsis*. *Science* **316**, 1030-1033.
- Costa, M.M., Fox, S., Hanna, A.I., Baxter, C., and Coen, E.** (2005). Evolution of regulatory interactions controlling floral asymmetry. *Development* **132**, 5093-5101.
- Coupland, G., Igeno, M.I., Simon, R., Schaffer, R., Murtas, G., Reeves, P., Robson, F., Pineiro, M., Costa, M., Lee, K., and Suarez-Lopez, P.** (1998). The regulation of flowering time by daylength in *Arabidopsis*. *Symp Soc Exp Biol* **51**, 105-110.
- Criqui, M.C., de Almeida Engler, J., Camasses, A., Capron, A., Parmentier, Y., Inze, D., and Genschik, P.** (2002). Molecular characterization of plant ubiquitin-conjugating enzymes belonging to the UbcP4/E2-C/UBCx/UbcH10 gene family. *Plant Physiol* **130**, 1230-1240.
- Crocco, C.D., Holm, M., Yanovsky, M.J., and Botto, J.F.** (2010). AtBBX21 and COP1 genetically interact in the regulation of shade avoidance. *Plant J* **64**, 551-562.
- Curtis, M.D., and Grossniklaus, U.** (2003). A gateway cloning vector set for high-throughput functional analysis of genes in planta. *Plant Physiol* **133**, 462-469.
- Datta, S., Hettiarachchi, G.H., Deng, X.W., and Holm, M.** (2006). *Arabidopsis* CONSTANS-LIKE3 is a positive regulator of red light signaling and root growth. *Plant Cell* **18**, 70-84.
- Datta, S., Hettiarachchi, C., Johansson, H., and Holm, M.** (2007). SALT TOLERANCE HOMOLOG2, a B-box protein in *Arabidopsis* that activates transcription and positively regulates light-mediated development. *Plant Cell* **19**, 3242-3255.
- Datta, S., Johansson, H., Hettiarachchi, C., and Holm, M.** (2008a). STH2 has 2 B there: An insight into the role of B-box containing proteins in *Arabidopsis*. *Plant Signal Behav* **3**, 547-548.
- Datta, S., Johansson, H., Hettiarachchi, C., Irigoyen, M.L., Desai, M., Rubio, V., and Holm, M.** (2008b). LZFI/SALT TOLERANCE HOMOLOG3, an *Arabidopsis* B-box

- protein involved in light-dependent development and gene expression, undergoes COP1-mediated ubiquitination. *Plant Cell* **20**, 2324-2338.
- Deng, X.-W., Caspar, T., and Quail, P.H.** (1991). *cop1*: A regulatory locus involved in light-controlled development and gene expression in *Arabidopsis*. *Genes Dev* **5**, 1172-1182.
- Deng, X.W., Matsui, M., Wei, N., Wagner, D., Chu, A.M., Feldmann, K.A., and Quail, P.H.** (1992). COP1, an *Arabidopsis* regulatory gene, encodes a protein with both a zinc-binding motif and a G beta homologous domain. *Cell* **71**, 791-801.
- Disch, S., Anastasiou, E., Sharma, V.K., Laux, T., Fletcher, J.C., and Lenhard, M.** (2006). The E3 ubiquitin ligase BIG BROTHER controls *Arabidopsis* organ size in a dosage-dependent manner. *Curr Biol* **16**, 272-279.
- Donnelly, P.M., Bonetta, D., Tsukaya, H., Dengler, R.E., and Dengler, N.G.** (1999). Cell cycling and cell enlargement in developing leaves of *Arabidopsis*. *Dev Biol* **215**, 407-419.
- Duek, P.D., and Fankhauser, C.** (2003). HFR1, a putative bHLH transcription factor, mediates both phytochrome A and cryptochrome signalling. *Plant J* **34**, 827-836.
- Duek, P.D., and Fankhauser, C.** (2005). bHLH class transcription factors take centre stage in phytochrome signalling. *Trends Plant Sci* **10**, 51-54.
- Duek, P.D., Elmer, M.V., van Oosten, V.R., and Fankhauser, C.** (2004). The degradation of HFR1, a putative bHLH class transcription factor involved in light signaling, is regulated by phosphorylation and requires COP1. *Curr Biol* **14**, 2296-2301.
- Edwards, K., Johnstone, C., and Thompson, C.** (1991). A simple and rapid method for the preparation of plant genomic DNA for PCR analysis. *Nucleic Acids Res* **19**, 1349.
- Efroni, I., Blum, E., Goldshmidt, A., and Eshed, Y.** (2008). A protracted and dynamic maturation schedule underlies *Arabidopsis* leaf development. *Plant Cell* **20**, 2293-2306.
- Endo, M., Nakamura, S., Araki, T., Mochizuki, N., and Nagatani, A.** (2005). Phytochrome B in the mesophyll delays flowering by suppressing FLOWERING LOCUS T expression in *Arabidopsis* vascular bundles. *Plant Cell* **17**, 1941-1952.
- Fackendahl, P.** (2005). Funktionelle Charakterisierung der Lichtsignaltransduktion bei *Arabidopsis thaliana*. In Institut für Entwicklungs- und Molekularbiologie der Pflanzen (Düsseldorf: Heinrich-Heine Universität).
- Fairchild, C.D., Schumaker, M.A., and Quail, P.H.** (2000). HFR1 encodes an atypical bHLH protein that acts in phytochrome A signal transduction. *Genes Dev* **14**, 2377-2391.
- Falke, C.** (2009). Biochemical and molecular analysis of light signal transduction in *Arabidopsis thaliana*. In Botanical Institute (Cologne: University of Cologne).
- Fankhauser, C., and Chory, J.** (2000). RSF1, an *Arabidopsis* locus implicated in phytochrome A signaling. *Plant Physiol* **124**, 39-45.
- Favory, J.J., Stec, A., Gruber, H., Rizzini, L., Oravecz, A., Funk, M., Albert, A., Cloix, C., Jenkins, G.I., Oakeley, E.J., Seidlitz, H.K., Nagy, F., and Ulm, R.** (2009). Interaction of COP1 and UVR8 regulates UV-B-induced photomorphogenesis and stress acclimation in *Arabidopsis*. *EMBO J* **28**, 591-601.
- Fittinghoff, K.** (2008). Functional Analysis of the SPA Gene Family in *Arabidopsis thaliana*. In Botanical Institute (Cologne: University of Cologne).
- Fittinghoff, K., Laubinger, S., Nixdorf, M., Fackendahl, P., Baumgardt, R.L., Batschauer, A., and Hoecker, U.** (2006). Functional and expression analysis of *Arabidopsis* SPA genes during seedling photomorphogenesis and adult growth. *Plant J* **47**, 577-590
- Fleet, C.M., and Sun, T.P.** (2005). A DELLAcate balance: the role of gibberellin in plant morphogenesis. *Curr Opin Plant Biol* **8**, 77-85.
- Fleming, A.J.** (2006). The integration of cell proliferation and growth in leaf morphogenesis. *J Plant Res* **119**, 31-36.
- Franklin, K.A., and Quail, P.H.** (2010). Phytochrome functions in *Arabidopsis* development. *J Exp Bot* **61**, 11-24.

- Franklin, K.A., Lerner, V.S., and Whitelam, G.C.** (2005). The signal transducing photoreceptors of plants. *Int J Dev Biol* **49**, 653-664.
- Fujii, H., and Zhu, J.K.** (2009). Arabidopsis mutant deficient in 3 abscisic acid-activated protein kinases reveals critical roles in growth, reproduction, and stress. *Proc Natl Acad Sci U S A* **106**, 8380-8385.
- Gonzalez, N., De Bodt, S., Sulpice, R., Jikumaru, Y., Chae, E., Dhondt, S., Van Daele, T., De Milde, L., Weigel, D., Kamiya, Y., Stitt, M., Beemster, G.T., and Inze, D.** (2010). Increased leaf size: different means to an end. *Plant Physiol* **153**, 1261-1279.
- Gou, M., Su, N., Zheng, J., Huai, J., Wu, G., Zhao, J., He, J., Tang, D., Yang, S., and Wang, G.** (2009). An F-box gene, CPR30, functions as a negative regulator of the defense response in Arabidopsis. *Plant J* **60**, 757-770.
- Guo, H., Yang, H., Mockler, T.C., and Lin, C.** (1998). Regulation of flowering time by Arabidopsis photoreceptors. *Science* **279**, 1360-1363.
- Guo, H., Duong, H., Ma, N., and Lin, C.** (1999). The Arabidopsis blue light receptor cryptochrome 2 is a nuclear protein regulated by a blue light-dependent post-transcriptional mechanism. *Plant J* **19**, 279-287.
- Hajdukiewicz, P., Svab, Z., and Maliga, P.** (1994). The small, versatile pPZP family of Agrobacterium binary vectors for plant transformation. *Plant Mol Biol* **25**, 989-994.
- Hay, A., Barkoulas, M., and Tsiantis, M.** (2004). PINning down the connections: transcription factors and hormones in leaf morphogenesis. *Curr Opin Plant Biol* **7**, 575-581.
- Hoecker, U.** (2005). Regulated proteolysis in light signaling. *Curr Opin Plant Biol* **8**, 469-476.
- Hoecker, U., and Quail, P.H.** (2001). The phytochrome A-specific signaling intermediate SPA1 interacts directly with COP1, a constitutive repressor of light signaling in Arabidopsis. *J Biol Chem* **276**, 38173-38178.
- Hoecker, U., Xu, Y., and Quail, P.H.** (1998). SPA1: A new genetic locus involved in phytochrome A - Specific signal transduction. *Plant Cell* **10**, 19-33.
- Hoecker, U., Tepperman, J.M., and Quail, P.H.** (1999). SPA1, a WD-repeat protein specific to phytochrome A signal transduction. *Science* **284**, 496-499.
- Holm, M., Ma, L.G., Qu, L.J., and Deng, X.W.** (2002). Two interacting bZIP proteins are direct targets of COP1-mediated control of light-dependent gene expression in Arabidopsis. *Genes Dev* **16**, 1247-1259.
- Horiguchi, G., Kim, G.T., and Tsukaya, H.** (2005). The transcription factor AtGRF5 and the transcription coactivator AN3 regulate cell proliferation in leaf primordia of Arabidopsis thaliana. *Plant J* **43**, 68-78.
- Horiguchi, G., Ferjani, A., Fujikura, U., and Tsukaya, H.** (2006a). Coordination of cell proliferation and cell expansion in the control of leaf size in Arabidopsis thaliana. *J Plant Res* **119**, 37-42.
- Horiguchi, G., Fujikura, U., Ferjani, A., Ishikawa, N., and Tsukaya, H.** (2006b). Large-scale histological analysis of leaf mutants using two simple leaf observation methods: identification of novel genetic pathways governing the size and shape of leaves. *Plant J* **48**, 638-644.
- Horton, R.M., Hunt, H.D., Ho, S.N., Pullen, J.K., and Pease, L.R.** (1989). Engineering hybrid genes without the use of restriction enzymes: gene splicing by overlap extension. *Gene* **77**, 61-68.
- Hu, Y., Xie, Q., and Chua, N.H.** (2003). The Arabidopsis auxin-inducible gene ARGOS controls lateral organ size. *Plant Cell* **15**, 1951-1961.
- Imaizumi, T., Tran, H.G., Swartz, T.E., Briggs, W.R., and Kay, S.A.** (2003). FKF1 is essential for photoperiodic-specific light signalling in Arabidopsis. *Nature* **426**, 302-306.
- Jackson, S., and Xiong, Y.** (2009). CRL4s: the CUL4-RING E3 ubiquitin ligases. *Trends Biochem Sci* **34**, 562-570.
- Jander, G., Norris, S.R., Rounsley, S.D., Bush, D.F., Levin, I.M., and Last, R.L.** (2002). Arabidopsis map-based cloning in the post-genome era. *Plant Physiol* **129**, 440-450.

- Jang, I.C., Yang, J.Y., Seo, H.S., and Chua, N.H.** (2005). HFR1 is targeted by COP1 E3 ligase for post-translational proteolysis during phytochrome A signaling. *Genes Dev* **19**, 593-602.
- Jang, I.C., Yang, S.W., Yang, J.Y., and Chua, N.H.** (2007). Independent and interdependent functions of LAF1 and HFR1 in phytochrome A signaling. *Genes Dev* **21**, 2100-2111.
- Jang, I.C., Henriques, R., Seo, H.S., Nagatani, A., and Chua, N.H.** (2010). Arabidopsis PHYTOCHROME INTERACTING FACTOR proteins promote phytochrome B polyubiquitination by COP1 E3 ligase in the nucleus. *Plant Cell* **22**, 2370-2383.
- Jang, S., Marchal, V., Panigrahi, K.C., Wenkel, S., Soppe, W., Deng, X.W., Valverde, F., and Coupland, G.** (2008). Arabidopsis COP1 shapes the temporal pattern of CO accumulation conferring a photoperiodic flowering response. *EMBO J* **27**, 1277-1288.
- Jiao, Y., Lau, O.S., and Deng, X.W.** (2007). Light-regulated transcriptional networks in higher plants. *Nat Rev Genet* **8**, 217-230.
- Jones, A.M., Im, K.H., Savka, M.A., Wu, M.J., DeWitt, N.G., Shillito, R., and Binns, A.N.** (1998). Auxin-dependent cell expansion mediated by overexpressed auxin-binding protein 1. *Science* **282**, 1114-1117.
- Kang, C.Y., Lian, H.L., Wang, F.F., Huang, J.R., and Yang, H.Q.** (2009). Cryptochromes, phytochromes, and COP1 regulate light-controlled stomatal development in Arabidopsis. *Plant Cell* **21**, 2624-2641.
- Karve, A., and Moore, B.D.** (2009). Function of Arabidopsis hexokinase-like1 as a negative regulator of plant growth. *J Exp Bot* **60**, 4137-4149.
- Kevei, E., Schafer, E., and Nagy, F.** (2007). Light-regulated nucleo-cytoplasmic partitioning of phytochromes. *J Exp Bot* **58**, 3113-3124.
- Kim, G.T., Tsukaya, H., and Uchimiya, H.** (1998). The ROTUNDIFOLIA3 gene of Arabidopsis thaliana encodes a new member of the cytochrome P-450 family that is required for the regulated polar elongation of leaf cells. *Genes Dev* **12**, 2381-2391.
- Kim, J.H., and Kende, H.** (2004). A transcriptional coactivator, AtGIF1, is involved in regulating leaf growth and morphology in Arabidopsis. *Proc Natl Acad Sci U S A* **101**, 13374-13379.
- Kim, J.H., Choi, D., and Kende, H.** (2003). The AtGRF family of putative transcription factors is involved in leaf and cotyledon growth in Arabidopsis. *Plant J* **36**, 94-104.
- Kircher, S., Kozma-Bognar, L., Kim, L., Adam, E., Harter, K., Schafer, E., and Nagy, F.** (1999). Light quality-dependent nuclear import of the plant photoreceptors phytochrome A and B. *Plant Cell* **11**, 1445-1456.
- Kircher, S., Gil, P., Kozma-Bognar, L., Fejes, E., Speth, V., Husselstein-Muller, T., Bauer, D., Adam, E., Schafer, E., and Nagy, F.** (2002). Nucleocytoplasmic partitioning of the plant photoreceptors phytochrome A, B, C, D, and E is regulated differentially by light and exhibits a diurnal rhythm. *Plant Cell* **14**, 1541-1555.
- Koornneef, M., Elgersma, A., Hanhart, C., Loenen, E., Rijn, L., and Zeevaart, J.** (1985). A gibberellin insensitive mutant of Arabidopsis thaliana. *Physiol Plant* **65**, 33-39.
- Koyama, T., Furutani, M., Tasaka, M., and Ohme-Takagi, M.** (2007). TCP transcription factors control the morphology of shoot lateral organs via negative regulation of the expression of boundary-specific genes in Arabidopsis. *Plant Cell* **19**, 473-484.
- Kozuka, T., Horiguchi, G., Kim, G.T., Ohgishi, M., Sakai, T., and Tsukaya, H.** (2005). The different growth responses of the Arabidopsis thaliana leaf blade and the petiole during shade avoidance are regulated by photoreceptors and sugar. *Plant Cell Physiol* **46**, 213-223.
- Krizek, B.A.** (2009). Making bigger plants: key regulators of final organ size. *Curr Opin Plant Biol* **12**, 17-22.
- Kwok, S.F., Piekos, B., Misera, S., and Deng, X.W.** (1996). A complement of ten essential and pleiotropic arabidopsis COP/DET/FUS genes is necessary for repression of photomorphogenesis in darkness. *Plant Physiol* **110**, 731-742.
- Laemmli, U.K.** (1970). Cleavage of structural proteins during the assembly of the head of bacteriophage T4. *Nature* **227**, 680-684.

- Lau, O.S., and Deng, X.W. (2010). Plant hormone signaling lightens up: integrators of light and hormones. *Curr Opin Plant Biol.*
- Laubinger, S., and Hoecker, U. (2003). The SPA1-like proteins SPA3 and SPA4 repress photomorphogenesis in the light. *Plant J* **35**, 373-385.
- Laubinger, S., Fittinghoff, K., and Hoecker, U. (2004). The SPA quartet: a family of WD-repeat proteins with a central role in suppression of photomorphogenesis in arabidopsis. *Plant Cell* **16**, 2293-2306.
- Laubinger, S., Marchal, V., Le Gourrierec, J., Wenkel, S., Adrian, J., Jang, S., Kulajta, C., Braun, H., Coupland, G., and Hoecker, U. (2006). Arabidopsis SPA proteins regulate photoperiodic flowering and interact with the floral inducer CONSTANS to regulate its stability. *Development* **133**, 3213-3222.
- Lee, B.H., Ko, J.H., Lee, S., Lee, Y., Pak, J.H., and Kim, J.H. (2009). The Arabidopsis GRF-INTERACTING FACTOR gene family performs an overlapping function in determining organ size as well as multiple developmental properties. *Plant Physiol* **151**, 655-668.
- Lee, J., and Zhou, P. (2007). DCAFs, the missing link of the CUL4-DDB1 ubiquitin ligase. *Mol Cell* **26**, 775-780.
- Lee, J., He, K., Stolc, V., Lee, H., Figueroa, P., Gao, Y., Tongprasit, W., Zhao, H., Lee, I., and Deng, X.W. (2007). Analysis of transcription factor HY5 genomic binding sites revealed its hierarchical role in light regulation of development. *Plant Cell* **19**, 731-749.
- Leivar, P., and Quail, P.H. (2011). PIFs: pivotal components in a cellular signaling hub. *Trends Plant Sci* **16**, 19-28.
- Leyser, H.M., Lincoln, C.A., Timpte, C., Lammer, D., Turner, J., and Estelle, M. (1993). Arabidopsis auxin-resistance gene AXR1 encodes a protein related to ubiquitin-activating enzyme E1. *Nature* **364**, 161-164.
- Li, C., Potuschak, T., Colon-Carmona, A., Gutierrez, R.A., and Doerner, P. (2005). Arabidopsis TCP20 links regulation of growth and cell division control pathways. *Proc Natl Acad Sci U S A* **102**, 12978-12983.
- Li, Y., Zheng, L., Corke, F., Smith, C., and Bevan, M.W. (2008). Control of final seed and organ size by the DA1 gene family in Arabidopsis thaliana. *Genes Dev* **22**, 1331-1336.
- Lin, C.T. (2002). Blue light receptors and signal transduction. *Plant Cell* **14**, S207-S225.
- Lin, C.T., Yang, H.Y., Guo, H.W., Mockler, T., Chen, J., and Cashmore, A.R. (1998). Enhancement of blue-light sensitivity of Arabidopsis seedlings by a blue light receptor cryptochrome 2. *Proc Natl Acad Sci USA* **95**, 2686-2690.
- Lin, M.K., Belanger, H., Lee, Y.J., Varkonyi-Gasic, E., Taoka, K., Miura, E., Xoconostle-Cazares, B., Gendler, K., Jorgensen, R.A., Phinney, B., Lough, T.J., and Lucas, W.J. (2007). FLOWERING LOCUS T protein may act as the long-distance florigenic signal in the cucurbits. *Plant Cell* **19**, 1488-1506.
- Liscum, E., and Briggs, W.R. (1995). Mutations in the NPH1 locus of Arabidopsis disrupt the perception of phototropic stimuli. *Plant Cell* **7**, 473-485.
- Liu, H., Yu, X., Li, K., Klejnot, J., Yang, H., Lisiero, D., and Lin, C. (2008a). Photoexcited CRY2 interacts with CIB1 to regulate transcription and floral initiation in Arabidopsis. *Science* **322**, 1535-1539.
- Liu, L.J., Zhang, Y.C., Li, Q.H., Sang, Y., Mao, J., Lian, H.L., Wang, L., and Yang, H.Q. (2008b). COP1-mediated ubiquitination of CONSTANS is implicated in cryptochrome regulation of flowering in Arabidopsis. *Plant Cell* **20**, 292-306.
- Lopez-Juez, E., Dillon, E., Magyar, Z., Khan, S., Hazeldine, S., de Jager, S.M., Murray, J.A., Beemster, G.T., Bogre, L., and Shanahan, H. (2008). Distinct light-initiated gene expression and cell cycle programs in the shoot apex and cotyledons of Arabidopsis. *Plant Cell* **20**, 947-968.
- Lyapina, S., Cope, G., Shevchenko, A., Serino, G., Tsuge, T., Zhou, C., Wolf, D.A., Wei, N., and Deshaies, R.J. (2001). Promotion of NEDD-CUL1 conjugate cleavage by COP9 signalosome. *Science* **292**, 1382-1385.

- Ma, L., Li, J., Qu, L., Hager, J., Chen, Z., Zhao, H., and Deng, X.W.** (2001). Light control of Arabidopsis development entails coordinated regulation of genome expression and cellular pathways. *Plant Cell* **13**, 2589-2607.
- Ma, L., Gao, Y., Qu, L., Chen, Z., Li, J., Zhao, H., and Deng, X.W.** (2002). Genomic evidence for COP1 as a repressor of light-regulated gene expression and development in Arabidopsis. *Plant Cell* **14**, 2383-2398.
- Mao, J., Zhang, Y.C., Sang, Y., Li, Q.H., and Yang, H.Q.** (2005). From The Cover: A role for Arabidopsis cryptochromes and COP1 in the regulation of stomatal opening. *Proc Natl Acad Sci U S A* **102**, 12270-12275.
- Mathieu, J., Warthmann, N., Kuttner, F., and Schmid, M.** (2007). Export of FT protein from phloem companion cells is sufficient for floral induction in Arabidopsis. *Curr Biol* **17**, 1055-1060.
- Matsushita, T., Mochizuki, N., and Nagatani, A.** (2003). Dimers of the N-terminal domain of phytochrome B are functional in the nucleus. *Nature* **424**, 571-574.
- McNellis, T.W., von Arnim, A.G., Araki, T., Komeda, Y., Misera, S., and Deng, X.W.** (1994). Genetic and molecular analysis of an allelic series of cop1 mutants suggests functional roles for the multiple protein domains. *Plant Cell* **6**, 487-500.
- Mizukami, Y., and Fischer, R.L.** (2000). Plant organ size control: AINTEGUMENTA regulates growth and cell numbers during organogenesis. *Proc Natl Acad Sci U S A* **97**, 942-947.
- Mizutani, M., and Ohta, D.** (2010). Diversification of P450 genes during land plant evolution. *Annu Rev Plant Biol* **61**, 291-315.
- Mockler, T., Yang, H., Yu, X., Parikh, D., Cheng, Y.C., Dolan, S., and Lin, C.** (2003). Regulation of photoperiodic flowering by Arabidopsis photoreceptors. *Proc Natl Acad Sci U S A* **100**, 2140-2145.
- Mockler, T.C., Guo, H., Yang, H., Duong, H., and Lin, C.** (1999). Antagonistic actions of Arabidopsis cryptochromes and phytochrome B in the regulation of floral induction. *Development* **126**, 2073-2082.
- Monte, E., Al-Sady, B., Leivar, P., and Quail, P.H.** (2007). Out of the dark: how the PIFs are unmasking a dual temporal mechanism of phytochrome signalling. *J Exp Bot* **58**, 3125-3133.
- Moore, B., Zhou, L., Rolland, F., Hall, Q., Cheng, W.H., Liu, Y.X., Hwang, I., Jones, T., and Sheen, J.** (2003). Role of the Arabidopsis glucose sensor HXK1 in nutrient, light, and hormonal signaling. *Science* **300**, 332-336.
- Nagatani, A.** (2004). Light-regulated nuclear localization of phytochromes. *Curr Opin Plant Biol* **7**, 708-711.
- Nakaya, M., Tsukaya, H., Murakami, N., and Kato, M.** (2002). Brassinosteroids control the proliferation of leaf cells of Arabidopsis thaliana. *Plant Cell Physiol* **43**, 239-244.
- Narita, N.N., Moore, S., Horiguchi, G., Kubo, M., Demura, T., Fukuda, H., Goodrich, J., and Tsukaya, H.** (2004). Overexpression of a novel small peptide ROTUNDIFOLIA4 decreases cell proliferation and alters leaf shape in Arabidopsis thaliana. *Plant J* **38**, 699-713.
- Nath, U., Crawford, B.C., Carpenter, R., and Coen, E.** (2003). Genetic control of surface curvature. *Science* **299**, 1404-1407.
- Neff, M.M., Fankhauser, C., and Chory, J.** (2000). Light: an indicator of time and place. *Genes Dev* **14**, 257-271.
- Nixdorf, M., and Hoecker, U.** (2010). SPA1 and DET1 act together to control photomorphogenesis throughout plant development. *Planta* **231**, 825-833.
- Onouchi, H., Igeno, M.I., Perilleux, C., Graves, K., and Coupland, G.** (2000). Mutagenesis of plants overexpressing CONSTANS demonstrates novel interactions among Arabidopsis flowering-time genes. *Plant Cell* **12**, 885-900.
- Oravec, A., Baumann, A., Mate, Z., Brzezinska, A., Molinier, J., Oakeley, E.J., Adam, E., Schafer, E., Nagy, F., and Ulm, R.** (2006). CONSTITUTIVELY PHOTOMORPHOGENIC1 is required for the UV-B response in Arabidopsis. *Plant Cell* **18**, 1975-1990.

- Osterlund, M.T., Ang, L.H., and Deng, X.W. (1999). The role of COP1 in repression of Arabidopsis photomorphogenic development. *Trends Cell Biol* **9**, 113-118.
- Osterlund, M.T., Wei, N., and Deng, X.W. (2000a). The roles of photoreceptor systems and the COP1-targeted destabilization of HY5 in light control of Arabidopsis seedling development. *Plant Physiol* **124**, 1520-1524.
- Osterlund, M.T., Hardtke, C.S., Wei, N., and Deng, X.W. (2000b). Targeted destabilization of HY5 during light-regulated development of *Arabidopsis*. *Nature* **405**, 462-466.
- Oyama, T., Shimura, Y., and Okada, K. (1997). The *Arabidopsis* HY5 gene encodes a bZIP protein that regulates stimulus-induced development of root and hypocotyl. *Genes Dev* **11**, 2983-2995.
- Palatnik, J.F., Allen, E., Wu, X., Schommer, C., Schwab, R., Carrington, J.C., and Weigel, D. (2003). Control of leaf morphogenesis by microRNAs. *Nature* **425**, 257-263.
- Perez-Perez, J.M., Serrano-Cartagena, J., and Micol, J.L. (2002). Genetic analysis of natural variations in the architecture of *Arabidopsis thaliana* vegetative leaves. *Genetics* **162**, 893-915.
- Potter, C.J., and Xu, T. (2001). Mechanisms of size control. *Curr Opin Genet Dev* **11**, 279-286.
- Putterill, J., Robson, F., Lee, K., Simon, R., and Coupland, G. (1995). The CONSTANS gene of *Arabidopsis* promotes flowering and encodes a protein showing similarities to zinc finger transcription factors. *Cell* **80**, 847-857.
- Quail, P.H. (2002). Phytochrome photosensory signalling networks. *Nat Rev Mol Cell Biol* **3**, 85-93.
- Ranjan, A., Fiene, G., Fackendahl, P., and Hoecker, U. (2011). The *Arabidopsis* repressor of light signaling SPA1 acts in the phloem to regulate seedling de-etiolation, leaf expansion and flowering time. *Development* **138**, 1851-1862.
- Rios, G., Lossow, A., Hertel, B., Breuer, F., Schaefer, S., Broich, M., Kleinow, T., Jasik, J., Winter, J., Ferrando, A., Farras, R., Panicot, M., Henriques, R., Mariaux, J.B., Oberschall, A., Molnar, G., Berendzen, K., Shukla, V., Lafos, M., Koncz, Z., Redei, G.P., Schell, J., and Koncz, C. (2002). Rapid identification of *Arabidopsis* insertion mutants by non-radioactive detection of T-DNA tagged genes. *Plant J* **32**, 243-253.
- Rockwell, N.C., Su, Y.S., and Lagarias, J.C. (2006). Phytochrome Structure and Signaling Mechanisms. *Annu Rev Plant Biol*.
- Rosler, J., Klein, I., and Zeidler, M. (2007). *Arabidopsis* fhl/fhy1 double mutant reveals a distinct cytoplasmic action of phytochrome A. *Proc Natl Acad Sci U S A* **104**, 10737-10742.
- Ruckle, M.E., DeMarco, S.M., and Larkin, R.M. (2007). Plastid signals remodel light signaling networks and are essential for efficient chloroplast biogenesis in *Arabidopsis*. *Plant Cell* **19**, 3944-3960.
- Saijo, Y., Sullivan, J.A., Wang, H., Yang, J., Shen, Y., Rubio, V., Ma, L., Hoecker, U., and Deng, X.W. (2003a). The COP1-SPA1 interaction defines a critical step in phytochrome A-mediated regulation of HY5 activity. *Genes Dev* **17**, 2642-2647.
- Saijo, Y., Sullivan, J.A., Wang, H.Y., Yang, J.P., Shen, Y.P., Rubio, V., Ma, L.G., Hoecker, U., and Deng, X.W. (2003b). The COP1-SPA1 interaction defines a critical step in phytochrome A-mediated regulation of HY5 activity. *Gene Develop* **17**, 2642-2647.
- Sakai, T., Wada, T., Ishiguro, S., and Okada, K. (2000). RPT2. A signal transducer of the phototropic response in *Arabidopsis*. *Plant Cell* **12**, 225-236.
- Sakai, T., Kagawa, T., Kasahara, M., Swartz, T.E., Christie, J.M., Briggs, W.R., Wada, M., and Okada, K. (2001). *Arabidopsis* nph1 and npl1: blue light receptors that mediate both phototropism and chloroplast relocation. *Proc Natl Acad Sci U S A* **98**, 6969-6974.
- Sakamoto, K., and Nagatani, A. (1996). Nuclear localization activity of phytochrome B. *Plant J* **10**, 859-868.

- Sambrook, J., Russell, D.** (2001). *Molecular Cloning: A Laboratory Manual*.
- Savaldi-Goldstein, S., Peto, C., and Chory, J.** (2007). The epidermis both drives and restricts plant shoot growth. *Nature* **446**, 199-202.
- Schommer, C., Palatnik, J.F., Aggarwal, P., Chetelat, A., Cubas, P., Farmer, E.E., Nath, U., and Weigel, D.** (2008). Control of jasmonate biosynthesis and senescence by miR319 targets. *PLoS Biol* **6**, e230.
- Schroeder, D.F., Gahrtz, M., Maxwell, B.B., Cook, R.K., Kan, J.M., Alonso, J.M., Ecker, J.R., and Chory, J.** (2002). De-etiolated 1 and damaged DNA binding protein 1 interact to regulate Arabidopsis photomorphogenesis. *Curr Biol* **12**, 1462-1472.
- Schroeder, J.I., Allen, G.J., Hugouvieux, V., Kwak, J.M., and Waner, D.** (2001). Guard Cell Signal Transduction. *Annu Rev Plant Physiol Plant Mol Biol* **52**, 627-658.
- Schultz, T.F., Kiyosue, T., Yanovsky, M., Wada, M., and Kay, S.A.** (2001). A role for LKP2 in the circadian clock of Arabidopsis. *Plant Cell* **13**, 2659-2670.
- Schwechheimer, C., and Willige, B.C.** (2009). Shedding light on gibberellic acid signalling. *Curr Opin Plant Biol* **12**, 57-62.
- Schwechheimer, C., and Isono, E.** (2010). The COP9 signalosome and its role in plant development. *Eur J Cell Biol* **89**, 157-162.
- Schwechheimer, C., Serino, G., Callis, J., Crosby, W.L., Lyapina, S., Deshaies, R.J., Gray, W.M., Estelle, M., and Deng, X.W.** (2001). Interactions of the COP9 signalosome with the E3 ubiquitin ligase SCF^{TIR1} in mediating auxin response. *Science* **292**, 1379-1382.
- Seo, H.S., Watanabe, E., Tokutomi, S., Nagatani, A., and Chua, N.H.** (2004). Photoreceptor ubiquitination by COP1 E3 ligase desensitizes phytochrome A signaling. *Genes Dev* **18**, 617-622.
- Seo, H.S., Yang, J.Y., Ishikawa, M., Bolle, C., Ballesteros, M.L., and Chua, N.H.** (2003). LAF1 ubiquitination by COP1 controls photomorphogenesis and is stimulated by SPA1. *Nature* **423**, 995-999.
- Sessa, G., Carabelli, M., Sassi, M., Ciolfi, A., Possenti, M., Mittempergher, F., Becker, J., Morelli, G., and Ruberti, I.** (2005). A dynamic balance between gene activation and repression regulates the shade avoidance response in Arabidopsis. *Genes Dev* **19**, 2811-2815.
- Sessions, A., Burke, E., Presting, G., Aux, G., McElver, J., Patton, D., Dietrich, B., Ho, P., Bacwaden, J., Ko, C., Clarke, J.D., Cotton, D., Bullis, D., Snell, J., Miguel, T., Hutchison, D., Kimmerly, B., Mitzel, T., Katagiri, F., Glazebrook, J., Law, M., and Goff, S.A.** (2002). A high-throughput Arabidopsis reverse genetics system. *Plant Cell* **14**, 2985-2994.
- Shalitin, D., Yang, H., Mockler, T.C., Maymon, M., Guo, H., Whitelam, G.C., and Lin, C.** (2002). Regulation of Arabidopsis cryptochrome 2 by blue-light-dependent phosphorylation. *Nature* **417**, 763-767.
- Sharrock, R.A., and Quail, P.H.** (1989). Novel phytochrome sequences in *Arabidopsis thaliana*: Structure, evolution, and differential expression of a plant regulatory photoreceptor family. *Genes Dev* **3**, 1745-1757.
- Shen, Y., Feng, S., Ma, L., Lin, R., Qu, L.J., Chen, Z., Wang, H., and Deng, X.W.** (2005). Arabidopsis FHY1 protein stability is regulated by light via phytochrome A and 26S proteasome. *Plant Physiol* **139**, 1234-1243.
- Sibout, R., Sukumar, P., Hettiarachchi, C., Holm, M., Muday, G.K., and Hardtke, C.S.** (2006). Opposite root growth phenotypes of hy5 versus hy5 hyh mutants correlate with increased constitutive auxin signaling. *PLoS Genet* **2**, e202.
- Silverstone, A.L., Mak, P.Y., Martinez, E.C., and Sun, T.P.** (1997). The new RGA locus encodes a negative regulator of gibberellin response in Arabidopsis thaliana. *Genetics* **146**, 1087-1099.
- Somers, D.E., Kim, W.Y., and Geng, R.** (2004). The F-box protein ZEITLUPE confers dosage-dependent control on the circadian clock, photomorphogenesis, and flowering time. *Plant Cell* **16**, 769-782.

- Somers, D.E., Sharrock, R.A., Tepperman, J.M., and Quail, P.H.** (1991). The hy3 Long Hypocotyl Mutant of Arabidopsis Is Deficient in Phytochrome B. *Plant Cell* **3**, 1263-1274.
- Spiegelman, J.I., Mindrinos, M.N., Fankhauser, C., Richards, D., Lutes, J., Chory, J., and Oefner, P.J.** (2000). Cloning of the Arabidopsis RSF1 gene by using a mapping strategy based on high-density DNA arrays and denaturing high-performance liquid chromatography. *Plant Cell* **12**, 2485-2498.
- Stokes, T.L., and Richards, E.J.** (2002). Induced instability of two Arabidopsis constitutive pathogen-response alleles. *Proc Natl Acad Sci U S A* **99**, 7792-7796.
- Suarez-Lopez, P., Wheatley, K., Robson, F., Onouchi, H., Valverde, F., and Coupland, G.** (2001). CONSTANS mediates between the circadian clock and the control of flowering in Arabidopsis. *Nature* **410**, 1116-1120.
- Subramanian, C., Kim, B.H., Lyssenko, N.N., Xu, X.D., Johnson, C.H., and von Arnim, A.G.** (2004). The Arabidopsis repressor of light signaling, COP1, is regulated by nuclear exclusion: Mutational analysis by bioluminescence resonance energy transfer. *Proc Nat Acad Sci Usa* **101**, 6798-6802.
- Sugimoto-Shirasu, K., and Roberts, K.** (2003). "Big it up": endoreduplication and cell-size control in plants. *Curr Opin Plant Biol* **6**, 544-553.
- Sun, T., Goodman, H.M., and Ausubel, F.M.** (1992). Cloning the Arabidopsis GA1 Locus by Genomic Subtraction. *Plant Cell* **4**, 119-128.
- Sweere, U., Eichenberg, K., Lohrmann, J., Mira-Rodado, V., Baurle, I., Kudla, J., Nagy, F., Schafer, E., and Harter, K.** (2001). Interaction of the response regulator ARR4 with phytochrome B in modulating red light signaling. *Science* **294**, 1108-1111.
- Szekeres, M., Nemeth, K., Koncz-Kalman, Z., Mathur, J., Kauschmann, A., Altmann, T., Redei, G.P., Nagy, F., Schell, J., and Koncz, C.** (1996). Brassinosteroids rescue the deficiency of CYP90, a cytochrome P450, controlling cell elongation and de-etiolation in Arabidopsis. *Cell* **85**, 171-182.
- Tepperman, J.M., Zhu, T., Chang, H.S., Wang, X., and Quail, P.H.** (2001). Multiple transcription-factor genes are early targets of phytochrome A signaling. *Proc Natl Acad Sci U S A* **98**, 9437-9442.
- Tsuge, T., Tsukaya, H., and Uchimiya, H.** (1996). Two independent and polarized processes of cell elongation regulate leaf blade expansion in Arabidopsis thaliana (L.) Heynh. *Development* **122**, 1589-1600.
- Tsukaya, H.** (2005). Leaf shape: genetic controls and environmental factors. *Int J Dev Biol* **49**, 547-555.
- Tsukaya, H.** (2006). Mechanism of leaf-shape determination. *Annu Rev Plant Biol* **57**, 477-496.
- Tsutsui, T., Kato, W., Asada, Y., Sako, K., Sato, T., Sonoda, Y., Kidokoro, S., Yamaguchi-Shinozaki, K., Tamaoki, M., Arakawa, K., Ichikawa, T., Nakazawa, M., Seki, M., Shinozaki, K., Matsui, M., Ikeda, A., and Yamaguchi, J.** (2009). DEAR1, a transcriptional repressor of DREB protein that mediates plant defense and freezing stress responses in Arabidopsis. *J Plant Res* **122**, 633-643.
- Turck, F., Fornara, F., and Coupland, G.** (2008). Regulation and identity of florigen: FLOWERING LOCUS T moves center stage. *Annu Rev Plant Biol* **59**, 573-594.
- Ulm, R., Baumann, A., Oravecz, A., Mate, Z., Adam, E., Oakeley, E.J., Schafer, E., and Nagy, F.** (2004). Genome-wide analysis of gene expression reveals function of the bZIP transcription factor HY5 in the UV-B response of Arabidopsis. *Proc Natl Acad Sci U S A* **101**, 1397-1402.
- Valverde, F., Mouradov, A., Soppe, W., Ravenscroft, D., Samach, A., and Coupland, G.** (2004). Photoreceptor regulation of CONSTANS protein in photoperiodic flowering. *Science* **303**, 1003-1006.
- Vandenbussche, F., Habricot, Y., Condiff, A.S., Maldiney, R., Van der Straeten, D., and Ahmad, M.** (2007). HY5 is a point of convergence between cryptochrome and cytokinin signalling pathways in Arabidopsis thaliana. *Plant J* **49**, 428-441.

- von Arnim, A.G., and Deng, X.W. (1994). Light inactivation of Arabidopsis photomorphogenic repressor COP1 involves a cell-specific regulation of its nucleocytoplasmic partitioning. *Cell* **79**, 1035-1045.
- von Arnim, A.G., Osterlund, M.T., Kwok, S.F., and Deng, X.W. (1997). Genetic and developmental control of nuclear accumulation of COP1, a repressor of photomorphogenesis in Arabidopsis. *Plant Physiol* **114**, 779-788.
- Wang, H., Ma, L.G., Li, J.M., Zhao, H.Y., and Deng, X.W. (2001). Direct interaction of Arabidopsis cryptochromes with COP1 in light control development. *Science* **294**, 154-158.
- Warrens, A.N., Jones, M.D., and Lechler, R.I. (1997). Splicing by overlap extension by PCR using asymmetric amplification: an improved technique for the generation of hybrid proteins of immunological interest. *Gene* **186**, 29-35.
- Wei, N., Serino, G., and Deng, X.W. (2008). The COP9 signalosome: more than a protease. *Trends Biochem Sci* **33**, 592-600.
- Wei, N., Kwok, S.F., von Arnim, A.G., Lee, A., McNellis, T.W., Piekos, B., and Deng, X.W. (1994). Arabidopsis COP8, COP10, and COP11 genes are involved in repression of photomorphogenic development in darkness. *Plant Cell* **6**, 629-643.
- Werner, T., and Schmulling, T. (2009). Cytokinin action in plant development. *Curr Opin Plant Biol* **12**, 527-538.
- Wertz, I.E., O'Rourke, K.M., Zhang, Z., Dornan, D., Arnott, D., Deshaies, R.J., and Dixit, V.M. (2004). Human De-etiolated-1 regulates c-Jun by assembling a CUL4A ubiquitin ligase. *Science* **303**, 1371-1374.
- Wigge, P.A., Kim, M.C., Jaeger, K.E., Busch, W., Schmid, M., Lohmann, J.U., and Weigel, D. (2005). Integration of spatial and temporal information during floral induction in Arabidopsis. *Science* **309**, 1056-1059.
- Wolters, H., and Jurgens, G. (2009). Survival of the flexible: hormonal growth control and adaptation in plant development. *Nat Rev Genet* **10**, 305-317.
- Wu, G., and Spalding, E.P. (2007). Separate functions for nuclear and cytoplasmic cryptochrome 1 during photomorphogenesis of Arabidopsis seedlings. *Proc Natl Acad Sci U S A* **104**, 18813-18818.
- Yanagawa, Y., Sullivan, J.A., Komatsu, S., Gusmaroli, G., Suzuki, G., Yin, J., Ishibashi, T., Saijo, Y., Rubio, V., Kimura, S., Wang, J., and Deng, X.W. (2004). Arabidopsis COP10 forms a complex with DDB1 and DET1 in vivo and enhances the activity of ubiquitin conjugating enzymes. *Genes Dev* **18**, 2172-2181.
- Yang, H.Q., Tang, R.H., and Cashmore, A.R. (2001). The signaling mechanism of Arabidopsis CRY1 involves direct interaction with COP1. *Plant Cell* **13**, 2573-2587.
- Yang, H.Q., Wu, Y.J., Tang, R.H., Liu, D.M., Liu, Y., and Cashmore, A.R. (2000). The C termini of Arabidopsis cryptochromes mediate a constitutive light response. *Cell* **103**, 815-827.
- Yang, J., and Wang, H. (2006). The central coiled-coil domain and carboxyl-terminal WD-repeat domain of Arabidopsis SPA1 are responsible for mediating repression of light signaling. *Plant J* **47**, 564-576.
- Yang, J., Lin, R., Hoecker, U., Liu, B., Xu, L., and Wang, H. (2005a). Repression of light signaling by Arabidopsis SPA1 involves post-translational regulation of HFR1 protein accumulation. *Plant J* **43**, 131-141.
- Yang, J., Lin, R., Sullivan, J., Hoecker, U., Liu, B., Xu, L., Deng, X.W., and Wang, H. (2005b). Light regulates COP1-mediated degradation of HFR1, a transcription factor essential for light signaling in Arabidopsis. *Plant Cell* **17**, 804-821.
- Yang, K.Y., Kim, Y.M., Lee, S., Song, P.S., and Soh, M.S. (2003). Overexpression of a mutant basic helix-loop-helix protein HFR1, HFR1-deltaN105, activates a branch pathway of light signaling in Arabidopsis. *Plant Physiol* **133**, 1630-1642.
- Yanovsky, M.J., and Kay, S.A. (2002). Molecular basis of seasonal time measurement in Arabidopsis. *Nature* **419**, 308-312.
- Yi, C., and Deng, X.W. (2005). COP1 - from plant photomorphogenesis to mammalian tumorigenesis. *Trends Cell Biol* **15**, 618-625.

- Yoo, S.K., Chung, K.S., Kim, J., Lee, J.H., Hong, S.M., Yoo, S.J., Yoo, S.Y., Lee, J.S., and Ahn, J.H.** (2005). CONSTANS activates SUPPRESSOR OF OVEREXPRESSION OF CONSTANS 1 through FLOWERING LOCUS T to promote flowering in Arabidopsis. *Plant Physiol* **139**, 770-778.
- Yu, X., Klejnot, J., Zhao, X., Shalitin, D., Maymon, M., Yang, H., Lee, J., Liu, X., Lopez, J., and Lin, C.** (2007). Arabidopsis cryptochrome 2 completes its posttranslational life cycle in the nucleus. *Plant Cell* **19**, 3146-3156.
- Zhu, D., Maier, A., Lee, J.H., Laubinger, S., Saijo, Y., Wang, H., Qu, L.J., Hoecker, U., and Deng, X.W.** (2008). Biochemical characterization of Arabidopsis complexes containing CONSTITUTIVELY PHOTOMORPHOGENIC1 and SUPPRESSOR OF PHYA proteins in light control of plant development. *Plant Cell* **20**, 2307-2323.

Danksagung

Zunächst möchte ich mich bei Prof. Dr. Ute Höcker bedanken. Für die Möglichkeit, sie nach Köln zu begleiten und meine Doktorarbeit in ihrer Arbeitsgruppe zu schreiben, für die tolle Betreuung und Unterstützung. Ich habe in den vergangenen Jahren viel gelernt.

Ich danke Prof. Dr. Hülkamp für die Übernahme des Zweitgutachtens und Prof. Dr. Werr danke ich für die Übernahme des Prüfungsvorsitzes.

Der gesamten AG Höcker bin ich dankbar für den alltäglichen Wahnsinn, den ich mit ihr erleben darf. Speziell Sebastian, Martin, Stefan, Xu und Leonie: Danke, dass ihr mich auch in stressigen Zeiten ertragen habt und für die ständige Versorgung mit Keksen ;-). Ganz besonders möchte ich mich bei Kirsten, Alex und Aashish bedanken, die das Abenteuer Köln von Anfang an mit mir zusammen miterlebt haben und natürlich bei Gabi für den technischen und vor allem beständigen seelischen Beistand – was würden wir nur ohne dich machen...? Danke auch an die Armee von Hiwis, die mich im Laufe der Zeit tatkräftig unterstützt haben.

Ich möchte der AG Hülkamp danken dafür, dass sie uns von Beginn an mit offenen Armen empfangen und unterstützt hat und für den kreativen Input aus unserem gemeinsamen Seminar.

Vielen Dank auch den Gärtnern, der Werkstatt und Siggie, die mir durch ihre Hilfsbereitschaft Vieles erleichtert haben.

Meinen Freunden, besonders Denise, Daniela und Eva möchte ich Danke sagen, dafür dass ich immer auf sie zählen kann – und dass Zeit keine Rolle spielt.

Meiner Familie möchte ich danken, Mama, Papa, Bärbel - und natürlich auch dem ganzen Rest der Bande - für den Halt und die immerwährende Unterstützung.

Erklärung

Ich versichere, dass ich die von mir vorgelegte Dissertation selbständig angefertigt, die benutzten Quellen und Hilfsmittel vollständig angegeben und die Stellen der Arbeit - einschließlich Tabellen, Karten und Abbildungen -, die anderen Werken im Wortlaut oder dem Sinn nach entnommen sind, in jedem Einzelfall als Entlehnung kenntlich gemacht habe; dass diese Dissertation noch keiner anderen Fakultät oder Universität zur Prüfung vorgelegen hat; dass sie – abgesehen von unten angegebenen Teilpublikationen – noch nicht veröffentlicht worden ist sowie, dass ich eine solche Veröffentlichung vor Abschluss des Promotionsverfahrens nicht vornehmen werde.

Die von mir vorgelegte Dissertation ist von Prof. Dr. Ute Höcker betreut worden.

Petra Fackendahl